ARTIFICIAL X-RAY IMAGING SYSTEM (AXIS) – DESIGN AND EVALUATION ON C-ARM PERFORMANCE IN OPERATING ROOM AND EDUCATIONAL SETTINGS

by

MICHÈLE TOUCHETTE

B.A., Concordia University, 2007
B.A.Sc., The University of British Columbia, 2014

A THESIS SUBMITTED IN PARTIAL FULFILLMENT OF THE REQUIREMENTS FOR THE DEGREE OF

MASTER OF APPLIED SCIENCE

in

THE FACULTY OF GRADUATE AND POSTDOCTORAL STUDIES

(Biomedical Engineering)

THE UNIVERSITY OF BRITISH COLUMBIA

(Vancouver)

April 2017

Abstract

Fluoroscopic C-arms are operated by medical radiography technologists (MRTs) in Canadian operating rooms (ORs). Newly trained MRTs often experience most of their practical learning curve with C-arms in the OR, where achieving the radiographic views requested by surgeons can be challenging. New MRTs often require several scout X-rays during C-arm positioning, resulting in unnecessary radiation exposure and added OR time. To address this problem we have designed an Artificial X-ray Imaging System (AXIS) in order to assess the utility of artificial X-rays in improving the C-arm positioning performance by inexperienced users. AXIS is designed to generate Digitally Reconstructed Radiographs (DRRs), or artificial X-ray images, based on the relative position of a C-arm and manikin.

We enrolled 30 participants into our user study, each of whom performed four activities: an introduction session, an AXIS-guided evaluation, a non-AXIS-guided evaluation, and a questionnaire. The main goal of the study was to compare C-arm positioning performance with and without AXIS guidance. For each evaluation, the participants had to replicate a set of target X-ray images by taking real radiographs of the manikin with the C-arm. During the AXIS evaluation, artificial X-rays were generated at 2 Hz for guidance, while in the non-AXIS evaluation, the participants had to acquire real X-rays to guide them toward the correct view. We recorded the number of real X-rays and time required per task, as well as tracked the C-arm's pose and compared it to the target pose to determine positioning accuracy.

We found that users required 53% fewer scout X-rays and achieved 10% better C-arm displacement accuracies when guided by AXIS, without requiring more time to complete the imaging tasks. From the questionnaires we found that, on average, participants felt significantly more confident in their ability to capture correct anatomical views when they were guided by AXIS. Moreover, the participants found the usefulness of AXIS in guiding them to the desired view to be 'very good'. Overall, we are encouraged by these findings and plan to further develop this system with the goal of deploying it both for training and intraoperative uses.

Lay Summary

C-arms (mobile X-ray equipment) provide surgeons with live views of the anatomy during surgery. However, radiation technologists, who operate these C-arms, receive little hands-on C-arm training. As a result, most of their learning curve is carried out during surgery, often causing them to inaccurately position the C-arm. This can slow the procedure down and expose the patient and staff to unnecessary radiation. To address this problem we have developed a system that generates X-rays artificially, without radiation. This artificial X-ray imaging system (AXIS) can guide inexperienced C-arm users during C-arm positioning. We carried out a user study with inexperienced C-arm users and found that they required half the number of X-rays to accomplish simulated imaging tasks when guided by AXIS. AXIS is a promising tool that has the potential to reduce radiation exposure, and improve C-arm positioning efficiency and accuracy in surgical and educational settings.

Preface

This thesis is an original piece of work by the author, Michèle Touchette. The original concept of designing the Artificial X-ray Imaging System (AXIS) as a means to evaluate the utility of artificial X-rays in educational and operating room settings was proposed by my co-supervisors, Dr. Antony Hodgson and Dr. Carolyn Anglin, who also provided guidance on its implementation and on revisions for the thesis writing.

The results of this work will be presented at the 17th annual meeting of the International Society for Computer Assisted Orthopaedic Surgery (CAOS) in Aachen, Germany, in June 2017.

The user study presented in this thesis was approved by the UBC Clinical Research Ethics Board (H15-00005) and by the BCIT Research Ethics Board (2016-09).

Figures that have been obtained from copyrighted sources throughout this thesis have been reproduced with the permission of the copyright owners.

Table of Contents

List of Tables

List of Figures

List of Abbreviations

API	Application Program Interface
AXIS	Artificial X-ray Imaging System
BioEng Lab	Biomedical Engineering Lab and Computer-Assisted Surgery Suite
BCIT	British Columbia Institute of Technology
CAMC	Camera-Augmented Mobile C-arm
CAOS	Computer-Assisted Orthopaedic Surgery
CHHM	Centre for Hip Health and Mobility
CLAHE	Contrast-Limited Adaptive Histogram Equalization
CT	Computer Tomography
DRR	Digitally Reconstructed Radiograph
FWER	Family-Wise Error Rate
GUI	Graphical User Interface
IMU	Inertial Measurement Unit
MRT	Medial Radiation Technologist
NDI	Northern Digital Instruments
OR	Operating Room
SCU	System Control Unit
UBC	University of British Columbia
VGH	Vancouver General Hospital

Acknowledgments

I would first like to thank Dr. Antony Hodgson and Dr. Carolyn Anglin, my research co-supervisors, for their ongoing guidance and support throughout my thesis project, as well as for being the inspiration behind the many medical innovations that grow from the Surgical Technologies Lab.

I would like to thank Dr. Meena Amlani, Francine Anselmo, and the rest of the Medical Radiography faculty at BCIT for providing their insight into the C-arm training world, as well as for their ongoing support with equipment and lab space resources.

I am tremendously thankful to the Centre for Hip Health and Mobility at Vancouver General Hospital for hosting me in their office and lab space throughout the life of this project, and for bringing so many brilliant and like-minded people together.

I am tremendously thankful to my colleagues in the UBC Surgical Technologies Lab for not only providing an excellent support network, but for their wide network of resources and for their forward-thinking approaches to medical innovation. Dr. Robyn Newell and Tiffany Ngo, your guidance and feedback have been paramount to the success of this project.

Dr. Pierre Guy and Dr. Kelly Lefaivre, I am thankful for the expertise you've offered from an orthopaedic standpoint and for the time you've provided to contribute to the project.

Lastly, I would like to thank the Canadian Institute of Health Research and the Natural Sciences and Engineering Research Council of Canada for their financial support.

Chapter 1

Introduction and Background

With fluoroscopic surgery becoming increasingly widespread in modern orthopaedics, matching such advancement with adequate training on fluoroscopic equipment is crucial to maximizing operating room efficiency. Additionally, with the evolution of these procedures, radiation exposure to patients and operating room staff is a growing cause for concern. These challenges are the motivation for this work, inspiring the proposed technical and clinical solution presented in this thesis.

1.1 Image-Guided Surgery

Image-guided surgeries that make use of intraoperative medical imaging, namely fluoroscopy, in order to help plan and guide the procedure, have become an important part of modern orthopaedics. Intraoperative fluoroscopy provides the surgeon with the ability to visualize internal structures and geometrical relationships with live imagery and direct views of the patient (Grimson 1999). One major advantage of such visualization capabilities are that they enable the surgeon to perform the procedure in a safer and less invasive manner, meaning that they can often make tiny incisions, rather than larger open ones. Minimally invasive surgery can benefit the patient in several ways when compared to traditional, open surgery, including: reduced trauma to the muscles, nerves, and surrounding tissues; reduced bleeding; reduced scarring; reduced pain and use of narcotics; reduced hospital time; and reduced impact on the immune system (MSMC 2016).

Fluoroscopy, a technology that makes use of X-rays to generate real-time still and video images of the patient, is the imaging modality most routinely used intraoperatively in orthopaedic procedures (Suhm

2003). With intraoperative fluoroscopy, the surgeon can visualize the placement of instruments and implants within the anatomy throughout the progression of the surgery while maintaining minimal invasiveness. The use of intraoperative fluoroscopy has also become the basis for many Computer-Assisted Orthopaedic Surgery techniques (CAOS, also known as navigation), which use computer-enabled tracking systems or robotic devices with the goal of improving application accuracy and visibility of the surgical field (Zheng 2015). Computer-assisted surgery has evolved from the desire to perform safer and less invasive surgical interventions, and has allowed for newer and what would have traditionally been more challenging approaches (Mezger 2013).

Since the mobile C-arm is central to the surgical problem being addressed and is a fundamental component of the system described in this thesis, some of its components and mechanisms are described in the following section to better understand the system design. The C-arm description is based on the model used for this work: a Siemens Arcadis Orbic 3D.

1.2 The Mobile C-arm Fluoroscopic X-ray System

Mobile C-arm fluoroscopic X-ray systems (Figure 1) are currently used in a variety of diagnostic imaging and minimally invasive surgical applications (Fornell 2011). One fundamental advantage of mobile C-arms is that they are capable of performing a variety of movements with a wide range of motion, allowing for quick alternation between multiple views in the operating room (OR). The basic components of a mobile C-arm are the X-ray source, the image detector, the C-shaped arm lending its name to the C-arm, the base (or electronic unit), and the workstation unit (Fujii 2003; Siemens 2006). The joint mechanisms between the base and the C-arm allow the source and detector to be repositioned by means of three rotational degrees of freedom, referred to as “orbit”, “wig-wag”, and “tilt”. The wheels supporting the base allow for three translational degrees of freedom, referred to as “up-and-down”, “in-and-out”, and “side-to-side” (or “along-the-table”) (Figure 2). When acquiring X-ray images, it is crucial to be aware of the radiation exposure that is delivered to the patient and anyone who may be present around the C-arm. To better understand this challenge, ionizing radiation exposure as it relates to the OR setting is discussed in the next section.

Figure 1: Mobile C-arm fluoroscopy X-ray system

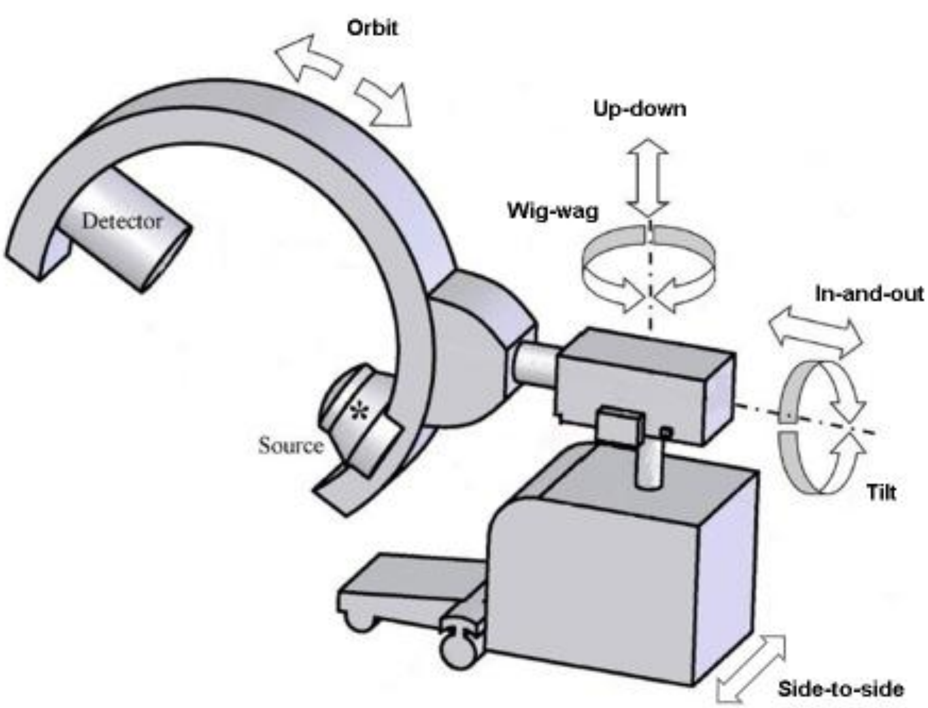

Figure 2: The C-arm's six degrees of freedom (©Amiri 2014, with permission)

1.3 Ionizing Radiation Exposure in the OR

In order to acquire an X-ray image of the patient, the radiation release footswitch is pressed, and the X-ray tube at the source emits X-rays that penetrate and interact with the patient's body tissue. The image intensifier then converts any incoming X-ray energy into visible light, which is in turn recorded by the integrated camera (Siemens 2006). The resulting image can be viewed on the workstation's monitors. It is important to note that not all X-rays produced by the X-ray tube interact with the patient tissue in such a way that they get directed towards the detector. Some incident X-rays penetrate the patient and do cause atom ionization, in turn producing the characteristic X-rays that get directed to the detector. However, some incident X-rays are absorbed by the patient tissue while others are scattered and contribute to radiation exposure of any surrounding persons (Boone 2000).

For physicians and surgeons who work with fluoroscopes, fluoroscopy can represent the largest component of the radiation exposure they receive throughout their careers. Given the increase in prominence of minimally-invasive procedures in modern surgery, the use of fluoroscopy has become indispensable and, as such, the use of fixed and mobile fluoroscopy units has increased dramatically over the last decade. Each contribution to radiation exposure is cumulative over the years and the long-term result can be substantial (Giordano 2011). As one would expect, radiation exposure resulting from medical imaging not only affects the physicians who call for it during interventions, but also affects anyone in the surroundings, including other health care employees and, of course, the patient. In the medical field, human factors play an important role in the amount of radiation exposure that occurs, as well as in its reduction potential, especially with regard to safety-related decision making and the choice of interventional techniques used. For example, maximizing the distance between the surgeon and X-ray source, or positioning the source under the surgical table helps reduce radiation exposure in the OR (Dresing 2011). We address the human factors issues with C-arm positioning as they relate to the contribution of radiation exposure in the OR in the following sections.

1.4 The role of Radiation Technologists in Fluoroscopy-Guided Orthopaedic Surgeries

Radiation technologists are crucial members of the team during image-guided interventions, and as in any other team-based task, communication plays a key role in the successful outcome of each procedure. However, frustration is a common experience when a new radiographer meets and tries to communicate with a surgeon about the fluoroscopic images required (Williams 2009). In the operating room, orthopaedic surgeons are part of the sterile environment, preventing them from coming into contact with items that are not sterile, including the C-arm and its base. As such, the surgeon must rely on external help in order to adjust the position of the mobile C-arm. In Canada, medical radiation technologists (MRTs) operate and manoeuvre C-arms in the operating room on surgeon vocal command. When the surgeon requires a specific radiographic view of tools, implants, and anatomy, they communicate this to the MRT, who in turn moves the C-arm into position accordingly before acquiring a still X-ray image, or a series of images in video mode. Indeed, poor communication between the two can lead to disruption, increased radiation exposure, frustration, and conflict (Pally 2013; Booij 2007). In a study on perioperative disruptive behaviour among operating room staff, a survey found that in 79% of the cases, disruption was due to yelling and shouting (Rosenstein 2006).

Communication between the MRT and the surgeon becomes especially crucial in orthopaedic tasks that require precise placement of the source with respect to an anatomical feature or implant, or that require alternating between two perpendicular views of the same feature of interest. For example, this requirement is common when measuring anatomical distances for screw sizing, aligning locking screws into intramedullary rods, or to ensure that the placement of a screw is not breaching bone and coming into contact with important surrounding tissues, blood vessels, or nerves. However, there is currently no consistent and widely used set of terms to facilitate communication between the surgeon and MRT when describing the positioning of the C-arm with respect to the patient's anatomy. Surgeons in the OR often use ambiguous language that inadequately conveys their request to MRTs, and the language used is often inconsistent from one surgeon to another (Pally 2013). When one of the members is new or inexperienced, or in the instance of an unusual case, this results in a situation where the MRT and surgeon must attempt to translate the language of the other. For example, "up" is a particularly ambiguous term that is used to describe both vertical elevation and movement toward the patient's head, while the terms "rotate," "tilt", and "angle" are used interchangeably to describe any of the rotational motions of a C-arm (Pally 2013). One can imagine that in these situations, incongruent language inevitably leads to delays and inaccuracies. In British Columbia, inexperienced MRTs are especially vulnerable to poor communication in this respect, and this is better understood when appreciating how limited their practical training is with C-arms in the OR.

1.5 Mobile C-arm Fluoroscopy Training

With increased pressure on the healthcare system to be safer and more efficient, the C-arm performance of MRTs becomes increasingly crucial in the OR with regard to imaging efficacy, conscientiousness with radiation exposure, and efficiency during procedures. Training in C-arm fluoroscopy, however, is often largely limited to learning the theory of operation and lacks hands-on practice in a learning environment, such as that carried out for standard radiographic training (i.e. non-C-arm X-ray imaging). Thus, the majority of their practical training and a large proportion of their learning curve is carried out in a real OR setting. This is less than ideal in light of the communication challenges that already often exist between MRTs and surgeons. The OR is a fast-paced and stressful environment; inadequate MRT training can therefore be stressful and frustrating for the MRT, the surgeon, and OR staff.

At the British Columbia Institute of Technology (BCIT), the Medical Radiography program is a two-year curriculum that trains its MRT students in medical X-ray imaging. The program is composed of classroom instruction, online courses, labs, and clinical rotations (BCIT 2016). For standard radiography training, in addition to theoretical classroom instruction and exercises, students get 129 hours of applied lab training, where they practice the patient and equipment positioning procedures they learned in the classroom. During the labs, they implement positioning procedures in pairs without radiation, as well as practice taking real X-rays on radiopaque mannequins (BCIT 2016). For the C-arm on the other hand, students only receive two hours of formal lab practice, which involves watching a demonstration of the rotational and translation C-arm motions by one of the instructors. The students usually are not allocated any additional C-arm and patient positioning practice time during the lab; therefore the majority of this is carried out during shadowing rotations as part of the curriculum, or when they begin work.

1.6 Problem Observation: Inexperienced MRTs in the OR

Overall, inadequate intraoperative communication between the MRT and surgeon, combined with the MRT's lack of practical experience with the mobile C-arm in an educational setting, can result in C-arm positioning accuracy challenges, requiring more scout (or "trial-and-error") X-ray images before achieving the desired radiographic view. Consequently, both the patient and OR team are exposed to increased radiation exposure and procedure time is longer (Klein 2007). One group from Basel, Switzerland, has shown that in intramedullary nailing procedures, the C-arm positioning process accounts for 80% of all fluoroscopic manoeuvres (Matthews 2007, Suhm 2004). Several groups have tried to address C-arm positioning issues by providing simulated X-ray images either on their own or as an augmentation to video imaging, which are described in the following section.

1.7 Currently Available Solutions and Gaps

One group from the Technische Universität München in Germany has developed a Camera Augmented Mobile C-arm (CamC) system, which computes Digitally Reconstructed Radiographs (DRRs, or artificial X-ray images) from pre- or intraoperative CT data based on the C-arm's current position (Chen 2013). To achieve this, the patient is registered to a pre- or intraoperative CT scan and tracked with a camera installed near the X-ray source. The group has evaluated the system in terms of registration accuracy and C-arm pose estimation using a lumbar spine phantom. They achieved submillimetric registration accuracy and less than 5 mm accuracy for C-arm pose estimation (Dressel 2010). In a separate study the group evaluated the potential of CamC to reduce radiation exposure and found that the mean number of X-rays required to perform cadaveric intramedullary nail interlocking was reduced by 28% when using the CamC compared to only the C-arm (Wang 2010). While these results are promising, both experiments were performed by experienced surgeons, whereas in a real OR situation, the C-arm would be operated by an MRT. As such, there remains a need for evaluation of intraoperative artificial X-rays when used by inexperienced MRTs.

Similarly, a group from Stanford University has taken a comparable approach by developing a fluoroscopy simulator that uses the Image-Guided Surgery Toolkit (IGSTK), an open-source software toolkit developed at Georgetown University (Gong 2014; Cleary 2004). A web camera is mounted on the C-arm's image detector and its relationship with respect to the X-ray source is calibrated. It then tracks a patient phantom using IGSTK, which allows for the generation of DRRs. The group has evaluated the system on the accuracy with which it mimics the clinical setting by surveying clinicians on a 1-5 Likert scale (5 indicating the most realism) after having used the simulator. The overall average was 4.0 among eleven clinicians. The system, however, was not assessed for its effect on C-arm positioning performance, such as radiation exposure, procedure times, or imaging accuracy.

A group from John Hopkins University has integrated surgical tracking and DRR generation with live video augmentation. This system, the Tracker-on-C, has been implemented by fixing a video-based tracker next to the C-arm's detector, registering the patient with a CT volume, and fixing them with tracking markers. They evaluated tracking and registration accuracy using a skull phantom with fiducials, as well as a hexagonal-face marker and achieved submillimetric accuracy results. Geometric accuracy of the DRRs was also evaluated by using a calibration phantom with embedded ball-bearings, then comparing the projection error between the virtual and real X-ray images; the errors were also submillimetric. Finally, in a similar fashion, projection errors were evaluated for overlay of DRRs and trajectory planning data onto video imaging, again resulting in submillimetric errors. The evaluations were performed by an experienced orthopaedic surgeon, and again, despite expressing potential for reducing radiation exposure and time, the group did not explicitly evaluate these in their experiments (Reaungamornat 2012).

In an area more focused on C-arm simulation training, a group from Hannover in Germany has developed a simulation package called virtX, which integrates a physical C-arm and patient manipulation with virtual software (Bott 2009; Bott 2011). virtX offers simulated training with two modules: 1) software that displays a virtual scene consisting of three-dimensional models of a C-arm, an operating room table, and a patient, and 2) motion trackers that enable physical manipulation of a real C-arm and a manikin to be used in combination with the aforementioned virtual scene. In both modules, DRRs are generated based on where the C-arm's position is relative to the patient. A user study was conducted where the time required to achieve certain tasks was compared between three groups: the group that practiced with the virtual component, the group that practiced with both the virtual and physical components, and the control group that performed the tasks without practicing on either of the components. The group that practiced with both the virtual and physical components took an average of 32 seconds (24%) less time to complete the exercise tasks than the control (Bott 2008). While the virtX group evaluated simulated fluoroscopy in the form of DRRs on time required to achieve radiographic views of a manikin, they did not evaluate the extent to which it might reduce radiation exposure in an OR setting.

Finally, one group that did measure radiation exposure in the context of the OR procedures, from RWTH Aachen University, developed a computer-assisted planning and navigation system that is integrated with a tool that enables virtual radiation-free previews of X-ray images, referred to as *zero-dose navigation*. This is achieved by tracking both the C-arm and the anatomy, and as part of the navigation system, subsequently overlaying 3D bone, guide-wire, or screw models onto a simulated X-ray image. The group measured the discrepancy between the models and the images to be a maximal error of 10 mm (Müller 2012, de la Fuente 2007). In a test experiment where a surgeon performed guide-wire and cannulated screw insertion procedures in cadavers with and without guidance from the system, the group found that with computer assistance, radiation exposure was reduced significantly by 89.6% and screw placement accuracy, as measured by screw parallelism and femoral neck width coverage, was significantly improved by 58%. However, mean operation time, from guide wire insertion up to final placement of screws, with the system's guidance was also significantly increased by 67.9% compared to without it (Müller 2011). While it is promising that this experiment has shown how a system incorporating simulated X-rays can significantly reduce radiation exposure and improve accuracy, the effect of the intraoperative artificial X-ray images alone cannot be assessed from these tests since they were part of a larger system that included a broader range of other guidance tools.

Overall, several groups have developed technologies that use artificial X-ray images either for training, or with the goal of guiding the surgeon in order to improve surgical accuracy and efficiency during orthopaedic tasks, such as the placement of screws or implants. However, most of them did not evaluate their systems in order to determine whether they have the potential to decrease radiation exposure to the patient, surgeon, and operating room staff, as well as decrease C-arm positioning time. If they did evaluate radiation exposure and time, it was for an integrated computer-assisted system rather than for artificial X-ray images alone, and the evaluations were performed with clinicians as participants who are rarely the ones operating the C-arm in the OR. None of the existing solutions were evaluated with inexperienced users, and additionally, the users were not assessed on the accuracy of their C-arm positioning in the context of a target radiographical view. As such this important gap still remains. Table 1 below summarizes the above-described existing solutions to C-arm positioning issues and indicates which elements, relevant to this thesis, they have assessed.

Table 1: Summary of issues addressed by previous studies of C-arm positioning technologies

Existing Solutions	Radiation Exposure	Task Time	C-arm Positioning Accuracy	New C-arm users	Artificial X-rays only
CamC	✓				
IGSTK-based simulator					
Tracker-on-C					
virtX		✓			
Zero-dose navigation	✓	✓			

1.8 Proposed Solution and Thesis Goal: System Design and User Study Hypothesis Testing

Several groups in the existing literature provide some evidence that artificial X-rays can improve C-arm positioning performance, but have not clearly evaluated some key issues including radiation exposure, C-arm positioning time, and C-arm positioning accuracy by inexperienced users in a simulated OR setting. Therefore, we have developed our own Artificial X-ray Imaging System (AXIS) to address these questions. AXIS can generate digitally reconstructed radiographs (DRRs), also referred to as artificial X-ray images, without the use of ionizing radiation, in order to guide radiation technologists during orthopaedic surgeries. The system can additionally be used by new MRTs and clinicians in training applications. The artificial X-ray images emulate what would be expected if the C-arm machine were activated in the same position relative to the patient. With the use of this intraoperative and training tool, MRTs can see an estimate of what the real X-ray image would look like in various views by generating artificial X-ray images as required while maneuvering towards the correct view. When in the OR, once they are satisfied with the estimated image, they can then take a real, clinical X-ray image to confirm and provide additional detail not captured in the artificial X-ray image.

We hypothesize that guidance with AXIS can significantly improve C-arm positioning accuracy and thus decrease the need for scout, or “trial and error” X-rays the MRTs normally take when trying to achieve the correct radiographic view requested by the surgeon. This could dramatically reduce the amount of ionizing radiation the patient and operating room personnel are exposed to. We also hypothesize that AXIS can help reduce surgical times by decreasing the time required by MRTs to obtain the correct anatomical views, by providing immediate, radiation-free visual feedback during communication between the surgeon and the MRT.

The goals of the work presented in this thesis are therefore to:

1) Develop an Artificial X-ray Imaging System (AXIS), which is described in detail in Chapter 2;

2) Design and implement a user study in a simulated OR setting in order to evaluate AXIS on its radiation and surgical time reduction potential when used as a guidance tool by inexperienced MRTs during simulated orthopaedic procedures. Additionally, the user study will serve to investigate the effect of guidance with artificial X-rays on C-arm positioning accuracy in the context of a target radiographic view. The study design and results are discussed in Chapter 3 and Chapter 4, respectively.

Chapter 2

AXIS Design Methods

The purpose of the Artificial X-ray Imaging System is to generate digitally reconstructed radiographs (DRRs), also referred to as artificial X-ray images, without the use of ionizing radiation. In order to assess the potential impact of artificial X-rays on C-arm performance, we developed an Artificial X-ray Imaging System and used it to conduct a user study in a simulated OR setting, in which participants who are inexperienced with C-arms were asked to achieve target X-ray views with and without AXIS guidance. This system allows us to determine whether inexperienced C-arm users who are guided by artificial X-rays during orthopaedic procedures are able to achieve intraoperative radiographic images with less radiation, in less time, and with better C-arm positioning accuracy, than without them.

AXIS can be fitted to an existing mobile C-arm and predicts what a fluoroscopic image would look like if a real X-ray were acquired given the current C-arm and patient position. It therefore requires the ability to track the relative position of the C-arm and a simulated patient, as well as a means for generating and displaying the predicted X-ray images. In addition, the ability to produce real X-ray images is necessary for comparison. Figure 3 summarizes how we accomplish these goals.

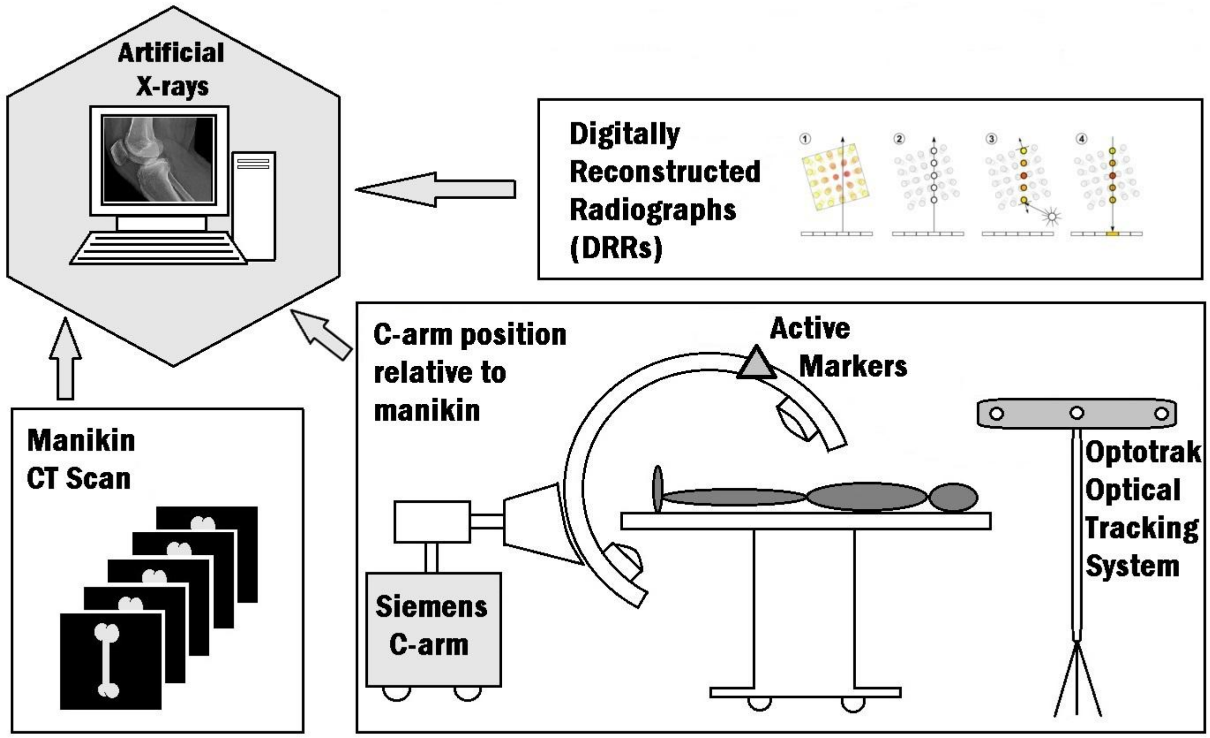

Figure 3: The main components of AXIS

AXIS consists of a manikin with radiopaque artificial bones, a CT scan of the manikin, a C-arm fluoroscopy machine, an optical tracking system to monitor the position of the C-arm, a Digitally Reconstructed Radiograph (DRR) algorithm, and a graphical user interface (GUI) that displays the artificial X-ray images as they are generated. Each of these components is described in detail in the following sections.

2.1 Manikin

A manikin with radiopaque artificial bones spanning the pelvis down to the feet was purchased from Pacific Research Laboratories (Vashon Island, WA, USA) (Figure 4). This portion of anatomy was chosen because the user study makes use of pelvic X-rays, for which positioning the C-arm adequately can vary in difficulty, as explained in more detail in Section 3.2. The manikin is scaled to an average Caucasian male and has limited range of motion within the joints. Since the bones are radiodense and the surrounding tissue-mimicking materials are not, the bone models are well-defined in X-ray images taken with the mobile C-arm.

Figure 4: Manikin with radiodense bones used for AXIS

2.2 CT Scan

In order to generate artificial X-rays, a reference 3D CT volume that matches the physical manikin is required. To do this, we acquired a full CT scan of the manikin from Canada Diagnostic Centre (Vancouver, BC), with a 0.80 mm transverse slice thickness and in-plane resolution of 0.94x0.94 mm.

In viewing the CT images, we discovered that the radiopaque property of the manikin bone models had been achieved by coating the bones with radiopaque material; the internal volume of the bone model material is therefore not radiodense, as it would be in real human bones. Therefore, the internal volume of the bone models has radiodensity values similar to the surrounding volume containing the tissue model. Consequently the ray-casting method employed by the DRR algorithm (described later in Section 2.7) produced images with the bones often indistinguishable from the surrounding tissue (Figure 5a).

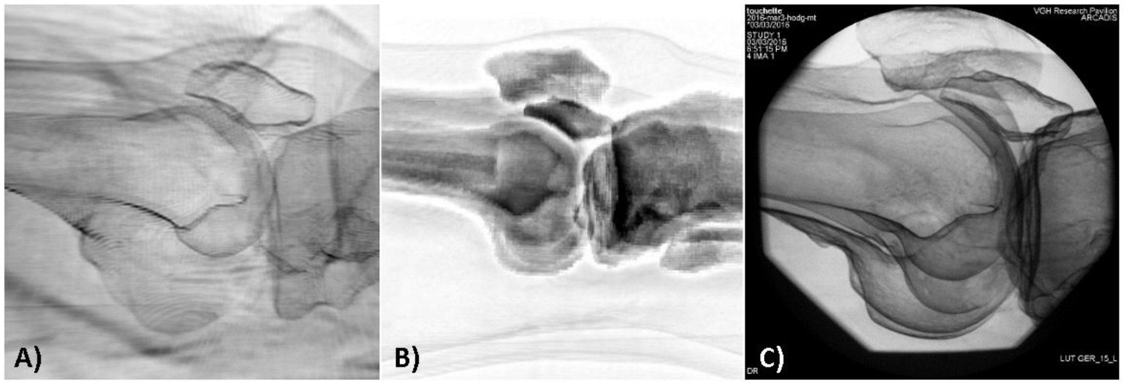

Figure 5: a) Artificial X-ray image of the knee before CT processing; b) Artificial X-ray image of the knee after CT & image post-processing; c) Real X-ray image of the knee for comparison

In order to produce a CT model with bones appearing more distinct, we imported the CT scan into Mimics, a medical image processing software package from Materialise (Leuven, Belgium). We segmented each bone of the manikin's CT scan, associating each segment with a mask of uniform Hounsfield value determined from the average Hounsfield value found in the radiopaque surface material portion (Figure 6a). The resulting exported CT gives the impression that for each different bone segment, the material is of uniform density and material across its entire volume (Figure 6b). In reality, human bone is composed of two main types of bone tissue (cortical and cancellous) that vary in density and composition, so the resulting uniform CT scan appears somewhat unrealistic. However, the artificial X-ray images that are generated by the DRR algorithm display the bone model in a comparatively realistic manner, which is acceptable for our intended application (Figure 5b, c).

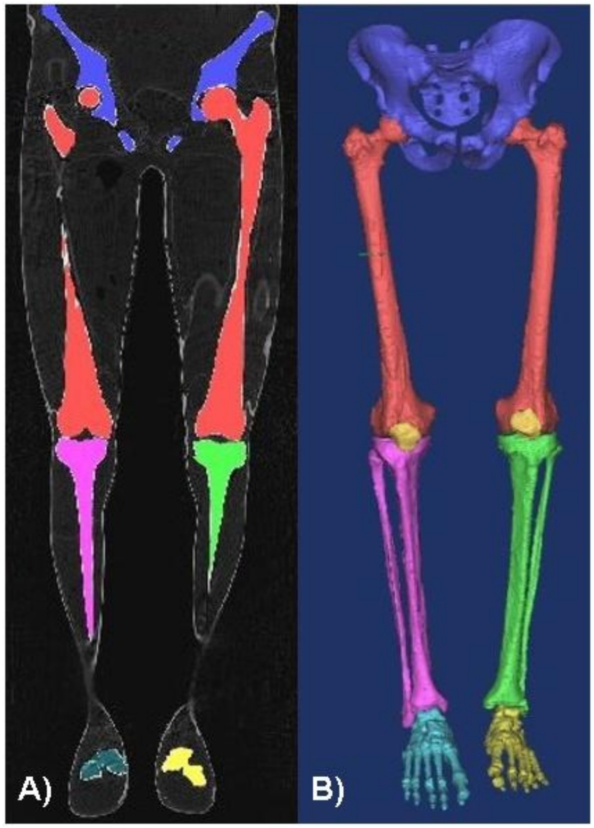

Figure 6: a) Masks for different bone segments with uniform Hounsfield values; b) Bone reconstruction after applying uniform Hounsfield masks

We imported the segmented CT volume into Matlab by means of a GUI that supports medical file format imports, which we obtained from Mathworks' file exchange (Kroon 2010). This function saves the volume data into a 3D matrix variable and the associated CT data information into a structure variable. The volume was further processed in Matlab in preparation for use in the DRR algorithm as follows:

- The volume was cropped to remove voxels that do not include any anatomy in order to reduce its size
- The volume's orientation was adapted to reflect the manikin being positioned in the supine position
- The voxel intensities were thresholded, by defining a minimum and maximum intensity value, below and above which voxel values were set to black or white, respectively, in order to optimize contrast resolution

The final dimensions of the reference CT volume used were 512 x 1413 x 354 voxels and 480 x 1130 x 332 mm (0.94 x 0.80 x 0.94 mm/voxel).

2.3 C-arm Optical Tracking

In order to simulate X-rays that are produced and intensified by the mobile C-arm, as well as attenuated by the anatomy, it is necessary to know where the C-arm is with respect to the anatomy in question when an artificial X-ray is generated. To achieve this, we use the Northern Digital Instruments (NDI, Waterloo, Ontario) Certus Optotrak optical tracking system (Figure 7).

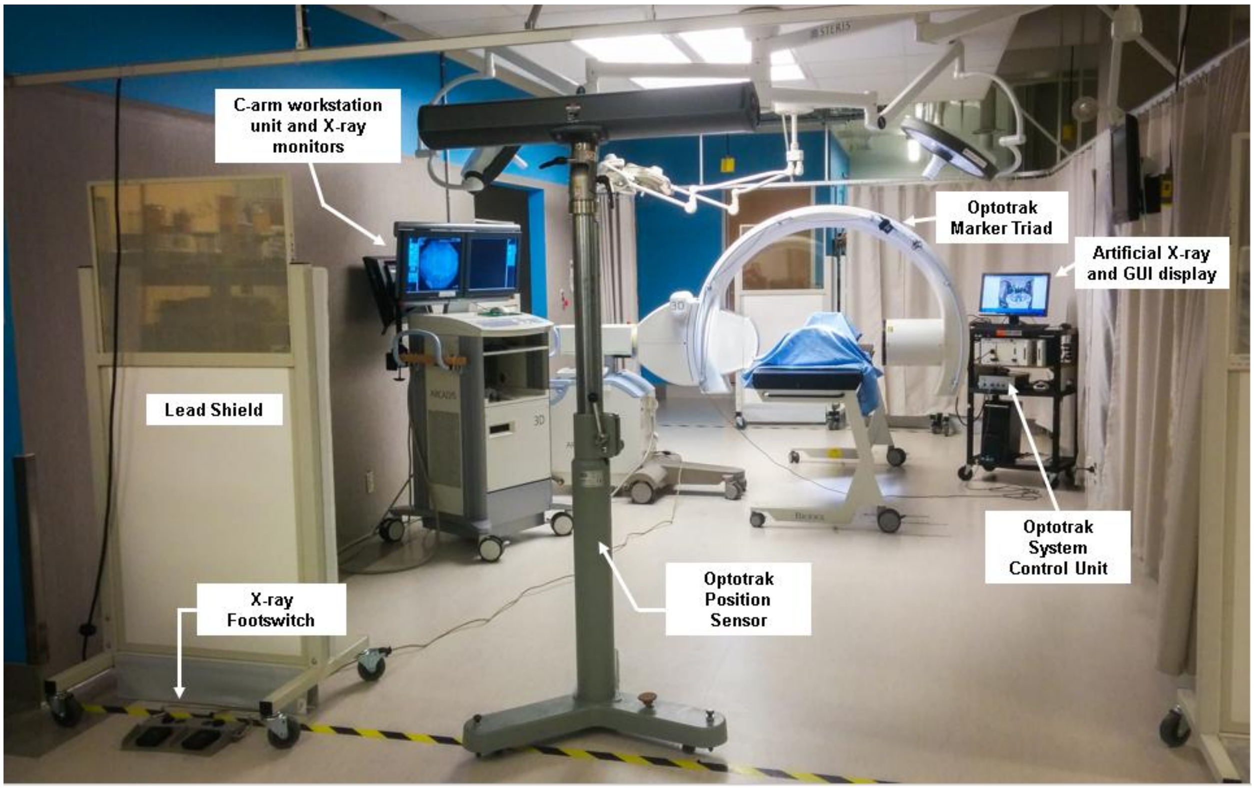

Figure 7: AXIS setup in the Biomedical Engineering Lab of the Centre for Hip Health and Mobility

The C-arm is instrumented with a triad of three active infrared markers (supplied by NDI) so that its three-dimensional pose can be measured. Each marker emits a uniquely-timed signal within the infrared range and is detected by the Optotrak position sensor, whose shutter is synchronized with the cycling of each marker's signal. The Optotrak system provides 0.01 mm resolution and 0.1 mm accuracy when positioned within the optimal ranges depicted in Figure 8. Since the markers in the triad are spaced approximately 45 mm apart, we estimate the angular accuracy to be approximately 0.13 degrees. For the position sensor to detect the infrared signals, the markers must not only be within the optimal range volume, but they must also be visible to the position sensor (i.e., must be in line-of-sight). The positional information is relayed to the Certus System Control Unit (SCU) for analysis in the Optotrak software programs: 1st Principles and 6D Architect.

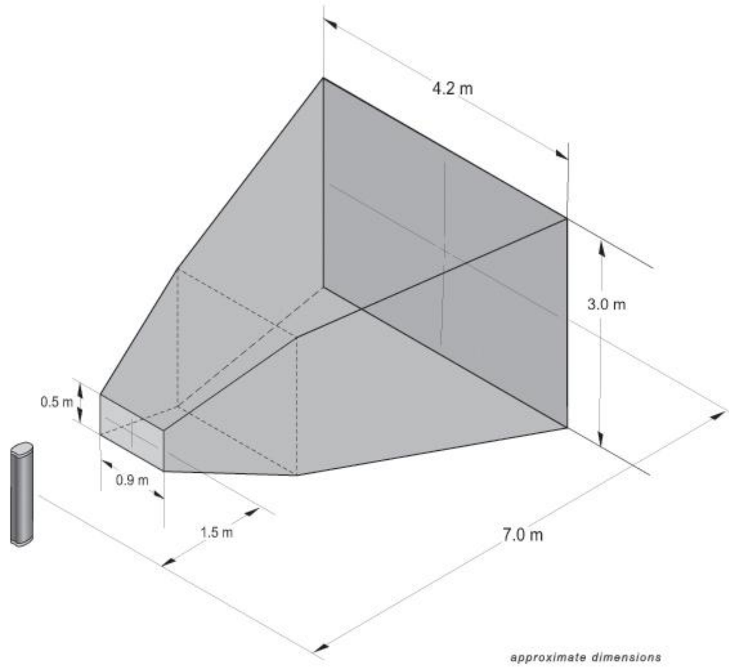

Figure 8: Optotrak range volume depicting placement of markers for optimal accuracy (©Northern Digital Inc. 2015, with permission)

2.4 Registering the CT Volume to the Manikin

The spatial relationship between the C-arm and the manikin is established with respect to the central voxel of the manikin's CT volume, which we take to be the coordinate system origin. The CT scan is approximately registered to the manikin by visual comparison of fluoroscopic images against artificial X-ray images acquired from the C-arm's position of origin (referred to as its home position), which we have arbitrarily defined as the pose when the C-arm is arched over the supine manikin and surgical table, with the X-ray source facing the manikin laterally on its left side and the image intensifier facing the manikin laterally on its right side, as depicted in Figure 7 above. The manikin is successfully registered to its CT scan when the C-arm, in its home position, is in line with the centre of the manikin's sagittal plane. The registration is verified by comparing a real X-ray taken in this position against an artificial X-ray image generated with AXIS in this corresponding home position.

The artificial datum image is obtained by manually setting the position of the X-ray source in the AXIS software so as to define its position to be in line with the CT's central voxel in the sagittal plane. The C-arm’s lateral position with respect to the manikin is defined as a 40 cm distance between the detector surface and the manikin’s midline. As a result, the 2D image produced will represent the central sagittal portion of the manikin’s anatomy, with the central voxel of the CT being mapped to the image’s central pixel. Once we know what the X-ray from the C-arm’s home position should look like, we position the physical manikin on the surgical table, with the C-arm in its home position, and visually line up the axis between the source and detector centres with the manikin sagittal plane’s centre. The manikin’s centre point is also laterally measured to be 40 cm away from the detector surface. A real, fluoroscopic X-ray image is acquired and compared to the reference artificial X-ray. If they do not match, the manikin is repositioned to try and correct for the image discrepancies. This process is reiterated (normally requiring approximately three to five X-rays) until the real X-ray and artificial X-ray images match, by visual inspection. Once the images match, the manikin and its CT scan volume are considered registered.

Since the manikin is not tracked, once the CT volume has been registered to the manikin, the manikin can no longer be repositioned without further registration and calibration. In order to speed up the registration process and avoid the requirement for several X-rays for future setups, crosshairs were drawn onto the manikin to mark where the C-arm’s laser crosshairs should meet the manikin both laterally and anteriorly. During each setup, this step is quickly verified by taking one X-ray and comparing it to the DRR. Notably, sources of error arise from this combination of steps, including the registration of a rigid CT scan to a non-rigid manikin, the use of the C-arm’s angle ruler (+/- 5° precision) to establish its home position angularly, and verifying the agreement of the DRRs with the real X-rays by visual inspection. While we did not explicitly perform tests to measure the angular and translational agreement between the DRRs and the X-rays, we estimate their matching accuracy to be within ± 1 cm and ± 3 degrees. The limitations associated with this setup and image agreement accuracy are discussed in more detail in Section 5.2.1.

2.5 Calculating the C-arm Position

In order to generate a DRR, we calculate the position of the C-arm relative to the manikin by determining the positions of the X-ray emitter and the image intensifier, and relating them to the manikin through a series of transformation matrices, which are described below and illustrated in Figure 12. Ultimately, the two principal parameters required to describe the C-arm pose and simulate the X-ray beam are “*startPt*” and “*endPt*”, a vector pointing from the centre of the CT volume to the centre of the X-ray source and a vector pointing from the centre of the CT volume to the currently indexed detector pixel, whose grayscale value is being calculated, respectively (Figure 10a). These two points of interest are tracked indirectly by creating a rigid body with the NDI marker triad instrumented on the C-arm and five digitized points (*V1*-*V5*) located on both the C-arm's X-ray gantry and the image intensifier (Figure 10b,c). By assuming that the C-arm, source, and detector are part of a rigid body, the five digitized points can be described in relation to the optical marker triad, so that whenever the markers are tracked by the Optotrak position sensor, the five points in space are also known. Additional points of interest can then be calculated, as discussed later in this section and summarized in Figure 9.

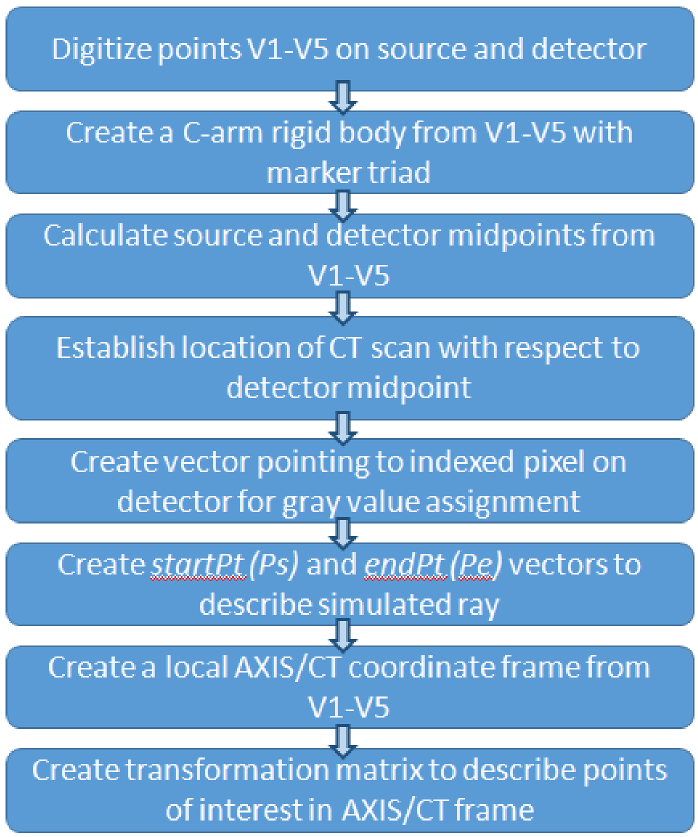

Figure 9: Summary of steps involved in calculating C-arm pose with respect to the manikin

Digitized points *V1* and *V2* are located on the source casing, in such a way that two imaginary perpendicular lines passing through each point, one of which is parallel to the axis line between the source and detector centres, would intersect where the ionizing radiation is emitted (Figure 10b). When the C-arm is in its home position, described in Section 2.4), points *V3*, *V4*, and *V5* are located on the top, right, and bottom screws securing the detector's surface plate to the gantry, respectively (Figure 10c).

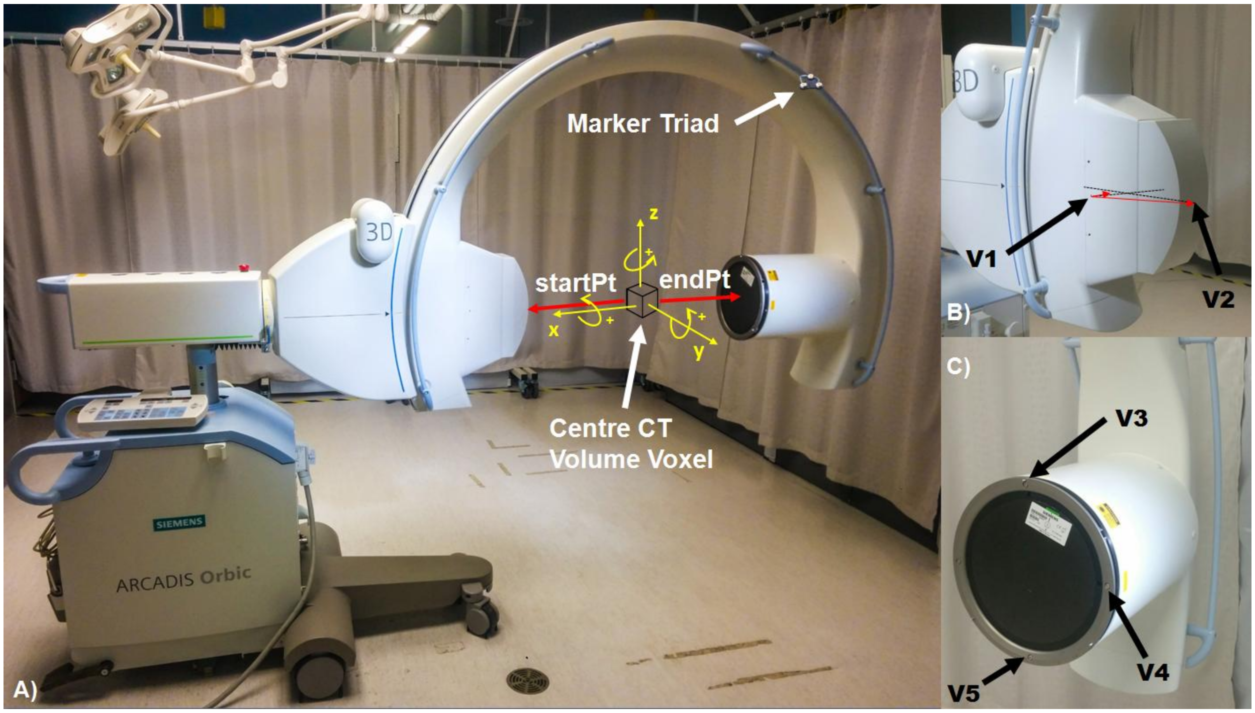

Figure 10: a) The C-arm in its home position, with the directions of startPt and endPt with respect to the central CT volume voxel; b) Digitized points V1 and V2 on the X-ray source casing; c) Digitized points V3, V4, and V5 on the detector casing

In order to digitize points *V1*-*V5*, their locations are collected using the NDI digitization probe (Figure 11). The digitization probe is calibrated using a pivot test with NDI's 3D Architect software. The calibration file that this step produces indicates the location of each of the four probe markers with respect to the tool tip, which is the probe's component that comes into direct contact with the point of interest to be digitized. For each digitization point, *V1*-*V5*, the location of the four probe markers, as well as the marker triad on the C-arm, are collected simultaneously. A coordinate system matrix, $[T_{GD}]$, is then created from three of the four markers on the digitization probe using the global coordinates output by Optotrak during the collection, and using marker 2 as its origin (Figure 11). Figure 12 is included below to help visualize how the various coordinate frames are defined and how each transformation matrix relates the different coordinate frames.

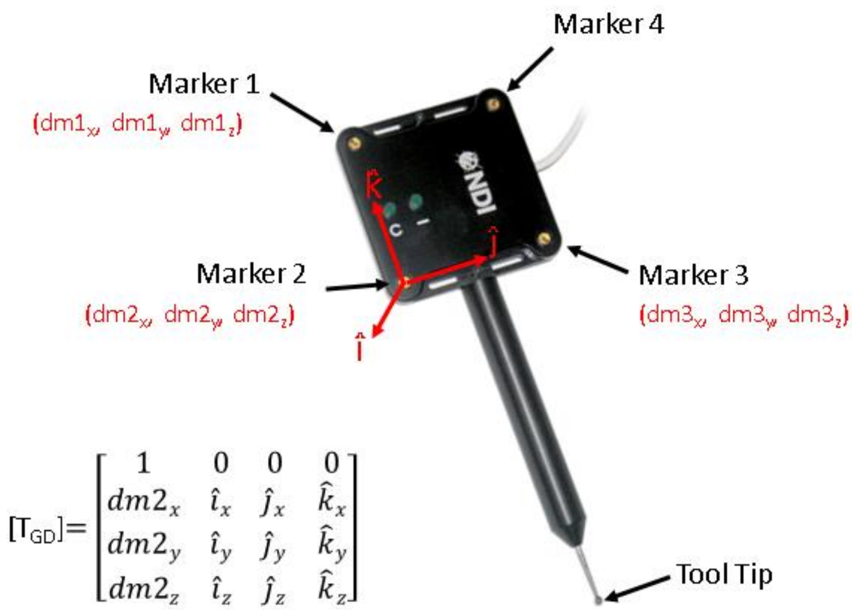

Figure 11: NDI Optotrak digitization probe tool and its local coordinate frame described in global coordinates [T_{GD}]

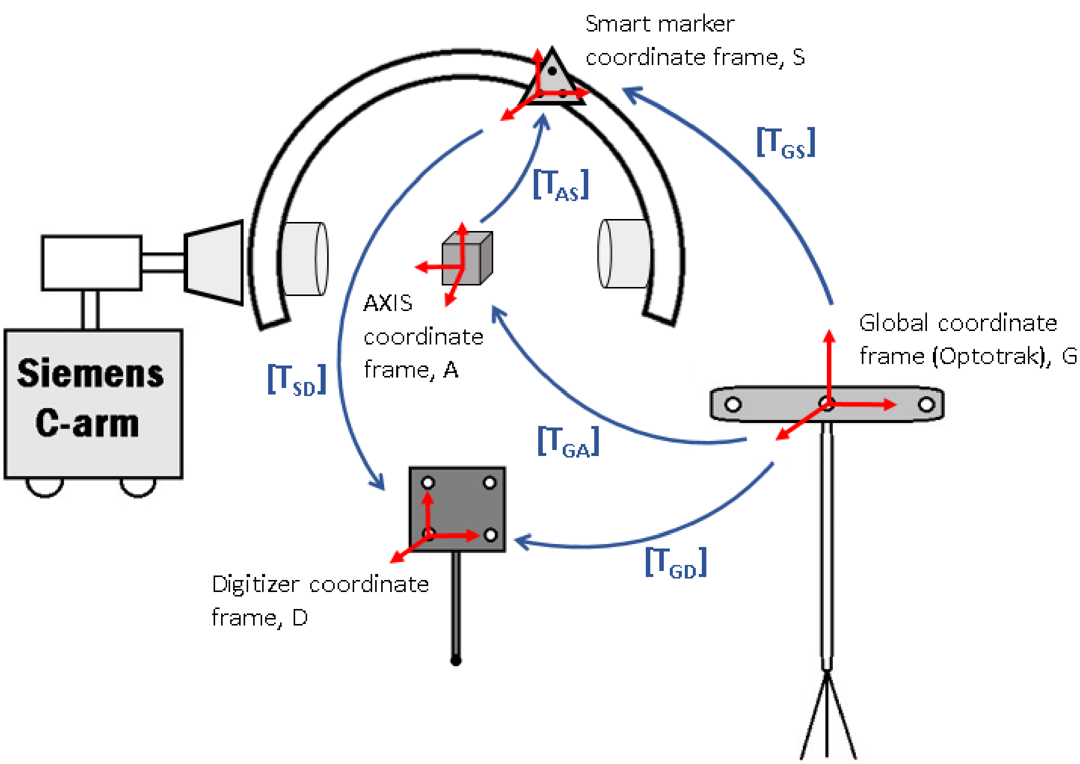

Figure 12: The global, smart marker, digitizer, and AXIS coordinate frames and the transformation matrices that relate them

The location of the probe's tip described in the global frame (Optotrak's position sensor frame) can then be calculated as:

$$\boldsymbol{tip_G} = [\boldsymbol{T_{GD}}] \cdot \boldsymbol{tip_D}, \qquad \textbf{[2.1]}$$

where tip_d is the location of the tip in the digitizer probe's local frame, as defined by the calibration file. A coordinate system matrix using Optotrak's output values during the digitization collection is also created for the three triad markers, similarly to the method shown in Figure 11:

$$[\boldsymbol{T_{GS}}] = \begin{bmatrix} \mathbf{1} & \mathbf{0} & \mathbf{0} & \mathbf{0} \\ \boldsymbol{sm2_x} & \hat{\imath}_x & \hat{\jmath}_x & \hat{\mathbf{k}}_x \\ \boldsymbol{sm2_y} & \hat{\imath}_y & \hat{\jmath}_y & \hat{\mathbf{k}}_y \\ \boldsymbol{sm2_z} & \hat{\imath}_z & \hat{\jmath}_z & \hat{\mathbf{k}}_z \end{bmatrix}. \qquad \textbf{[2.2]}$$

$[T_{GS}]$ is then used to obtain the transformation matrix $[T_{SD}]$, which describes the digitization probe markers in the smart marker triad's frame as follows:

$$[\boldsymbol{T_{SD}}] = [\boldsymbol{T_{GS}}]^{-1}[\boldsymbol{T_{GD}}]. \qquad \textbf{[2.3]}$$

The location of each digitization point can then be described with respect to the marker triad, tip_S, as follows:

$$\boldsymbol{tip_S} = [\boldsymbol{T_{SD}}] \cdot \boldsymbol{tip_D}. \qquad \textbf{[2.4]}$$

Once points *V1-V5* have been calibrated to be part of the C-arm's rigid body, their positions will remain constant relative to the marker triads when tracked, so their positions can be calculated at all times in the global coordinate frame. Thus, for the CT-manikin registration process described previously in Section 2.4, when the C-arm is in its home position, the marker triad's position can be collected and points *V1-V5* can be deduced accordingly. Once the registration process is completed and the C-arm's home orientation is established, any subsequent C-arm motion can be tracked in real-time, and its pose can be defined in relation to its home position.

As mentioned previously, from digitized points *V1-V5*, additional points of interest are calculated. *startPt*, the point where perpendicular lines passing through V1 and V2 intersect, is the location where X-rays are produced and the point at which each mathematical ray for the artificial X-ray image at the current C-arm position begins. The calculation of *startPt*, along with other vectors and points described in this section, are illustrated in Figure 13.

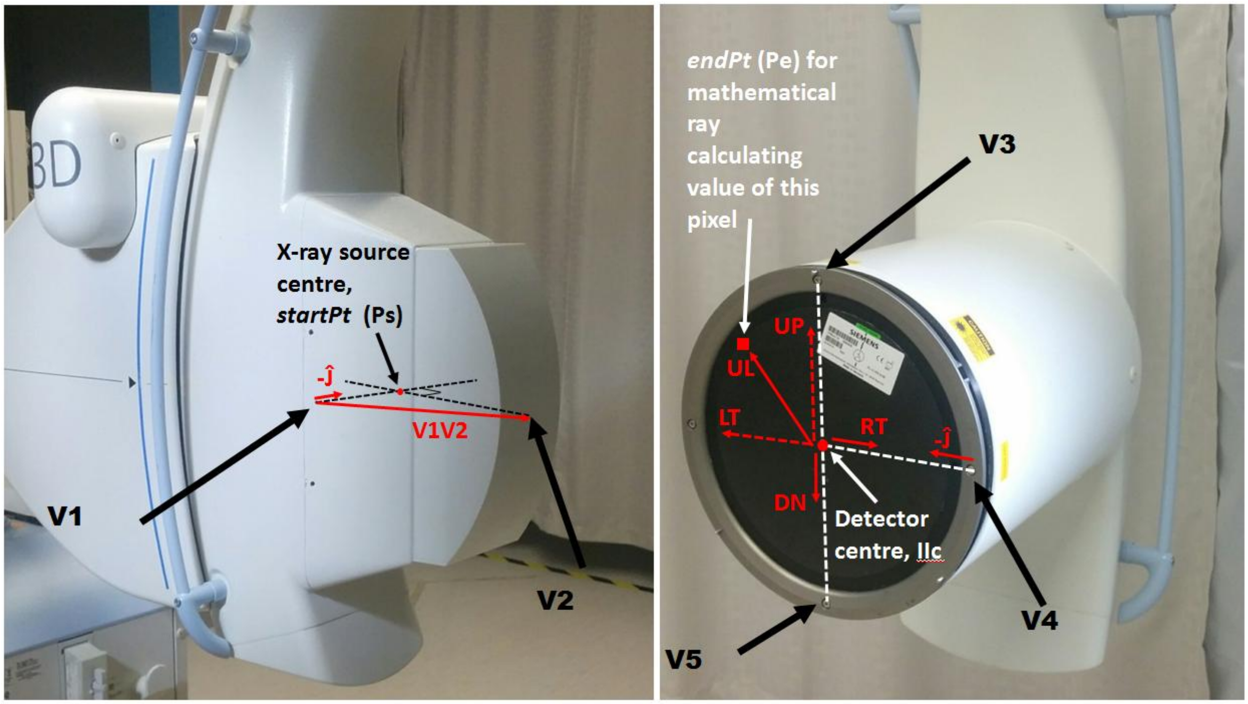

Figure 13: Visualization of the points and vectors calculated in this section

startPt, or *Ps*, is calculated by first defining a unit vector that points in the negative y-direction, $-\hat{J}$, which serves the purpose of defining the first perpendicular line, passing through V1. We achieve this by calculating the center point of the image intensifier, *IIc*, then calculating the $-\hat{\jmath}$ unit vector from *IIc* and *V4*:

$$IIc_G = \frac{V3_G + V5_G}{2} \quad [2.5]$$

$$-\hat{\jmath}_G = \frac{IIc_G - V4_G}{\|IIc_G - V4_G\|}. \quad [2.6]$$

A vector pointing from V1 to V2 is calculated and projected onto $-\hat{J}$ to determine the distance of *Ps* from V1 along $-\hat{J}$. The location of the X-ray source's centre, *startPt* or *Ps,* is then defined in the global coordinate frame:

$$\overrightarrow{V1V2_G} = \begin{bmatrix} (V2_{G,x} - V1_{G,x}) \\ (V2_{G,y} - V1_{G,y}) \\ (V2_{G,z} + V1_{G,z}) \end{bmatrix} \quad [2.7]$$

$$Ps_G = \overrightarrow{V1V2_G} \cdot -\hat{\jmath}_G. \quad [2.8]$$

Once *Ps* is calculated, the end point of the mathematical ray, *endPt or Pe*, is calculated for each pixel on the detector. *Pe* is determined by first calculating a vector that points to the upper-left corner pixel of the detector, $\overrightarrow{UL}$. We create a vector that points in the upward direction on the detector, $\overrightarrow{UP}$, using IIc_G and V3, then creating a unit vector and multiplying by half of the image's height, *H*:

$$\overrightarrow{\boldsymbol{UP_G}} = \frac{\boldsymbol{V3_G - IIc_G}}{\|\boldsymbol{V3_G - IIc_G}\|} * \left(\frac{1}{2}\right) * \boldsymbol{H}. \quad \textbf{[2.9]}$$

The leftward vector $\overrightarrow{LT}$ uses $-\hat{\jmath}_G$, calculated above, multiplied by half of the image's width, *W:*

$$\overrightarrow{\boldsymbol{LT_G}} = -\hat{\jmath}_G * \left(\frac{1}{2}\right) * \boldsymbol{W}. \quad \textbf{[2.10]}$$

Finally we add $\overrightarrow{UP_G}$ and $\overrightarrow{LT_G}$ to get the $\overrightarrow{UL_G}$ vector:

$$\overrightarrow{\boldsymbol{UL_G}} = \overrightarrow{\boldsymbol{UP_G}} + \overrightarrow{\boldsymbol{LT_G}}. \quad \textbf{[2.11]}$$

Rightward and downward unit vectors are also created using IIc_G, $V4_G$, and $V5_G$ in a similar fashion, named $\overrightarrow{RT_g}$ and $\overrightarrow{DN_g}$, which are used to incrementally change the pixel index (to which *endPt* must point for each mathematical ray) by moving across rows of pixels to the right, then down each row.

In order for the above-calculated vectors to be used in the DRR algorithm, they must be described in a reference frame in which the CT volume's central voxel is the origin, which we name the AXIS coordinate frame, A. This is achieved by first creating the x-, y-, and z-axes (Figure 10a), using points *V1-V5* and the source and detector midpoints:

$$\overrightarrow{\boldsymbol{A_{z,guess}}} = \boldsymbol{V3_g - V5_g} \quad \textbf{[2.12]}$$

$$\overrightarrow{\boldsymbol{A_y}} = \boldsymbol{V4_g - IIc_g} \quad \textbf{[2.13]}$$

$$\overrightarrow{\boldsymbol{A_x}} = \boldsymbol{A_y \; x \; A_{z,guess}} \quad \textbf{[2.14]}$$

$$\overrightarrow{\boldsymbol{A_z}} = \boldsymbol{A_x \; x \; A_y}. \quad \textbf{[2.15]}$$

$\overrightarrow{A_x}$, $\overrightarrow{A_y}$, and $\overrightarrow{A_z}$ are then calculated as unit vectors (not shown here). The volume's centre, Vc_G, is calculated by describing a vector that points from the detector midpoint towards the volume, along the x-axis, with a set length of 400 mm from the detector:

$$\boldsymbol{Vc_G = IIc_G + 400} * \overrightarrow{\boldsymbol{A_x}} \quad \textbf{[2.16]}$$

A transformation matrix is then set up to define the AXIS coordinate frame described in global coordinates, with Vc_G as its origin:

$$[\boldsymbol{T_{GA}}] = \begin{bmatrix} \mathbf{1} & \mathbf{0} & \mathbf{0} & \mathbf{0} \\ \boldsymbol{Vc_{G,x}} & \boldsymbol{Ax_x} & \boldsymbol{Ay_x} & \boldsymbol{Az_x} \\ \boldsymbol{Vc_{G,y}} & \boldsymbol{Ax_y} & \boldsymbol{Ay_y} & \boldsymbol{Az_y} \\ \boldsymbol{Vc_{G,z}} & \boldsymbol{Ax_z} & \boldsymbol{Ay_z} & \boldsymbol{Az_z} \end{bmatrix}. \quad \textbf{[2.17]}$$

We use this transformation to describe the parameters of interest in the AXIS coordinate frame so we can ultimately input them into the DRR algorithm. In order to verify that the above calculations were performed correctly, we calculated the rotation angles and translation distances from transformation matrices between different C-arm poses and compared them to the C-arm's physical observed pose. To achieve this we first define $[T_{GS,Home}]$, which is done similarly to $[T_{GS}]$, above, but where the origin is specific to the 'home' position of the current calibration:

$$[\boldsymbol{T_{GS,home}}] = \begin{bmatrix} \mathbf{1} & \mathbf{0} & \mathbf{0} & \mathbf{0} \\ \boldsymbol{sm2_{x,home}} & \hat{\imath}_x & \hat{\jmath}_x & \hat{\mathbf{k}}_x \\ \boldsymbol{sm2_{y,home}} & \hat{\imath}_y & \hat{\jmath}_y & \hat{\mathbf{k}}_y \\ \boldsymbol{sm2_{z,home}} & \hat{\imath}_z & \hat{\jmath}_z & \hat{\mathbf{k}}_z \end{bmatrix} \quad \textbf{[2.18]}$$

We then define the transformation matrix $[T_{AS,Home}]$, which describes the location of the smart marker triad during the 'home' collection in the AXIS coordinate system:

$$[\boldsymbol{T_{AS,Home}}] = [\boldsymbol{T_{GA}}]^{-1}[\boldsymbol{T_{GS,Home}}]. \quad \textbf{[2.19]}$$

We can then describe the source center from the 'home' pose in the AXIS frame, $[T_{ASc,Home}]$, as follows:

$$[\boldsymbol{T_{ASc,Home}}] = \begin{bmatrix} \mathbf{1} & \mathbf{0} & \mathbf{0} & \mathbf{0} \\ \boldsymbol{Sc_{A,Home,x}} & \boldsymbol{T_{AS,Home,xx}} & \boldsymbol{T_{AS,Home,xy}} & \boldsymbol{T_{AS,Home,xz}} \\ \boldsymbol{Sc_{A,Home,y}} & \boldsymbol{T_{AS,Home,yx}} & \boldsymbol{T_{AS,Home,yy}} & \boldsymbol{T_{AS,Home,yz}} \\ \boldsymbol{Sc_{A,Home,z}} & \boldsymbol{T_{AS,Home,zx}} & \boldsymbol{T_{AS,Home,zy}} & \boldsymbol{T_{AS,Home,zz}} \end{bmatrix}. \quad \textbf{[2.20]}$$

Similarly, we define $[T_{GS,Live}]$ in the same way as $[T_{GS,Home}]$ described above; however using the C-arm's live marker triad coordinates (after manoeuvring the C-arm away from the home position) as the origin:

$$[\boldsymbol{T_{GS,live}}] = \begin{bmatrix} \mathbf{1} & \mathbf{0} & \mathbf{0} & \mathbf{0} \\ \boldsymbol{sm2_{x,live}} & \hat{\imath}_x & \hat{\jmath}_x & \hat{\mathbf{k}}_x \\ \boldsymbol{sm2_{y,live}} & \hat{\imath}_y & \hat{\jmath}_y & \hat{\mathbf{k}}_y \\ \boldsymbol{sm2_{z,live}} & \hat{\imath}_z & \hat{\jmath}_z & \hat{\mathbf{k}}_z \end{bmatrix} \quad \textbf{[2.21]}$$

The transformation matrix that describes the live position of the marker triad in the AXIS coordinate frame is:

$$[\boldsymbol{T_{AS,Live}}] = [\boldsymbol{T_{GA}}]^{-1}[\boldsymbol{T_{GS,Live}}], \quad \textbf{[2.22]}$$

then describe the source centre from the C-arm's live pose in the AXIS frame:

$$[\boldsymbol{T_{ASc,Live}}] = \begin{bmatrix} \mathbf{1} & \mathbf{0} & \mathbf{0} & \mathbf{0} \\ \boldsymbol{Sc_{A,Live,x}} & \boldsymbol{T_{AS,Live,xx}} & \boldsymbol{T_{AS,Live,xy}} & \boldsymbol{T_{AS,Live,xz}} \\ \boldsymbol{Sc_{A,Live,y}} & \boldsymbol{T_{AS,Live,yx}} & \boldsymbol{T_{AS,Live,yy}} & \boldsymbol{T_{AS,Live,yz}} \\ \boldsymbol{Sc_{A,Live,z}} & \boldsymbol{T_{AS,Live,zx}} & \boldsymbol{T_{AS,Live,zy}} & \boldsymbol{T_{AS,Live,zz}} \end{bmatrix}. \quad \textbf{[2.23]}$$

Finally, we can define the transformation matrix for the source centre from the 'home' pose to the live pose:

$$[\boldsymbol{T_{ASc,HtoL}}] = [\boldsymbol{T_{ASc,Live}}][\boldsymbol{T_{ASc,Home}}]^{-1}. \quad \textbf{[2.24]}$$

$[T_{ASc,HtoL}]$ is in the form of:

$$[\boldsymbol{T_{ASc,HtoL}}] = \begin{bmatrix} \mathbf{1} & \mathbf{0} & \mathbf{0} & \mathbf{0} \\ \boldsymbol{d_x} & \boldsymbol{r_{xx}} & \boldsymbol{r_{xy}} & \boldsymbol{r_{xz}} \\ \boldsymbol{d_y} & \boldsymbol{r_{yx}} & \boldsymbol{r_{yy}} & \boldsymbol{r_{yz}} \\ \boldsymbol{d_z} & \boldsymbol{r_{zx}} & \boldsymbol{r_{zy}} & \boldsymbol{r_{zz}} \end{bmatrix}, \quad \textbf{[2.25]}$$

where d_x, d_y, and d_z are the displacements along each axis of the AXIS-coordinate frame made by the source centre with respect to the C-arm's 'home' position, described in the AXIS frame. We determine the C-arm's tilt, orbit, and wig-wag rotations (corresponding to rotations about the x-, y-, and z-axes, respectively, shown in Figure 10) by using an Euler angle decomposition matrix from multiplying the three Euler rotation matrices sequentially:

$$[\boldsymbol{R}] = [\boldsymbol{R_x}][\boldsymbol{R_z}][\boldsymbol{R_y}]$$

$$= \begin{bmatrix} \cos\theta_y \cos\theta_z & -\sin\theta_z & \cos\theta_z \sin\theta_y \\ \sin\theta_x \sin\theta_y + \cos\theta_x \cos\theta_y \sin\theta_z & \cos\theta_x \cos\theta_z & -\cos\theta_y \sin\theta_x + \cos\theta_x \sin\theta_y \sin\theta_z \\ -\cos\theta_x \sin\theta_y + \cos\theta_y \sin\theta_x \sin\theta_z & \cos\theta_z \sin\theta_x & \cos\theta_x \cos\theta_y + \sin\theta_x \sin\theta_y \sin\theta_z \end{bmatrix}. \quad \textbf{[2.26]}$$

We then solve for θ_x, θ_y, and θ_z using values from $[T_{ASc,HtoL}]$ as follows:

$$\boldsymbol{\theta_z} = -\arcsin(\boldsymbol{r_{xy}}) \quad \textbf{[2.27]}$$

$$\boldsymbol{\theta_y} = \arctan\left(\frac{r_{xz}}{r_{xx}}\right) \quad \textbf{[2.28]}$$

$$\boldsymbol{\theta_x} = \arctan\left(\frac{r_{zy}}{r_{yy}}\right). \quad \textbf{[2.29]}$$

We can use the values obtained from θ_x, θ_y, and θ_z, as well as d_x, d_y, and d_z in order to verify by visual inspection that they reasonably match the physical situation. Note that we used $[R_x][R_z][R_y]$ as the order of matrix rotations for the Euler angle decomposition matrix because as can be seen from Figure 10 , R_z represents the wig-wag rotation of the C-arm. Since the maximum wig-wag C-arm rotation is 10°

in each direction, it will never attain 90°, which will avoid the problem of singularity, or Gimbal Lock, where the first and third axes of rotation would be parallel and their angles undeterminable.

2.6 NDI Marker Data Acquisition from Matlab

In order to calculate the points of interest using the methods discussed in Section 2.5, the live location of the Optotrak marker triad must be retrieved and input into Matlab. Normally, however, the Optotrak system control unit streams data into its proprietary software (1st Principles, or 6D Architect); there is no simple, well-established method for streaming data directly into Matlab, or between 1st Principles and Matlab, so we needed to develop such a technique.

A group from the University of Lethbridge has devised a method to control an Optotrak Certus system from Matlab, but this method is described for 32-bit platforms (Blinch 2010). We have adapted this method to be used on a 64-bit Windows system so as to retain the capability of accessing the amount of RAM required for the DRR algorithm to run efficiently with large volume sizes. This method makes use of Matlab Executable (MEX) files written in C++ that call Optotrak's C++ Application Program Interface (API). The MEX file was compiled using Microsoft Visual Studio, and the C++ scripts were then written, based on Blinch's work, to access Optotrak's API tools. Matlab can then be used to call the C++ scripts by using the compiled MEX file as a language interface. When using AXIS, a Matlab script must first be used to initiate Optotrak; when a DRR image is to be generated, the script is used to collect the live positional data from the marker triad; and when use of AXIS is complete, the script is used to terminate Optotrak. We posted a detailed step-by-step document describing this process, adapted from Blinch's work, on the Mathworks Community Website (Touchette 2016).

2.7 The Digitally Reconstructed Radiograph (DDR) Algorithm

In order to generate an artificial X-ray image, an incremental ray-casting algorithm is used, which simulates radiographic image formation by modeling the attenuation of X-rays through radiodense materials (Wang 2002). The algorithm we used is based on Siddon's method of calculating the radiological path for a specified ray through a CT array (Siddon 1985). In this algorithm, a simulated ray is cast from *startPt,* the current position of the source as described in Section 2.5, to each pixel on the detector, pointed to by *endPt*. For each ray that is cast, the estimated attenuation is related to the sum:

$$d = \sum_{i,j,k} l(i,j,k)\mu(i,j,k), \quad [2.30]$$

where $\mu(i,j,k)$ is the intersected voxels' gray value (or attenuation coefficient) distribution and is weighted by $l(i,j,k)$, the intersecting length of the path within the voxel (i,j,k) (Han 2000). The resulting gray value, d, is assigned to the associated detector pixel, thus creating the overall DRR image by incrementally moving through each detector pixel (Figure 14). In Matlab, the value of each pixel is calculated by calling the DRR algorithm:

```
DRR_rayTrace(startPt,endPt(:,col),offset,voxDim,voxSize,voxData);
```

where *startPt* and *endPt* are the two parameters that describe the pose of the C-arm, as described in Section 2.5, and the rest of the parameters include the CT volume data and information about its dimensions.

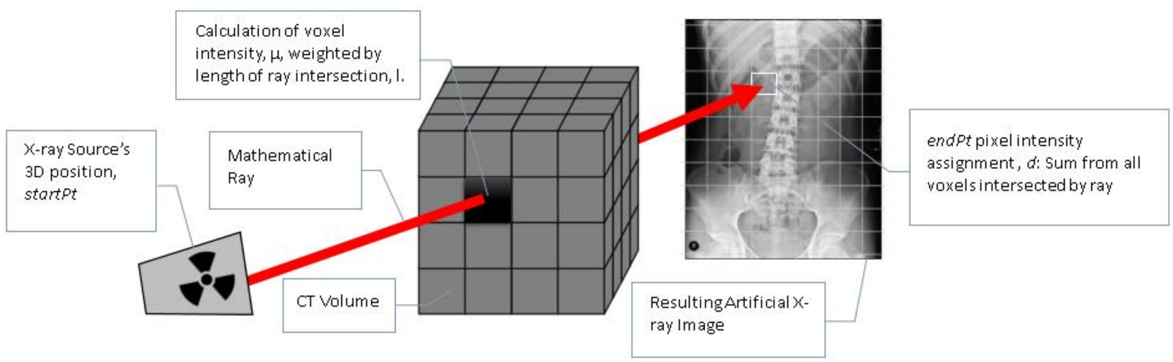

Figure 14: Digital simulation of a 2D X-ray from a CT volume using a ray-casting algorithm

A number of groups have proposed more computationally efficient ray-casting methods that build on Siddon's method, such as Han and Jacobs, who report 3-7.5 times quicker DRR generation times (Han 2000; Jacobs 1996). Other groups have proposed different algorithms altogether such as cylindrical harmonics (Wang 2002) or wobble splatting (Spoert 2007, Birkfellner 2005), which are also claimed to be more efficient, but also to yield more realistic images. However, a DRR script based on Siddon's method from University of California, San Diego, was freely available on GitHub (Folkerts 2012). The script is written in C++ and includes the MEX wrapper to compile the MEX interface file. In the script's original form, DRR images were originally generated within 1-2 seconds. The rate-limiting step in the script was the double-nested loop where *endPt* is established for each pixel index and the rays are calculated for each pixel by calling an external C++ function. In an attempt to speed up this step, we tried implementing three approaches: parallel computing, *gpuArrays*, and serialization. Parallel computing requires too much overhead time when data is transferred between workers to be worth the shortened loop-time trade-off; in this case the DRRs were taking approximately 1-2 seconds longer to be generated. The use of the GPU to carry out a Matlab function using *arrayfun* only supports element-wise operations, which is not what is needed with the DRR function, and it also requires a MEX extension in order for the C++ function to run on the GPU, which is not convenient in our situation since the original MEX wrapper is not written to read and write *gpuArrays*. However, in the serialization approach, *endPt'*s values were set up to be pre-calculated and allocated in a serialized array, allowing the loops to be unnested. Images are now generated in 0.5-0.7 seconds, which is sufficiently fast for the purpose of designing a working system to be evaluated in a user study.

2.8 Artificial X-ray Image Generation

Once all of the necessary inputs for the DRR algorithm are established, and the intensity values are calculated for each pixel on the detector, the following series of image processing techniques are applied to the resulting image in order to improve the image quality and appearance:

- Image sharpening
- Image rotation (90 degrees clockwise) to represent the manikin in a standing position, the way they are normally displayed in the OR
- Image mirroring along its vertical axis to be representative of the fluoroscopic perspective (view from detector rather than from source)
- Contrast enhancement using Contrast-Limited Adaptive Histogram Equalization (CLAHE)
- Image complement to reverse the intensity range for fluoroscopic appearance (i.e. bone tissue appears dark), rather than the radiographic convention (i.e. bone tissue appears light)
- Red region-of-interest overlay: since the C-arm we use has a 9-inch image intensifier tube rather than the 12-inch one that we can simulate, the resulting DRR image appears wider than the real fluoroscopic image. A red circle is superimposed onto the DRR image in order to indicate approximately the area that the real X-ray image will include.

Figure 15 below includes some sample DRR images acquired during the user study, next to the six target X-ray images for reference.

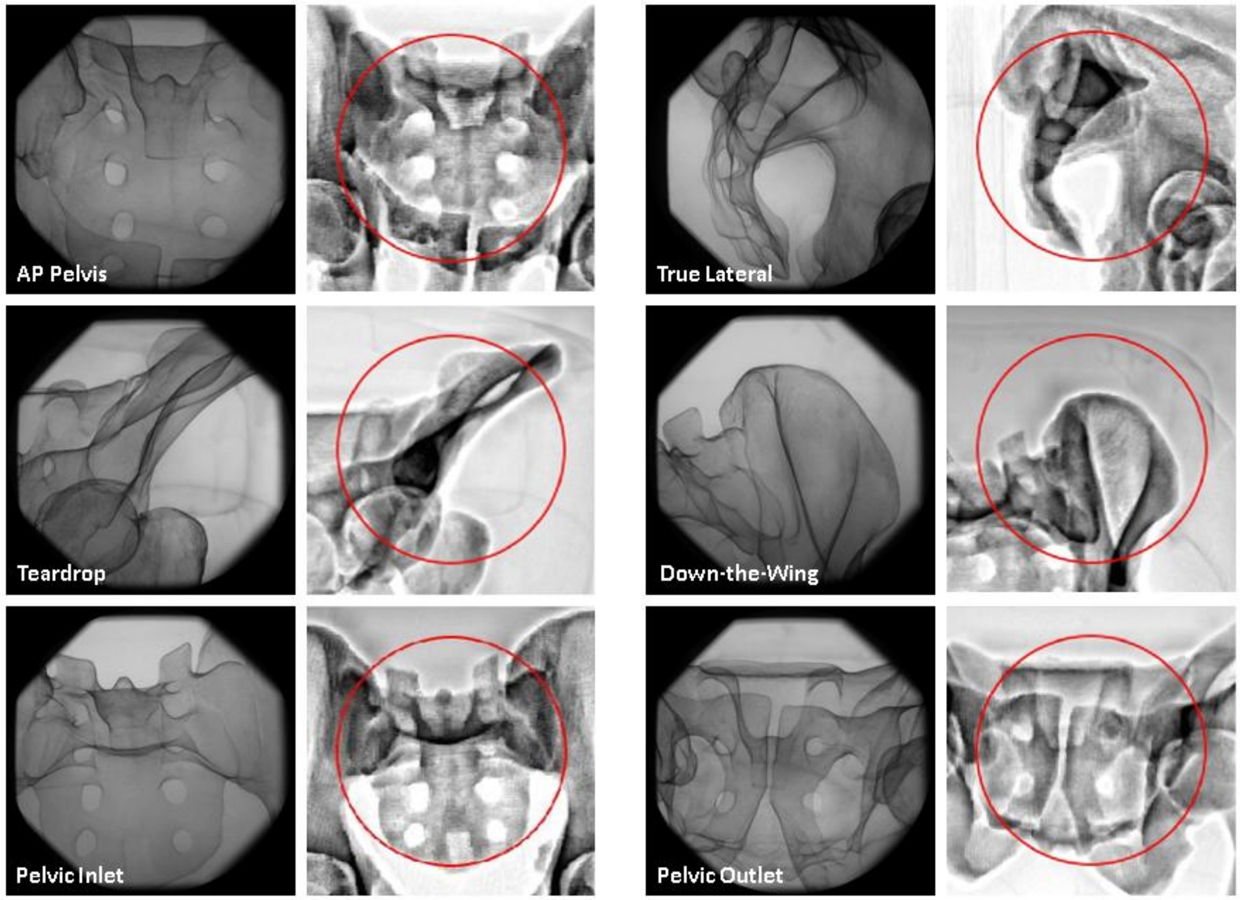

Figure 15: Six sample artificial X-ray images next to the six corresponding target X-ray images for reference

2.9 Graphical User Interface for Study Participants

A graphical user interface (GUI) was designed in Matlab to provide an easy-to-use interface for the study participants and study co-investigators (Figure 16). The GUI is used to display the DRR images, as well as to write the tracked C-arm position data to files, which are collected for study analysis. The GUI allows the user to perform the following tasks:

- Upload the CT volume data and the CT volume info
- Initiate Optotrak for C-arm tracking
- Choose between wide-view DRR images or a standard view DRR images (Figure 16)
- Choose between displaying single DRR images at a time or displaying them in semi-continuous mode (~2 Hz)
- Write the following AXIS data to file (done automatically in DRR generation mode):
    - Marker triad x-, y-, and z-coordinates in Optotrak frame

- C-arm Euler angles with respect to home position
    - C-arm translation magnitude along x-, y-, and z-axes with respect to home position
    - C-arm's current central X-ray beam axis vector (X-ray source midpoint to detector midpoint)
    - Midpoint along C-arm's current central X-ray beam
    - Clock timestamp
- End DRR generation when in semi-continuous mode
- Clear the data files
- Terminate Optotrak to stop C-arm tracking

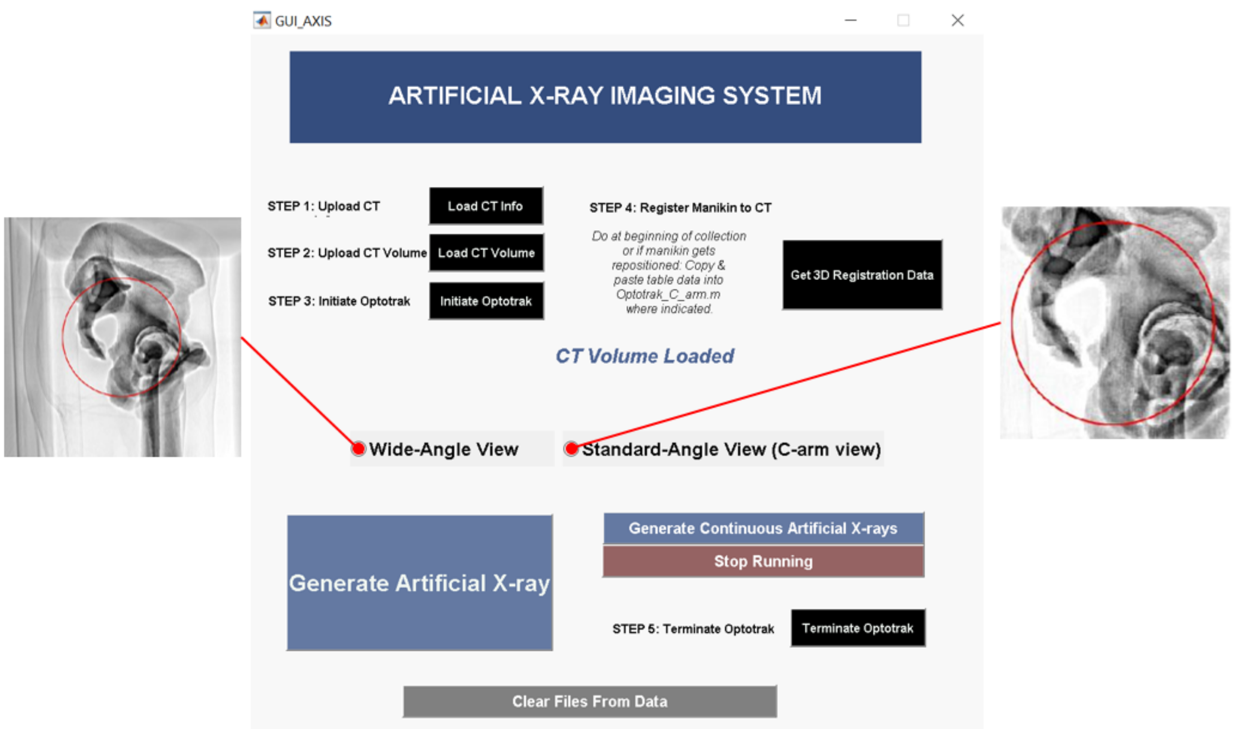

Figure 16: AXIS graphical user interface, with sample DRR images in wide- and standard-angle views

2.10 AXIS Design Summary

To summarize the steps involved with the design of AXIS, we created a 512 x 1413 x 354 voxel volume (480 x 1130 x 332 mm) from a CT scan of a manikin with radiodense bones we acquired. We registered the CT scan to the manikin by visually comparing a datum DRR to a real X-ray image taken from the same C-arm position, a process that we estimate results in an image matching accuracy of ± 1 cm and ±

3 degrees. We used an Optotrak optical tracking system with 0.1 mm accuracy to track the position of the C-arm, and developed a method to stream this data into Matlab. With this data, we calculated the relative positions of the C-arm source and detector, relative to the manikin, to simulate the X-ray beam and reconstruct a 2D artificial X-ray image. Image post-processing techniques were implemented to improve the appearance of the image, and finally the images were displayed on a monitor using a GUI.

Chapter 3

Clinical User Study Methods

In order to assess the utility of AXIS as an intraoperative and educational guidance tool, we conducted a user trial primarily aimed at determining whether the use of artificially generated X-ray images improves C-arm performance during specific orthopaedic surgery imaging tasks in a simulated OR setting. We recruited participants with little or no previous C-arm experience to approximate the experience level of newly graduated MRTs who learn to operate a C-arm for the first time in the OR. We hypothesized that users with comparatively little C-arm experience can perform simulated orthopaedic surgery tasks with fewer radiographic C-arm images, in less time, and with greater accuracy if they are using artificial X-ray images to guide them as compared to using the conventional technique without the guidance of artificial X-ray images. To test this, we measured the number of X-ray images, task time, and image accuracy relative to a pre-defined target specified by an expert surgeon when the participants carried out a set of simulated surgically-inspired imaging tasks as described below.

3.1 User Study Design Overview

After receiving ethics approval from the University of British Columbia's (UBC) Clinical Research Ethics Board and the British Columbia Institute of Technology's (BCIT) Research Ethics Board, we recruited 30 participants with varying levels of radiography experience, but most of whom had no previous experience with radiography (Table 2). We contacted students who were either currently enrolled in BCIT's Medical Radiography program or who had graduated within a year of the study. We also invited participants from the general public, most of whom were students at UBC in health-related programs, such as Biomedical Engineering, Kinesiology and Health Science, and Biological and Medicinal Chemistry. We chose to recruit participants with little or no C-arm experience rather than trained radiographers so that the effect of AXIS guidance on C-arm performance could be assessed at this early stage of professional development.

Table 2: Participants' level of C-arm experience prior to study

Level of experience	Frequency
No hands-on experience	18
Manoeuvred a C-arm, without taking X-rays	3
Taken X-rays with a C-arm under supervision / during rotations	8
Professional work experience with C-arm	1

When the participants agreed to join the study, they signed a consent form and each one of them was assigned a study participant number at the time of enrolment in order to anonymize their data. The study was carried out using the mobile C-arm in the Biomedical Engineering Laboratory and Computer-Assisted-Surgery Suite (the BioEng Lab) of the Centre for Hip Health and Mobility (CHHM). The study lasted approximately an hour and a half per participant and consisted of the following series of steps for all participants:

- An introduction session ("INTRO"),
- Control evaluation tasks (without AXIS guidance) ("CTRL"),
- Evaluation tasks with AXIS guidance ("AXIS"),
- A questionnaire ("QNR").

The aim of this series of tasks was to evaluate C-arm positioning performance with and without the use of AXIS when acquiring target radiographic X-ray images with the C-arm.

3.2 C-arm Positioning Task Sets

We asked each participant to perform a total of six C-arm positioning tasks, which were divided into two sets (Set 1 and Set 2) based on imaging difficulty level. The tasks were described in a "casebook" we provided to the participants at the beginning of the study, which included six target images (three per set), as well as additional guidance information described in more detail in Section 3.5. Both sets consisted of one easy, one medium, and one difficult target image of the pelvis (Figure 17). The difficulty levels of the images were established by two faculty members and classroom instructors from the Medical Radiography Technology program at BCIT, who have a good sense of which imaging views new C-arm users tend to find more difficult. An experienced orthopaedic trauma surgeon at Vancouver General Hospital, who we refer to as Surgeon-A in this thesis for anonymity, also reviewed the difficulty levels we assigned to each image and agreed with these classifications based on his experience with MRTs of varying experience levels. The purpose of using two different tasks at each difficulty level was to allow us to have each participant perform one task of each difficulty level both with and without AXIS guidance; if we had asked participants to repeat the same task with and without guidance, they may have been able to simply remember the correct position from the first attempt, which could confound our results. Surgeon-A acquired the target radiographs using the C-arm and manikin in BioEng Lab. The X-ray views he acquired are what he considers optimal views in his daily practice and are based on the standard views in image-guided pelvic trauma procedures (Bates 2011). Both the position of the C-arm with respect to the manikin and the C-arm's radiographs were stored for use as target C-arm poses and images during the study. After the study, we asked Surgeon-A to repeat the image acquisition for the same views to assess repeatability, and we also asked a second trauma surgeon from VGH, who we refer to as Surgeon-B in this thesis, to independently produce the pelvic images for inter-expert analysis, discussed further in Section 3.11.

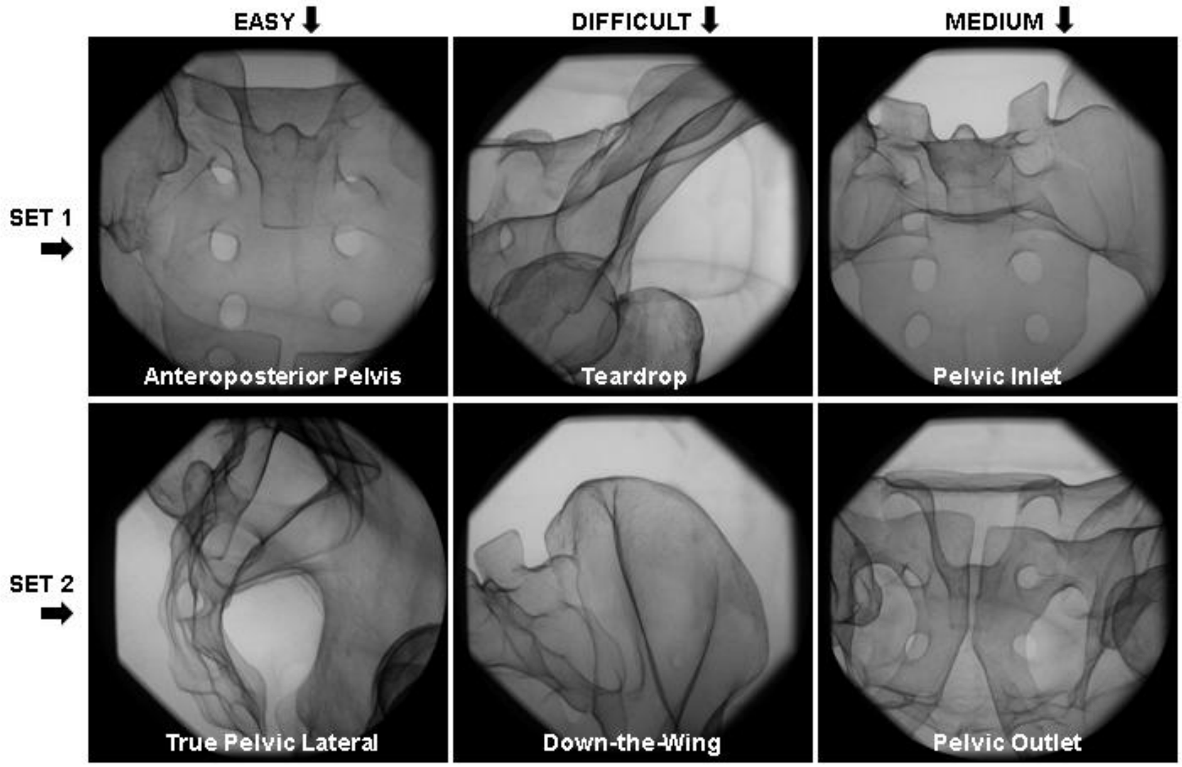

Figure 17: Imaging task sets and assigned difficulty level for each task, in order of implementation during the user study

3.3 Randomization of Evaluations and Task Sets

When the participants enrolled in the study, we randomized them into one of the two evaluations (CTRL or AXIS), as well as one of the two task sets (Set 1 or Set 2) in order to establish which evaluation they performed first and with which task set. Randomizing the order of evaluations for this crossover design allowed for us to control for improvements in the participants' performance that are based on repeating the evaluation rather than being primarily an effect of the AXIS surgical tool. Although we organized each task set to include one easy, one medium, and one difficult target pelvic image in the same order of difficulty as depicted in Figure 17, it is still possible for one set to be inherently more challenging than the other, hence why we randomized the ordering of the task sets. Incidentally, we ordered the imaging tasks within each set to be easy first, difficult second, and medium third, rather than in increasing level of difficulty, in case we ran out of time allotted for the evaluation session and needed to stop after two tasks instead of the three; this way we would still have evaluated the participant on one easy and one difficult task, at least providing results for both extremes. In randomizing the orders of both the evaluations and the task sets, four combinations of experimental treatments were possible:

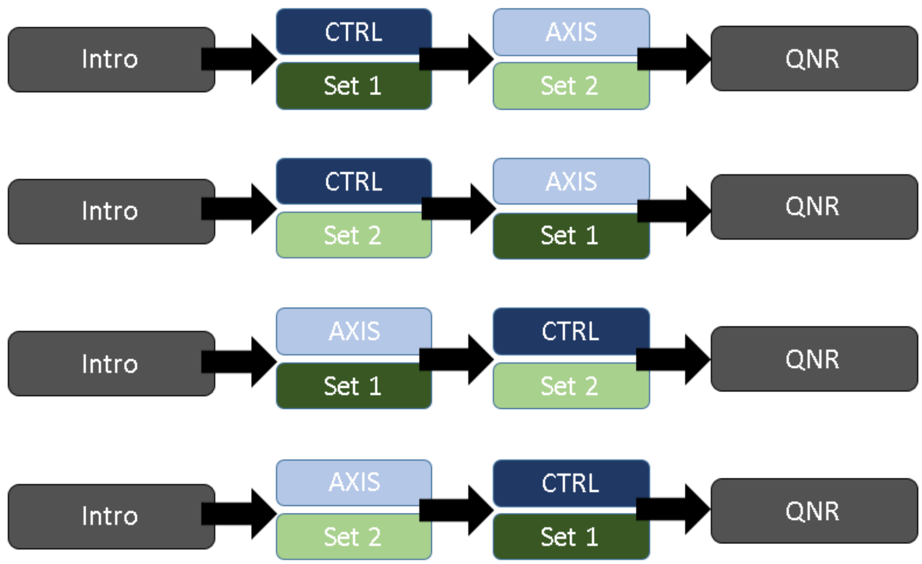

Figure 18: Randomization of evaluations and task sets: four possible combinations of experimental treatments

3.4 Introduction Session

Before beginning the study, the study investigator gave the participants a 10-15 minute information session about the activities that would be required of them for the study, as well as basic C-arm fluoroscopy use, techniques, and safety precautions. Specifically, the goals for the study tasks were explained in detail, including the six target images, what we would be measuring, and the participant material "casebook" they could refer to (described in Section 3.5). The C-arm's basic operation guidelines were also described so they could manoeuvre the C-arm and acquire X-ray images safely, even if they had not previously used a C-arm. Optotrak's line-of-sight constraint was explained to them, so they could position themselves so as to avoid interfering with its measurements, and they were also asked not to move the manikin or Optotrak markers on the C-arm since they were registered and calibrated once at the beginning of the session. During this session, they were also provided with a lead apron to be worn for the duration of the study, in addition to the requirement of standing behind the lead shields placed at least three meters away from the C-arm during the acquisition of X-ray images. During this session, the participants were able to ask questions, as well as practice manoeuvring the C-arm if they wished.

3.5 Participant Reference Casebook

Throughout the study tasks, the participants had access to a reference "casebook" binder that included copies of the target radiographs for both task sets, as well as reference information for each image to help guide them through the task (Figure 19). They were allowed to bring the binder with them and refer to it as much as they needed. The following information was provided for each imaging task:

- One clean copy of the target X-ray image
- One copy of the target X-ray image with notes highlighting the main features or anatomical landmarks that should be included
- A brief summary including the C-arm's approximate position and orientation with respect to the patient, a description of the most important features to include, some additional notes specific to each view, and in some cases, the clinical application
- Two images that demonstrate the approximate position of the C-arm with respect to the patient; one image is viewed sagittally and one viewed transversely, in order to better visualize the orbital and tilt rotations of the C-arm
- An image of a pelvic model, in the target image's perspective orientation, as seen from the detector's point of view, including a red circle overlaid on top of the image to indicate the approximate field of view

The reference information included in the binder was gathered from *The Percutaneous Treatment of Pelvic and Acetabular Fractures* (Bates 2011) as well as from Surgeon-A, and is included in detail (identical to that used during the study) in Appendix A.

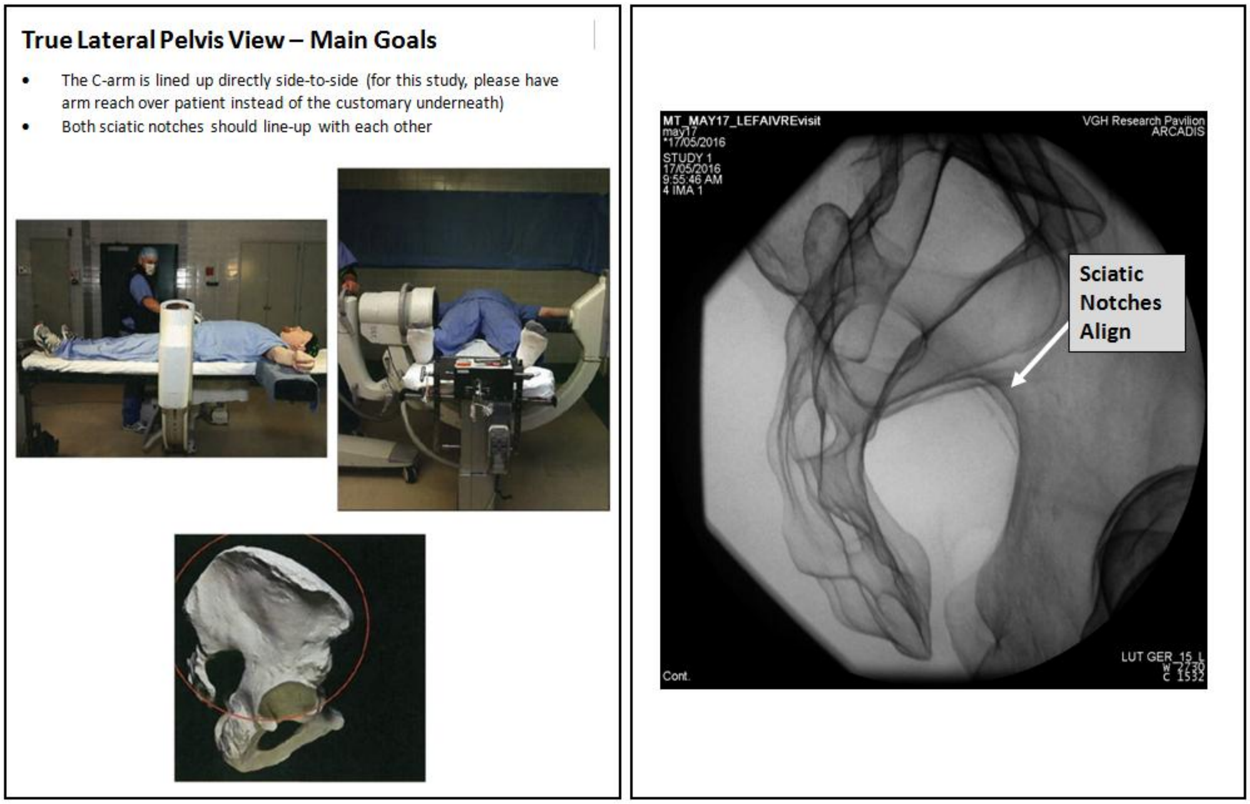

Figure 19: Sample imaging task found in user study casebook (a 'clean' X-ray of the view is provided on the third page but is not shown here)(three left-images, © Bates 2011, with permission)

3.6 Control Evaluation Exercise

During the control evaluation, the participants were asked to acquire X-ray images that replicated as closely as possible each of the three target images shown in the casebook. For each image, they were allowed to acquire as many real X-rays and take as much time as they wanted to until they were satisfied with their result; the investigator did not provide any suggestions or recommendations as to when the image was sufficiently accurate. If the participant was noticeably struggling after having attempted several X-ray images, or expressed that they were having difficulties, we provided some hints about how to better achieve the X-ray image. For example, if the C-arm was rotated in an inappropriate direction, this was pointed out. The participants were the ones to choose when to submit their radiograph. We recorded all forms of help and input during data collection.

While the evaluation exercise did not involve the use of AXIS for guidance, the software was still being run in the background during each of the control tasks so that the position of the C-arm could still be tracked, collected, and written to data files. However, the computer monitor that is used to display the AXIS GUI and artificial X-rays was turned off during this evaluation.

3.7 AXIS Evaluation Exercise

The AXIS evaluation exercise was identical to the control evaluation exercise, except that the participants were shown the set of target X-ray images they had not yet worked with, and the computer monitor used to display the AXIS GUI and artificial X-rays was turned on for this portion. The participants were able to view the artificial X-ray images that simulated what a real X-ray would look like at the current C-arm position. They were still required to acquire and submit real X-ray images to complete each task, and could still take as many real X-rays and as much time as needed to do so. The artificial X-rays were generated automatically during C-arm repositioning at a rate of approximately 2Hz.

3.8 Collection and evaluation metrics

For each radiographic task performed, we recorded the number of real X-ray images acquired, noted the X-ray image the participant chose to submit, and saved the image files. We timed the participants from when they began an imaging task until they had submitted the image they deemed to satisfactorily match the target image. Throughout each task, the C-arm's position was tracked and a file was written, which included the following information for each generated DRR:

- The x-, y-, and z-coordinates for the three markers instrumented on the C-arm, in the Optotrak global coordinate frame
- The C-arm's relative rotation, in degrees, about the three AXIS coordinate frame axes, with respect to the C-arm's home position
- The C-arm source's relative translation, in mm, in the three AXIS coordinate frame axes, with respect to the C-arm's home position
- The C-arm's central beam axis vector – a vector pointing from the C-arm's source to the image detector's centre point
- The C-arm's axis midpoint – the midpoint of the C-arm's central beam axis vector
- The timestamp for which the DRR was generated

At the end of the study, the participants were given a questionnaire to fill out, which included questions regarding their basic demographic information, their level of experience with radiography prior to the study, their confidence levels with and without AXIS, their impressions of AXIS in terms of usefulness, image realism, and accuracy, as well as what they liked and areas for improvement. The participants were not required to answer any questions they did not wish to. The survey questions can be found in Appendix B. Additionally, we recorded whether the participant required hints during any of the tasks.

3.9 Image Accuracy Metrics: Lateral Distance and Angular Difference Calculations

In order to assess how accurate the participants' X-ray images were, the C-arm's tracked position throughout the task was compared to the target C-arm position for the target image in question, which had been collected when Surgeon-A acquired the target radiographs. Specifically, the central beam axis running from the C-arm's source to the image detector's midpoint was used to define the C-arm's pose and location in space for each position. The two image accuracy metrics used to compare the C-arm's axis throughout the task to the target axis are lateral distance and angular difference. The lateral distance describes how laterally far apart the current C-arm axis's midpoint is from that of the target position, and the angular difference describes the angle between them. Figure 20 illustrates these accuracy metrics and the equations to calculate them are shown below.

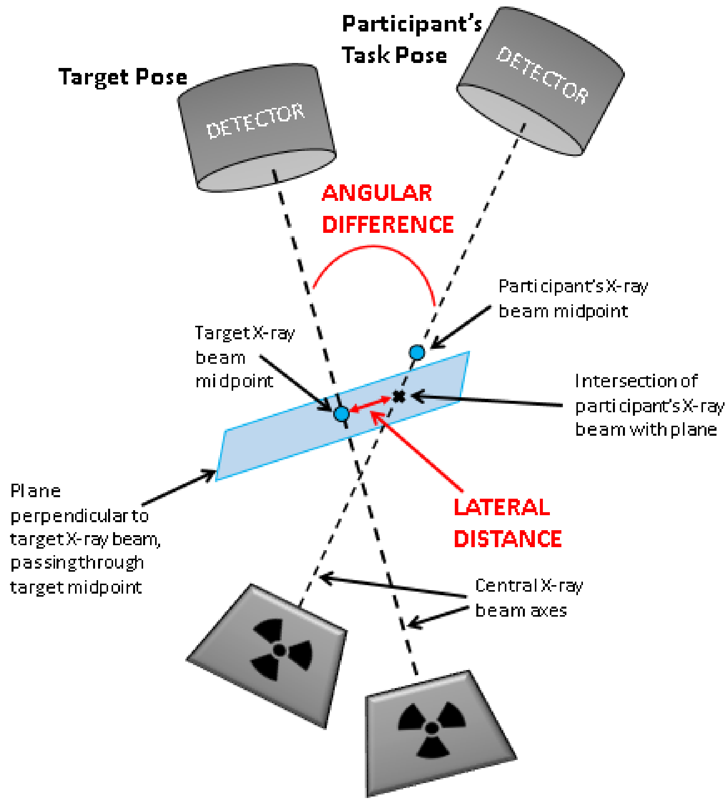

Figure 20: The two accuracy metrics used to compare the participant's C-arm pose to the target pose are lateral distance and angular difference

3.9.1 Calculating the lateral distance between the user and target C-arm poses

The general equation of a plane is:

$$(\vec{p} - \vec{p_0}) \cdot \vec{n} = 0, \qquad \textbf{[3.1]}$$

for $\vec{p} = [x, y, z]$, $\vec{p_0}$ a point on the plane, and $\vec{n}$, a vector than is normal to the plane.

The general equation of a line is:

$$\vec{p} = d \cdot \vec{l} + \vec{l_0} \text{ , for } d \in \mathbb{R}, \qquad \textbf{[3.2]}$$

for d, the magnitude of the line, $\vec{l}$ a vector in the direction of the line, and $\vec{l_0}$ a point on the line.

To find d, we sub **[3.2]** into **[3.1]** as follows:

$$\left(d \cdot \vec{l} + \vec{l_0} - \vec{p_0}\right) \cdot \vec{n} = 0 \qquad \textbf{[3.3]}$$

$$d\vec{l} \cdot \vec{n} + \left(\vec{l_0} - \vec{p_0}\right) \cdot \vec{n} = 0 \qquad \textbf{[3.4]}$$

$$\boldsymbol{d} = \frac{(\overrightarrow{\boldsymbol{p_0}} - \overrightarrow{\boldsymbol{l_0}}) \cdot \vec{\boldsymbol{n}}}{\vec{\boldsymbol{l}} \cdot \vec{\boldsymbol{n}}}. \quad \textbf{[3.5]}$$

The point of intersection between the line and plane is:

$$\overrightarrow{\boldsymbol{p_i}} = \boldsymbol{d}\vec{\boldsymbol{l}} + \overrightarrow{\boldsymbol{l_0}}. \quad \textbf{[3.6]}$$

In our case, if we set the midpoint of the target beam, $\overrightarrow{M_{targ}}$, to be $\overrightarrow{p_0}$, the target central X-ray beam axis, $\overrightarrow{B_{targ}}$to be $\vec{n}$, the user's central X-ray beam axis, $\overrightarrow{B_{user}}$, to be $\vec{l}$, and the midpoint of the user beam, $\overrightarrow{M_{user}}$, to be $\overrightarrow{l_0}$, we get:

$$\boldsymbol{d} = \frac{(\overrightarrow{\boldsymbol{M_{targ}}} - \overrightarrow{\boldsymbol{M_{user}}}) \cdot \overrightarrow{\boldsymbol{B_{targ}}}}{\overrightarrow{\boldsymbol{B_{user}}} \cdot \overrightarrow{\boldsymbol{B_{targ}}}}, \quad \textbf{[3.7]}$$

and therefore,

$$\overrightarrow{\boldsymbol{p_i}} = \left(\frac{(\overrightarrow{\boldsymbol{M_{targ}}} - \overrightarrow{\boldsymbol{M_{user}}}) \cdot \overrightarrow{\boldsymbol{B_{targ}}}}{\overrightarrow{\boldsymbol{B_{user}}} \cdot \overrightarrow{\boldsymbol{B_{targ}}}}\right) \overrightarrow{\boldsymbol{B_{user}}} + \overrightarrow{\boldsymbol{M_{user}}}. \quad \textbf{[3.8]}$$

The lateral distance is thus calculated:

$$\boldsymbol{D_L} = \sqrt{(\boldsymbol{p_{i,x}} - \boldsymbol{M_{targ,x}})^2 + (\boldsymbol{p_{i,y}} - \boldsymbol{M_{targ,y}})^2 + (\boldsymbol{p_{i,z}} - \boldsymbol{M_{targ,z}})^2}. \quad \textbf{[3.9]}$$

3.9.2 Calculating the angular difference between the user and target C-arm poses

To find the angle between two vectors we use the general equation:

$$\cos \boldsymbol{\theta} = \frac{(\vec{\boldsymbol{u}} \cdot \vec{\boldsymbol{v}})}{(\|\vec{\boldsymbol{u}}\| \cdot \|\vec{\boldsymbol{v}}\|)}. \quad \textbf{[3.10]}$$

In our case, to calculate the angular difference, θ_d, we use the two vectors of interest, $\overrightarrow{B_{user}}$ and $\overrightarrow{B_{targ}}$:

$$\boldsymbol{\theta_d} = \frac{(\overrightarrow{\boldsymbol{B_{user}}} \cdot \overrightarrow{\boldsymbol{B_{targ}}})}{(\|\overrightarrow{\boldsymbol{B_{user}}}\| \cdot \|\overrightarrow{\boldsymbol{B_{targ}}}\|)}. \quad \textbf{[3.11]}$$

3.10 Most Accurate Images, "X-rays-to-Best-Image", and "Time-to-Best-Image"

Throughout the user study imaging tasks, it was common that a participant would manoeuvre the C-arm into a position that was close to the target, but then continue with the task, possibly in an attempt to get the C-arm even closer to the target or because they were not aware of how acceptably close they were in the first place, or they wished to explore the surrounding anatomy. It was common that the participant's final image submission was less accurate than some of their previous images for the same task. In any case, the C-arm's pose when it was closest to the target pose was recorded for each task, referred to as the C-arm's *Best Image* (most accurate pose). The DRR timestamps collected by AXIS were used in order to calculate secondary X-ray and time metrics: the number of X-rays and the time taken to achieve the most accurate image throughout the task, referred to as *X-rays-to-Best-Image* and *Time-to-Best-Image*, respectively. These are indicators of how many X-rays and how long it actually takes a user to achieve their most accurate image and are perhaps more relevant indicators of their performance since in a training or intraoperative scenario, either the system or the surgeon could indicate that the level of accuracy was acceptable. To illustrate these secondary evaluation metrics, we plotted the C-arm accuracy traces against task time, along with the time at which real X-rays were acquired and the time at which the best accuracy was achieved. A sample of these plots is presented in Section 4.4.

3.11 Expert Target Tests

In order to provide a baseline regarding the acceptability of image accuracies resulting from the participants' imaging tasks, two experts were invited to perform the control evaluation task (without AXIS guidance) for all six target images. Surgeon-A, who had acquired the target X-ray images for the study, performed the tasks to provide information on repeatability; if an expert attempts to replicate their own acquired images and achieves a certain accuracy, then the participants with varying levels of radiography and OR experience should not be expected to achieve a better accuracy. Surgeon-B performed the control tasks on Surgeon-A's target images; her image accuracies provided context regarding how closely another expert can replicate the target images, helping us gauge the significance of residual deviations produced by the subjects.

During the expert target tests, both surgeons chose to perform the imaging tasks by acquiring the X-rays with the foot pedal near the surgical table rather than having to walk behind the lead shields, in order to better simulate how they perform these tasks in the OR. The time required to perform each imaging task would therefore be shorter and comparing these results to those of the participants, who had to walk behind the lead shields each time, would be unfair. We therefore calculated a corrected task time by estimating the time required to walk behind the lead shields when acquiring an X-ray based on observations of the thirty participants who had participated in the study. The corrected task times were therefore calculated by adding 10 seconds per X-ray acquired; this allows us to make more realistic comparisons between the surgeons and participants.

3.12 Statistical analysis: Means, Hypothesis Testing, and Paired t-Tests

After completion of the study, each participant's three imaging task results were averaged for the control and AXIS evaluations for the ten following evaluation metrics:

- Number of X-rays required
- Time required per task
- Lateral distance for their submitted X-ray
- Angular difference for their submitted X-ray
- Lateral distance for their best X-ray
- Angular difference for their best X-ray
- Time to best distance
- Time to best angle
- X-rays to best distance
- X-rays to best angle

In order to assess whether the averages for the control and AXIS evaluations were statistically different, hypothesis testing on the difference in means was performed between the AXIS and non-AXIS evaluations. Additionally, paired t-tests were performed in order to account for differences within each individual participant. The difference in means between the control and AXIS evaluation exercises were therefore calculated for each individual and averaged for t-testing.

Although the order in which each participant performed the control and AXIS evaluations was randomized, we were interested in finding out whether there were any significant differences between the participants who performed the control tasks first and those who performed the AXIS tasks first. We therefore performed hypothesis tests on the difference in means for each participant based on which evaluation they performed first, for the same above-listed ten evaluation metrics. For all of the statistical tests we used a significance level of $\alpha=0.05$ and considered the sample distributions to be normal according to the Central Limit Theorem, whereby sufficiently large samples tend to be normally distributed, and moreover, the means of random samples of any distribution tend themselves to be normally distributed.

In testing ten hypotheses on the same data set, we increase their susceptibility to the multiple comparisons problem, or finding significant results by chance. The multiple comparisons problem is characterized by the family-wise error rate (FWER), which is the probability of making one or more type I errors when performing multiple hypothesis tests. The FWER is calculated as:

$$\bar{\boldsymbol{\alpha}} = \mathbf{1} - (\mathbf{1} - \boldsymbol{\alpha})^{\boldsymbol{m}}, \qquad \textbf{[3.12]}$$

where α is the significance level used in the statistical test, and m is the number of hypothesis tests for the sample. In our case, for α=0.05 and m=10, the probability of making at least one type I error is 40%. To control the FWER at a level of α=0.05, we apply the Holm-Bonferroni correction method, which is valid for both dependent and independent samples, and is more powerful than the Bonferroni correction (one of the most commonly used approaches). We begin by sorting the P-values obtained from the hypothesis tests in ascending order and comparing them to the corrected P-values, $P_{c,}$ which are calculated as:

$$\boldsymbol{P_c} = \frac{\boldsymbol{\alpha}}{\boldsymbol{m}+\mathbf{1}-\boldsymbol{k}}, \qquad \textbf{[3.13]}$$

where k is the index of the hypothesis test P-value, P_k, being corrected. While the Holm-Bonferroni method does control the FWER by decreasing the probability of making type I errors, it does increase the probability of making type II errors. As such, due to the pilot nature of this study, we still consider the near-significant results to help determine the most important parameters for future considerations in the development of AXIS.

Finally, in order to determine whether participant C-arm experience level had any effect on their performance, one-way ANOVA tests were performed on four experience levels (from none to high) for the number of X-rays, time, submitted lateral distance, and submitted angular difference. ANOVA tests were not performed for the secondary evaluation metrics because tracking data is unavailable for the first six participants (explained in more detail later in Section 4.3.), which make up most of the “highly-experienced” cohort. Post hoc tests were then performed, in order to determine which of the experience level groups had the significantly different means, when applicable. For this we used the Tukey post hoc test because it compares each mean to every other mean, rather than to just a control.

Chapter 4

User Study Results

In order to evaluate AXIS on its potential to reduce the radiation exposure and time required to complete an imaging task, as well as to increase the accuracy of the radiographic images, a user study was conducted with 30 participants, most of whom had little or no experience in radiography. A cross-over design was used to evaluate the participants on their ability to replicate target X-ray images with and without AXIS guidance by measuring the number of X-ray images and time required to achieve each radiographic task. Additionally, the position of the C-arm was compared to the target position for each imaging task in order to evaluate each participant's imaging accuracy.

The section that follows includes a summary graph that provides the overall results for each evaluation metric obtained during the control tasks (without AXIS), the AXIS tasks, and those obtained by two experts – orthopaedic surgeons. Then, in the following sections, results from the study are presented in more detail.

4.1 Results Overview

Figure 21 provides a visual summary of the user study results for the participants performing tasks with and without AXIS, compared to the experts' average performance. Raw data graphs and detailed values, including the means, standard deviations, and statistical results, are shown in the subsequent sections.

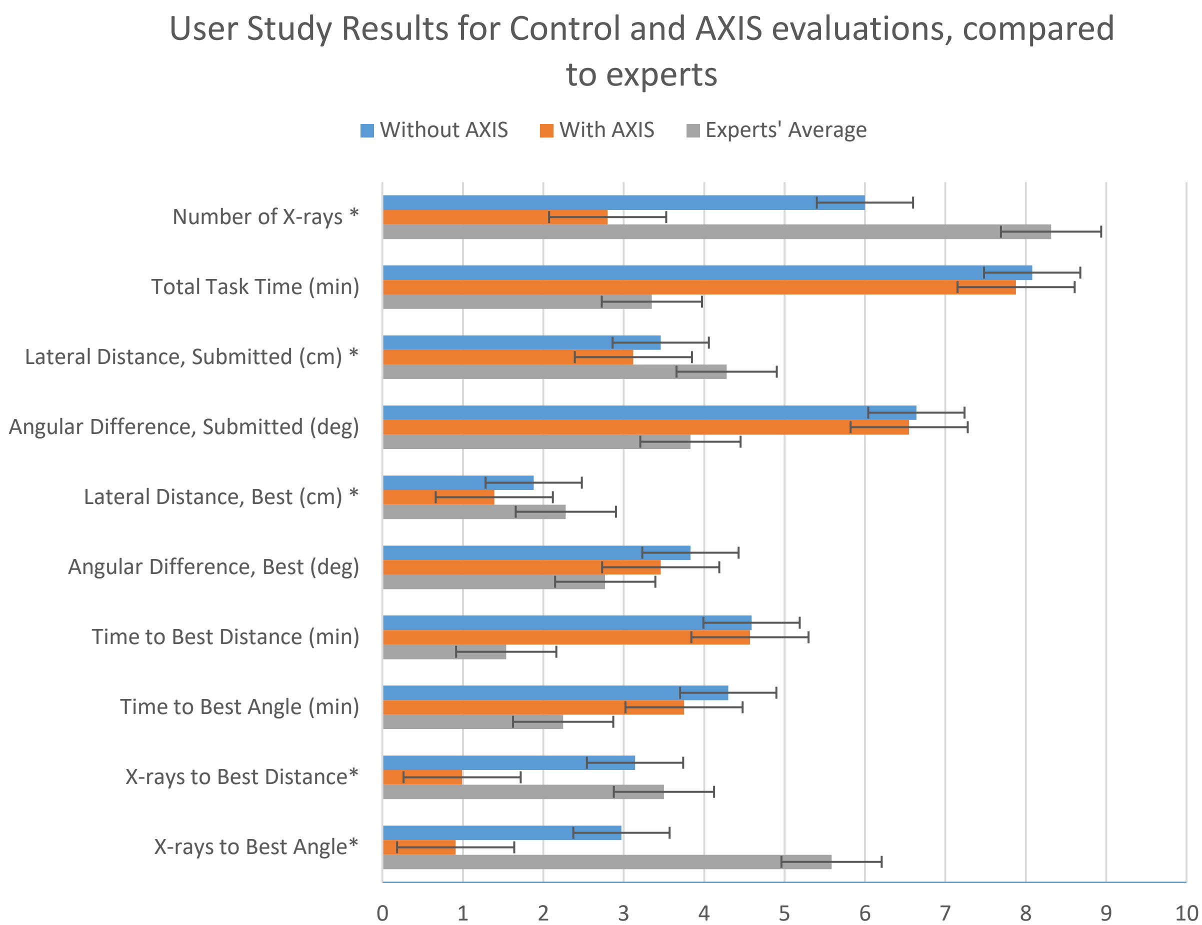

Figure 21: Overview of user study results for control and AXIS imaging tasks, compared to experts, with standard error bars (*statistically significant results excluding experts, after Holm-Bonferroni multiple comparison correction)

4.2 Number of X-rays and Task Time

For each of the imaging tasks carried out by the participants, we recorded the number of X-rays and time required per task, then plotted the results in raw data form for all six tasks per participant in Figure 22 and Figure 23 on the left, as well as in cumulative distribution function (CDF) plots on the right. The plots show that the participants took fewer X-rays overall when guided by AXIS; however we see no obvious trends from the task time data. Note that we applied a jitter function to the results in the raw data plots in this section as well as the following sections in order to separate them slightly along the x-axis for clarity. The results from statistical tests on these samples are presented in Section 4.6.

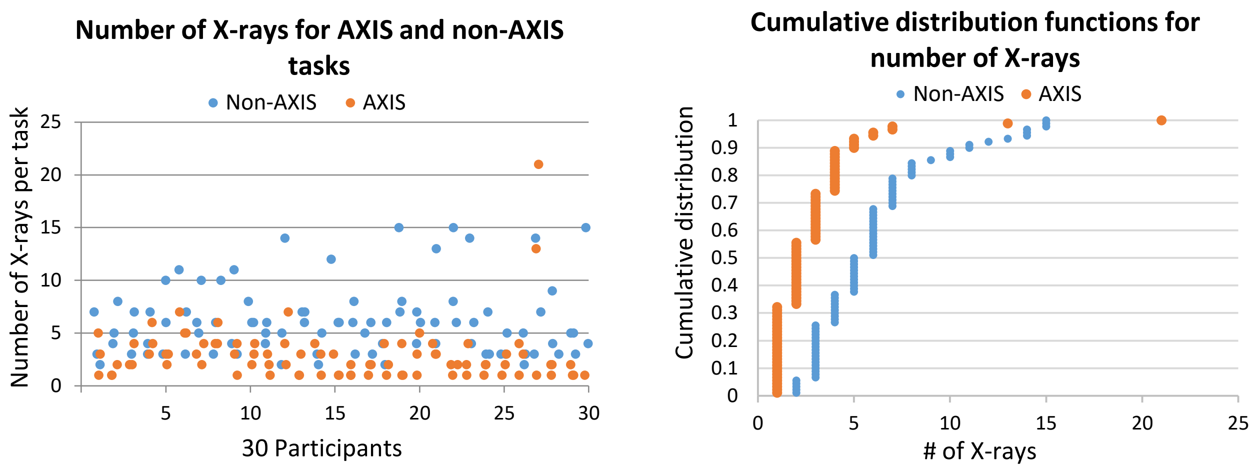

Figure 22: Number of X-rays acquired by participants for AXIS and non-AXIS tasks (left) and corresponding CDF plot (right)

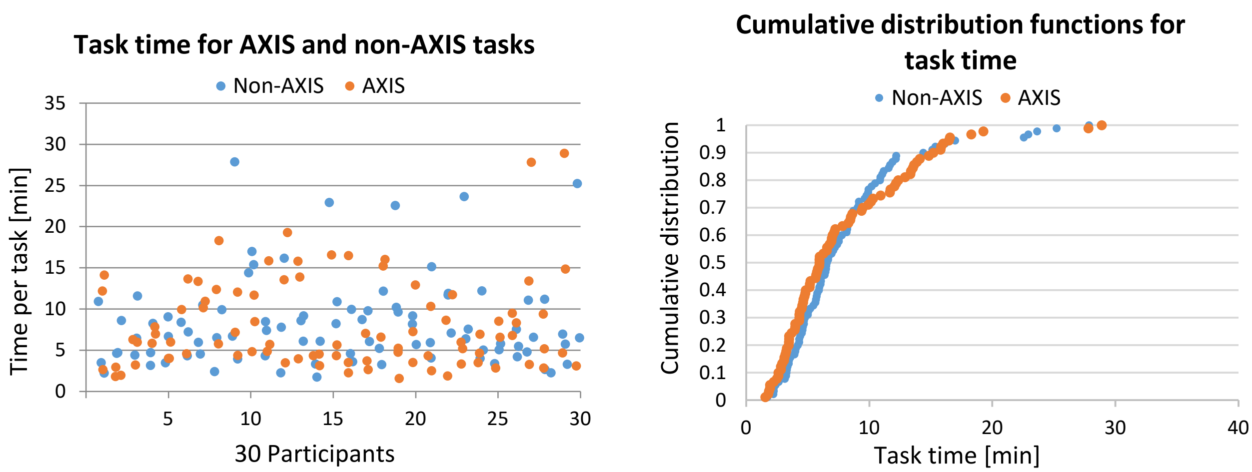

Figure 23: Time required by participants for AXIS and non-AXIS tasks (left) and corresponding CDF plot (right)

4.3 Accuracy Evaluation Metrics

In order to assess the accuracy of the images, we tracked the C-arm's pose in space and compared it to the target C-arm pose for the target X-ray image in question. The two accuracy metrics used to determine how close the C-arm pose was to the target pose were the lateral distances and angular differences, as we described in Section 3.9. We recorded these two accuracy metrics for each participant's final X-ray image submission, as well as for the C-arm position that was the closest to the target throughout each imaging task (*best image)*, whether the participant knew it or not. These results are presented in raw data plots for all six tasks per participant in Figure 24 through Figure 27 on the left, as well as in CDF plots on the right. Note that for the best-image plots, non-AXIS data is unavailable for the first six participants for reasons we discuss in the following section. The CDF plot in Figure 26 shows that the participants achieved better lateral accuracies in their 'best images' when they were guided by AXIS. We observe no other obvious trends from these plots; however we present the results from the statistical analyses in Section 4.6.

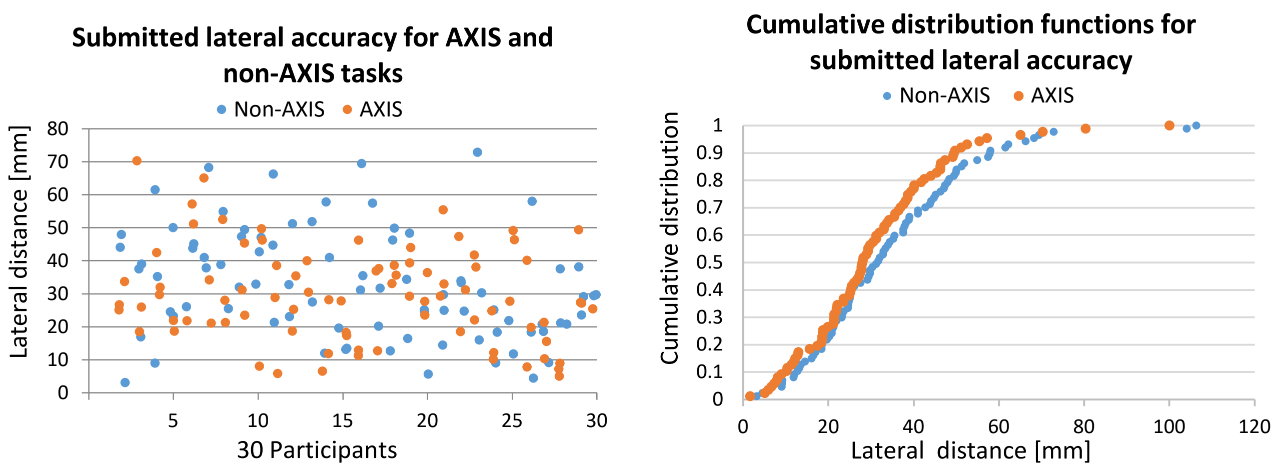

Figure 24: Submitted lateral distances obtained by participants at the end of AXIS and non-AXIS imaging tasks (left) and corresponding CDF plot (right)

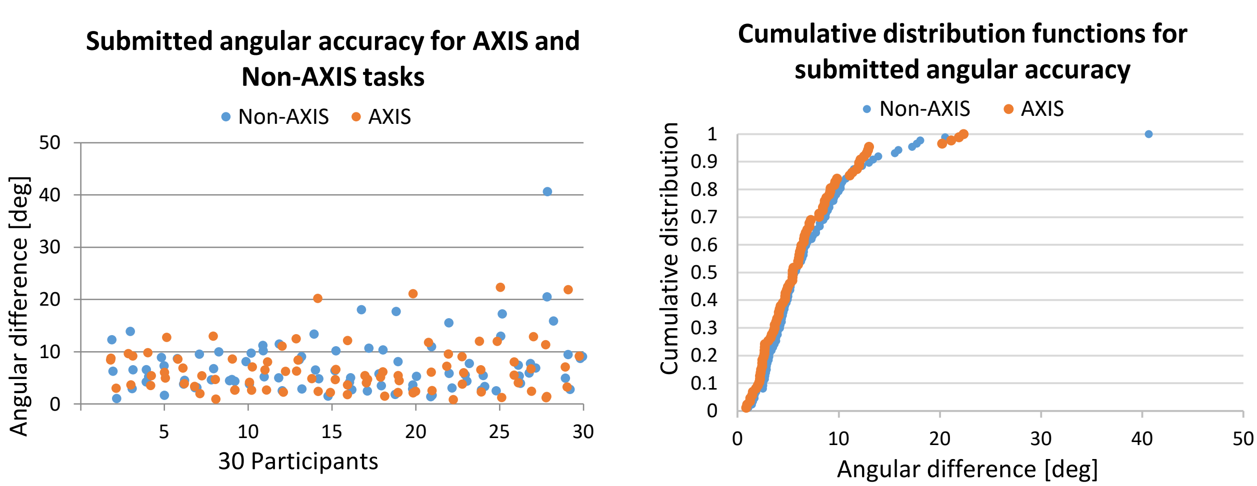

Figure 25: Submitted angular differences obtained by participants at the end of AXIS and non-AXIS imaging tasks (left) and corresponding CDF plot (right)

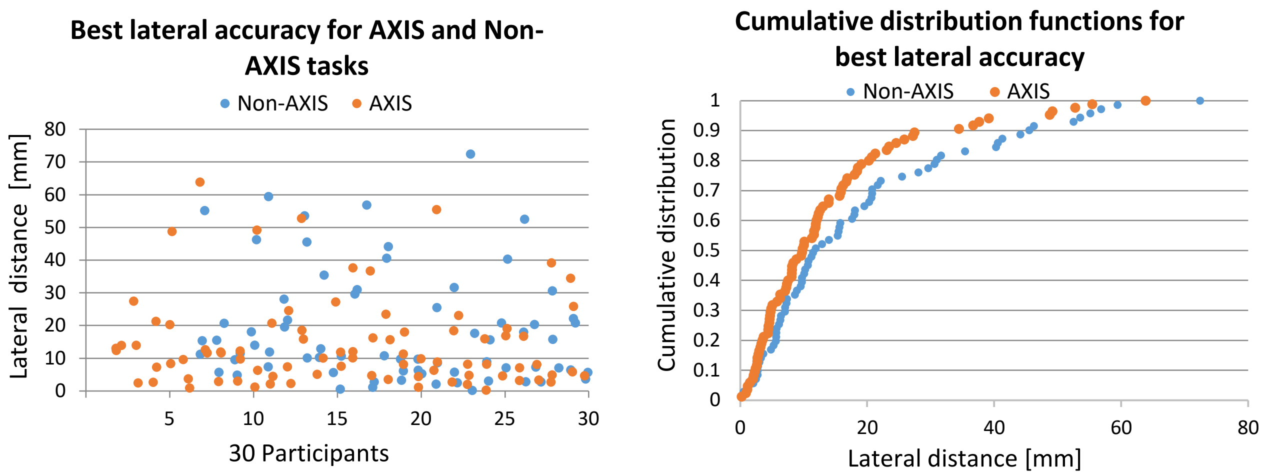

Figure 26: Best lateral distances obtained by participants during AXIS and non-AXIS imaging tasks (left) and corresponding CDF plot (right)

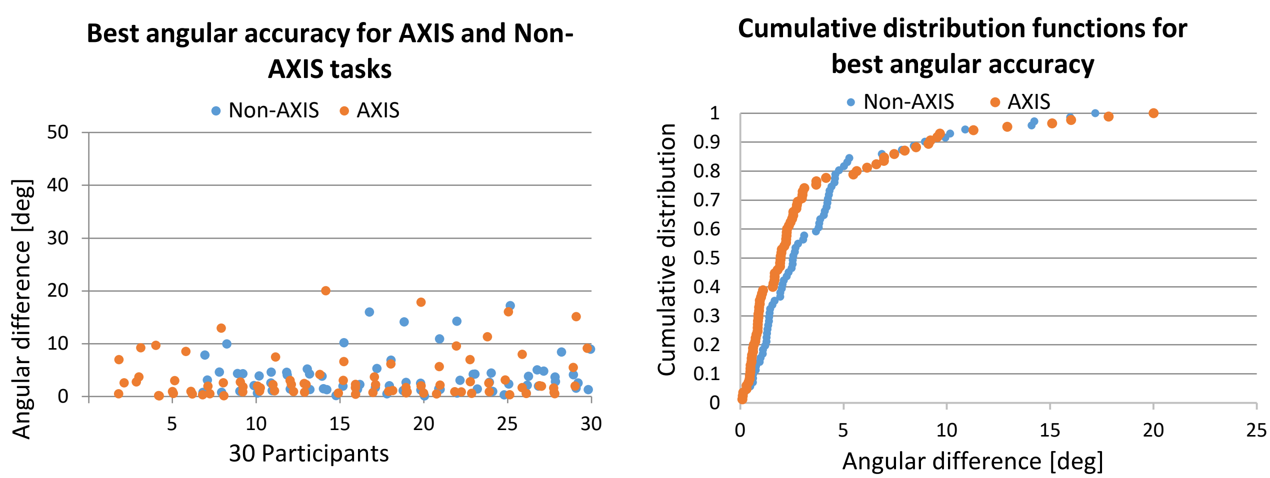

Figure 27: Best angular differences obtained by participants for AXIS and non-AXIS imaging tasks (left) and corresponding CDF plot (right)

4.4 Progression of Accuracy Throughout the Imaging Tasks

In Section 3.10, we discussed a common occurrence that we observed throughout the user study: during imaging tasks the participants would position the C-arm in such a way that it was close to the target, but they would continue with the task anyway, for a variety of possible reasons, and it was common that the participant's final image submission was less accurate than some of their previous images for the same task. In order to better visualize this, we have plotted the accuracies of two sample participants against task time for some sample AXIS and control imaging tasks, overlaid with their respective cumulative best accuracy traces. Additionally, the graphs display the times at which the real X-rays were acquired throughout each task (depicted by black dotted vertical lines), as well as the time at which the best accuracy (smallest lateral distance or angular difference) was achieved, time-to-best-image (depicted by a red circle). The two participants were chosen arbitrarily from pools of participants based on their level of C-arm experience: one with no previous C-arm experience and one with intermediate C-arm experience (has manoeuvred a C-arm and taken a limited number of X-rays before). Figure 28 through Figure 31 show the lateral accuracy traces for both participants for one AXIS and one non-AXIS task, while Figure 28 through Figure 31 show the angular accuracy traces for on AXIS and one non-AXIS task. Note that in these samples, for both lateral and angular accuracies, the participants' best accuracies are achieved before the end of the task in each case.

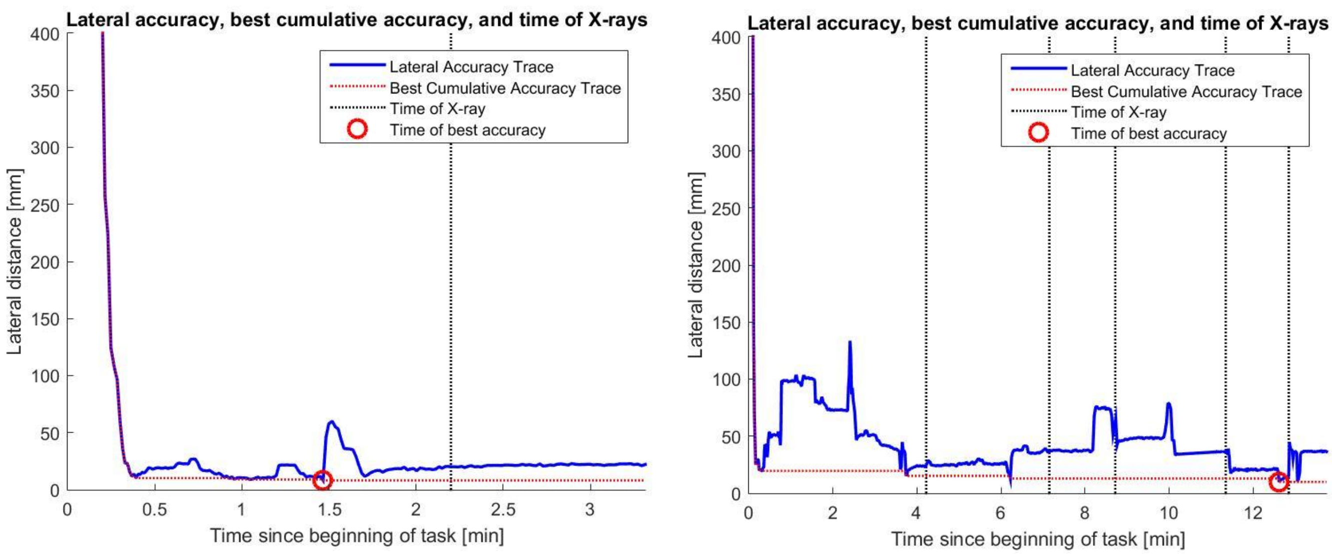

Figure 28: Lateral distance trace over time for inexperienced (left) and intermediate (right) participants during AXIS pelvic lateral imaging task

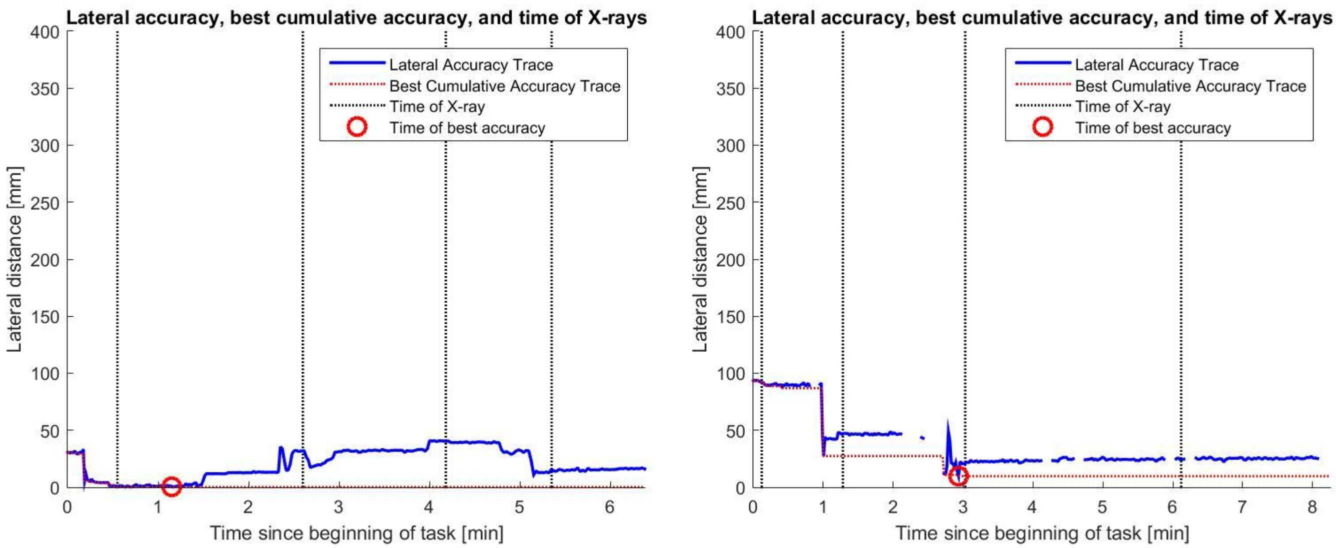

Figure 29: Lateral distance trace over time for inexperienced (left) and intermediate (right) participants during control AP pelvic imaging task

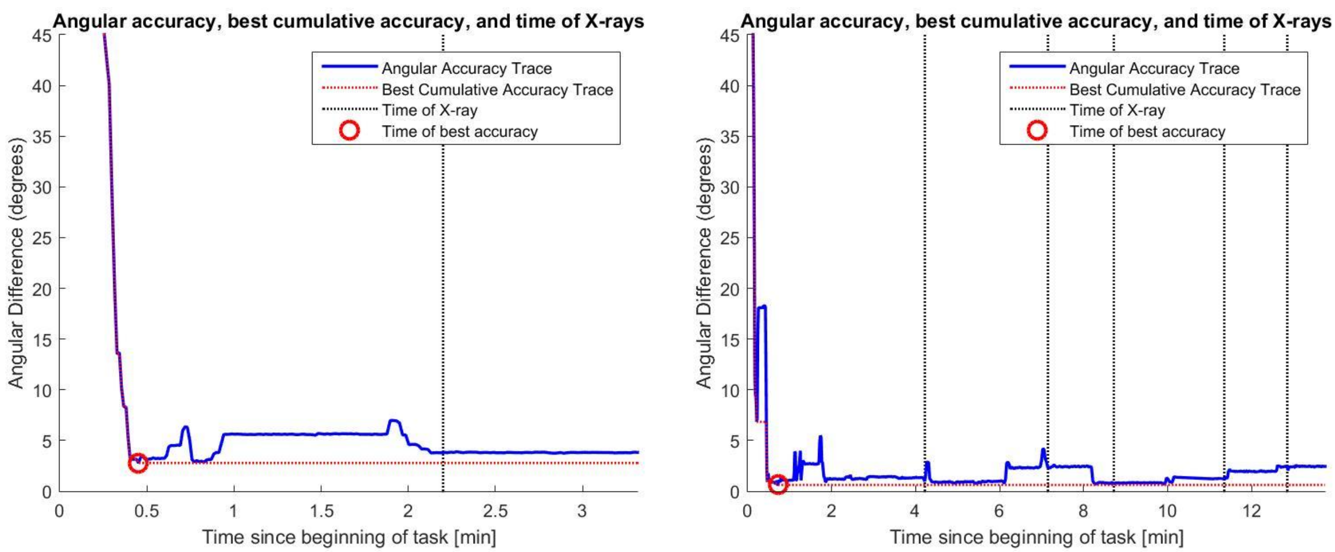

Figure 30: Angular distance trace over time for inexperienced (left) and intermediate (right) participants during AXIS pelvic lateral imaging task

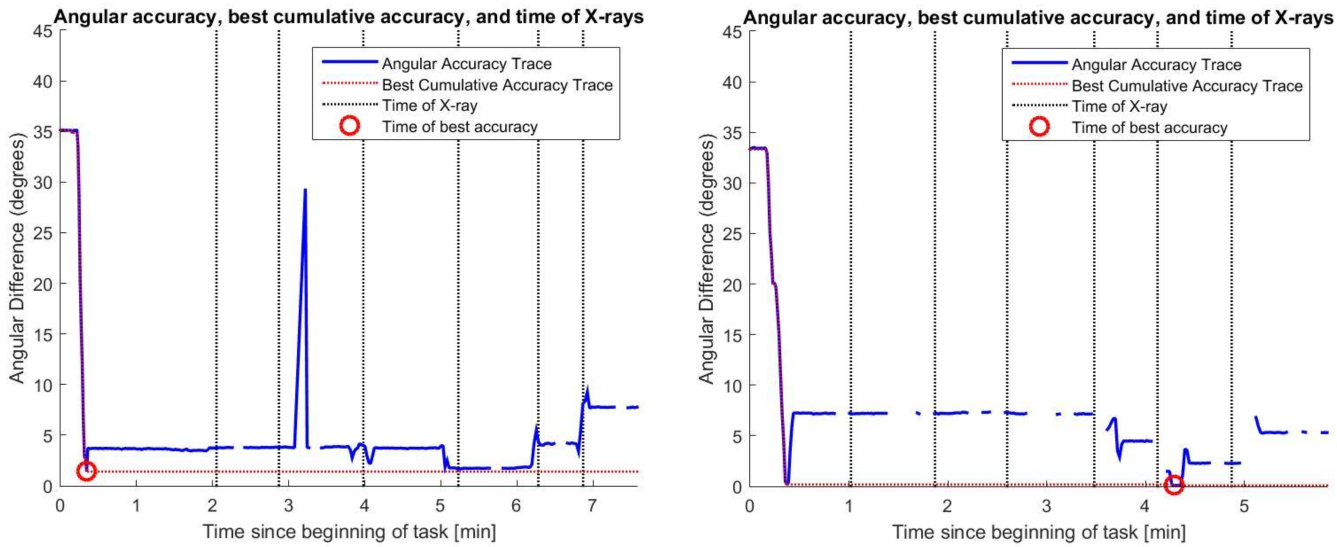

Figure 31: Angular distance trace over time for inexperienced (left) and intermediate (right) participants during control pelvic inlet imaging task

Overall, for the 30 participants, out of a total of 156 measurements made for each of the accuracy metrics, 141 measurements (90%) showed that the C-arm had been positioned at some point throughout the imaging task with greater lateral accuracy (smaller lateral distance, with > 1 mm difference) than what was measured at the end of the task, and similarly, 135 measurements (87%) showed that the C-arm had been positioned at some point throughout the imaging task with greater angular accuracy (smaller angle, with >0.1° difference) than what was measured at the end of the task. Incidentally, the reason we report 156 measurements rather than the expected 180 measurements for 30 participants who each performed six tasks, was that we were only tracking the C-arm for AXIS-specific tasks for the first six participants, and did not start tracking it for the control tasks as well until the seventh participant. Additionally, during a handful of tasks, the optical trackers had been obstructed, resulting in lack of tracking data for those tasks. This also accounts for the inconsistent sample sizes across the different evaluation metrics below.

4.5 Secondary X-ray and Time Evaluation Metrics

For the most accurate C-arm positions achieved throughout the imaging tasks, we recorded the number of X-rays and time required to achieve such positions. These results are presented in raw data plots for all six tasks per participant in Figure 32 through Figure 35 on the left, as well as in CDF plots on the right. Again, non-AXIS data are unavailable for the first six participants for reasons discussed in the previous section. Figure 34 and Figure 35 both show that the participants took fewer X-rays to achieve their most accurate images (both lateral and angular). We find no other obvious trends from these plots, however the statistical test results are presented in Section 4.6.

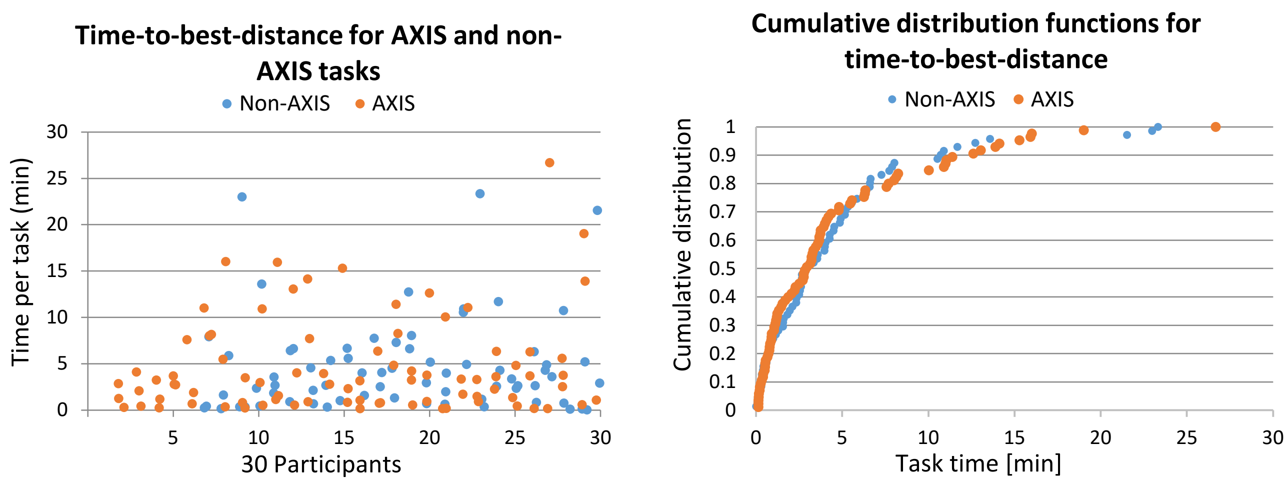

Figure 32: Time-to-best-distance for AXIS and non-AXIS tasks (left) and corresponding CDF plot (right)

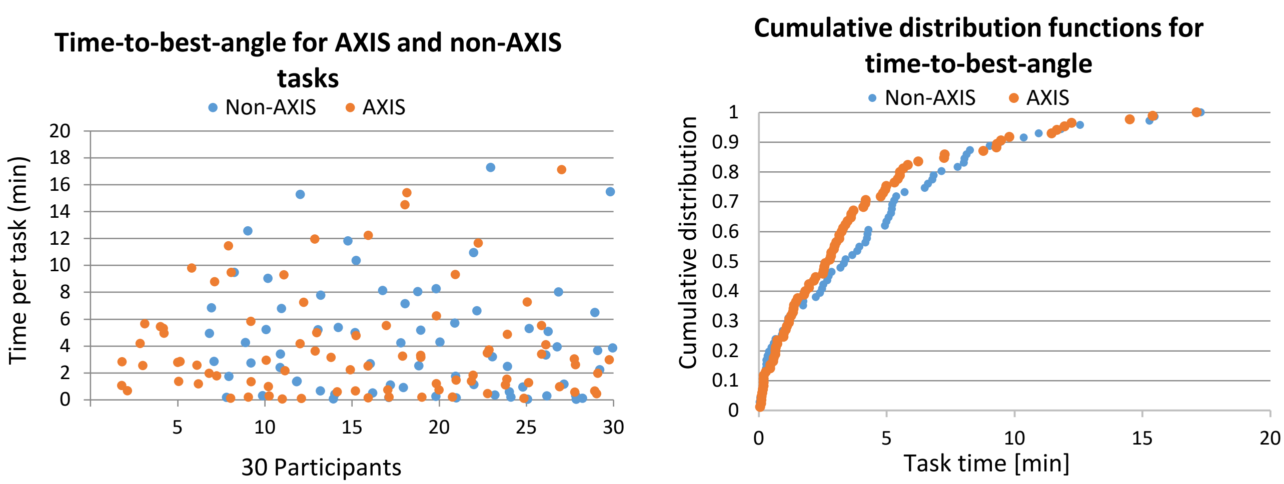

Figure 33: Time-to-best-angle for AXIS and non-AXIS tasks (left) and corresponding CDF plot (right)

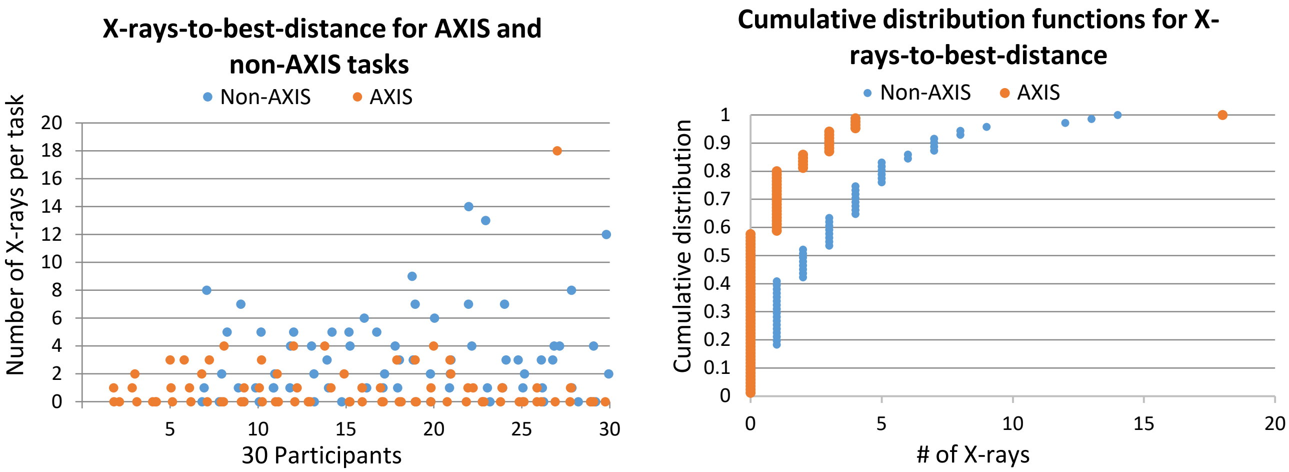

Figure 34: X-rays-to-best-distance for AXIS and non-AXIS tasks (left) and corresponding CDF plot (right)

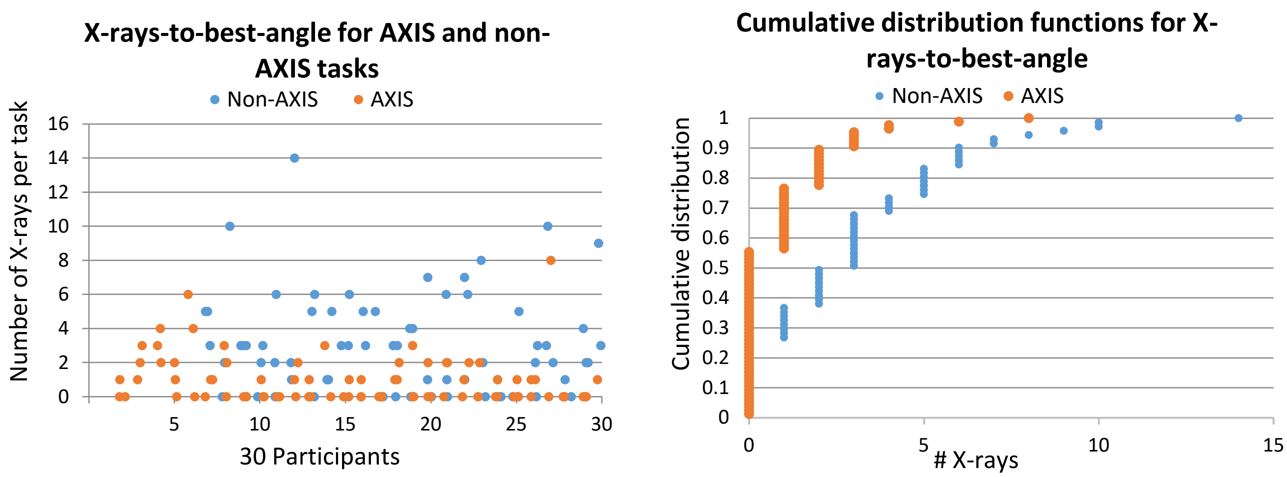

Figure 35: X-rays-to-best-angle for AXIS and non-AXIS tasks (left) and corresponding CDF plot (right)

4.6 Statistical Analysis for AXIS and Control Imaging Tasks

Each participant's three imaging task results were averaged for the control and AXIS evaluations for the ten evaluation metrics. We performed statistical analyses on the difference in group means, as well as the differences in each individual's means. We applied the Holm-Bonferroni method to the tests in order to correct for the multiple comparisons problem. Table 3 presents the descriptive statistics, hypothesis testing on the difference in group means, and paired t-testing on individual mean differences between AXIS and non-AXIS tasks, before the multiple comparison corrections. Table 4 then presents the statistical results from after we applied the Holm-Bonferroni correction. The accuracies achieved at the end of each task are indicated as "*submitted*" and those achieved for their most accurate C-arm positions are indicated as "*best".* Moreover, as explained previously in Section 4.3, the sample sizes are inconsistent across the different evaluation metrics due to occasional unavailability of C-arm tracking data for certain participants.

To summarize, in testing the hypotheses on the means, participants took significantly fewer X-rays overall (53% fewer), they took fewer X-rays to achieve their best lateral distance (68% fewer), and their submitted lateral accuracies were significantly better (10% better) when they were guided by AXIS. The paired t-tests on individual mean differences resulted in the same statistical inferences for the overall number of X-rays and for the submitted lateral accuracies as for the group means. Additionally, the paired t-tests showed that the participants' best lateral accuracies were significantly better (26% better) and that the participants required fewer X-rays to achieve their best angular accuracy (69% fewer) when they were guided by AXIS. On average, the point estimates for task time, time-best-distance, time-to-best-angle, and submitted and best angular accuracies were better for AXIS-guided tasks, though these differences were not statistically significant.

Table 3: Statistical analysis for comparison of AXIS and Non-AXIS imaging tasks (before Holm-Bonferroni correction)

	Hypothesis test on group means (z-test)					Paired t-tests on mean differences:			
	Mean	Sample Size	Stand. Dev.	Var.	P-value	Mean Diff.	Sample Size	Stand. Dev.	P-value
NUMBER OF X-RAYS, H1									
AXIS	2.83	90	2.68	7.17	<0.001	3.200	90	2.422	<0.001
Non-AXIS	6.03	90	3.27	10.68					
TIME [min], H2									
AXIS	7.88	90	5.48	30.07	0.802	0.198	90	4.991	<0.8
Non-AXIS	8.08	90	5.24	27.41					
LATERAL DISTANCE, SUBMITTED [mm], H3									
AXIS	31.21	87	9.63	92.75	0.026	3.400	87	9.752	<0.002
Non-AXIS	34.61	87	10.50	110.16					
ANGULAR DIFFERENCE, SUBMITTED [deg], H4									
AXIS	6.55	87	1.96	3.84	0.756	0.088	87	2.501	<0.8
Non-AXIS	6.64	87	1.79	3.22					
LATERAL DISTANCE, BEST [mm], H5									
AXIS	13.92	85	13.48	181.58	0.048	5.245	69	9.160	<0.001
Non-AXIS	18.84	71	17.03	289.95					
ANGULAR DIFFERENCE, BEST [deg], H6									
AXIS	3.46	85	4.21	17.72	0.562	0.220	69	3.335	<0.8
Non-AXIS	3.83	71	3.75	14.08					
TIME TO BEST LATERAL DISTANCE [min], H7									
AXIS	4.57	85	5.13	26.27	0.976	-0.576	69	4.575	<1
Non-AXIS	4.59	71	5.03	25.34					
TIME TO BEST ANGLE [deg], H8									
AXIS	3.75	85	3.85	14.79	0.39	0.418	69	3.319	<0.5
Non-AXIS	4.30	71	4.08	16.64					
X-RAYS TO BEST LATERAL DISTANCE, H9									
AXIS	0.99	85	2.20	4.85	<0.001	0.418	69	3.319	<0.5
Non-AXIS	3.14	71	3.13	9.78					
X-RAYS TO BEST ANGLE, H10									
AXIS	0.91	85	1.42	2.01	<0.001	2.243	69	1.384	<0.001
Non-AXIS	2.97	71	2.91	8.46					

Table 4: Holm-Bonferroni correction for multiple comparisons problem and statistical results for AXIS vs. non-AXIS imaging tasks

Holm-Bonferroni correction for multiple comparisons and statistical results									
		Hypothesis test on the means				Paired t-tests on mean differences			
K index value	**Corrected P-value, P_c**	**Hypothesis Test P-values**	**Ascending Order, P_k**	**P_k<P_c?**	**Statistical Test Result**	**Paired t-test P-values**	**Ascending Order, P_k**	**P_k<P_c?**	**Statistical Test Result**
1	0.005	P1<0.001	P1<0.001	Yes	**Reject $H_{1,0}$**	P1<0.001	P1<0.001	Yes	**Reject $H_{1,0}$**
2	0.006	P2=0.802	P9<0.001	Yes	**Reject $H_{9,0}$**	P2<0.8	P5<0.001	Yes	**Reject $H_{5,0}$**
3	0.006	P3=0.026	P10<0.001	Yes	**Reject $H_{3,0}$**	P3<0.002	P10<0.001	Yes	**Reject $H_{10,0}$**
4	0.007	P4=0.756	P3=0.026	No	No diff. found	P4<0.8	P3<0.002	Yes	**Reject $H_{3,0}$**
5	0.008	P5=0.048	P5=0.048	No	No diff. found	P5<0.001	P8<0.5	No	No diff. found
6	0.010	P6=0.562	P8=0.39	No	No diff. found	P6<0.8	P9<0.5	No	No diff. found
7	0.013	P7=0.976	P6=0.562	No	No diff. found	P7<1	P2<0.8	No	No diff. found
8	0.017	P8=0.39	P4=0.756	No	No diff. found	P8<0.5	P4<0.8	No	No diff. found
9	0.025	P9<0.001	P2=0.802	No	No diff. found	P9<0.5	P6<0.8	No	No diff. found
10	0.050	P10<0.001	P7=0.976	No	No diff. found	P10<0.001	P7<1	No	No diff. found

4.7 Treatment Order Significance

While the order in which the participants performed the AXIS tasks and the control tasks was randomized to allow us to control for improvements in the participants' performance based on simply repeating the tasks, we were interested in finding out whether there was, in fact, any difference between those who performed the AXIS tasks first and those who performed the control tasks first. Table 5 displays the descriptive statistics and hypothesis tests on the means for AXIS-first and control-first treatment orders. The means that are used are each individual's difference in means between AXIS and non-AXIS tasks. We then applied the Holm-Bonferroni method to correct for the multiple comparisons problem. The statistical results after this correction are shown in Table 6. In summary, after correcting for multiple comparisons, no statistically significant differences were found between the AXIS-first and control-first treatment orders for any of the evaluation metrics. However, it is worth noting that two of the three time-related metric results are nearly significant (both of which were significant before the correction), indicating that whichever evaluation the participants performed first ended up taking more time than the subsequent evaluation.

Table 5: Statistical analysis for comparison of AXIS-first and control-first treatment orders (before Holm-Bonferroni correction)

	Hypothesis Testing on Means				
	Mean Diffs.	Sample Size	Stand. Dev.	Var.	P-value
NUMBER OF X-RAYS, H1					
AXIS-first	3.178	15	2.011	4.043	0.960
Control-First	3.222	15	2.725	7.426	
TIME [min], H2					
AXIS-first	-1.947	15	3.911	15.298	0.008
Control-First	2.343	15	4.908	24.091	
LATERAL DISTANCE, SUBMITTED [mm], H3					
AXIS-first	34.418	15	5.819	33.862	0.045
Control-First	30.636	14	4.188	17.540	
ANGULAR DIFFERENCE, SUBMITTED [deg], H4					
AXIS-first	7.445	15	2.011	4.043	0.215
Control-First	6.340	14	2.725	7.426	
LATERAL DISTANCE, BEST [mm], H5					
AXIS-first	5.558	12	8.792	77.305	0.865
Control-First	4.932	12	9.251	85.588	
ANGULAR DIFFERENCE, BEST [deg], H6					
AXIS-first	0.540	12	2.190	4.796	0.631
Control-First	-0.101	12	4.076	16.612	
TIME TO BEST LATERAL DISTANCE [min], H7					
AXIS-first	-2.662	12	3.362	11.306	0.010
Control-First	1.510	12	4.533	20.546	
TIME TO BEST ANGLE [deg], H8					
AXIS-first	-0.210	12	3.301	10.895	0.337
Control-First	1.047	12	3.117	9.713	
X-RAYS TO BEST LATERAL DISTANCE, H9					
AXIS-first	2.083	12	1.772	3.138	0.834
Control-First	1.889	12	2.767	7.654	
X-RAYS TO BEST ANGLE, H10					
AXIS-first	2.500	12	1.339	1.793	0.347
Control-First	1.986	12	1.340	1.796	

Table 6: Holm-Bonferroni correction for multiple comparisons problem and statistical results for AXIS-first vs. control-first treatment order comparison

Holm-Bonferroni correction for multiple comparisons and statistical results	
	Hypothesis test on the means

k index value	Corrected P-value, P_c	Hypothesis Test P-values	Ascending Order, P_k	P_k<P_c?	Statistical Test Result
1	0.005	P1=0.960	P2=0.008	No	No diff. found
2	0.006	P2=0.008	P7=0.010	No	No diff. found
3	0.006	P3=0.045	P3=0.045	No	No diff. found
4	0.007	P4=0.215	P4=0.215	No	No diff. found
5	0.008	P5=0.865	P8=0.337	No	No diff. found
6	0.010	P6=0.631	P10=0.347	No	No diff. found
7	0.013	P7=0.010	P6=0.631	No	No diff. found
8	0.017	P8=0.337	P9=0.834	No	No diff. found
9	0.025	P9=0.834	P5=0.865	No	No diff. found
10	0.050	P10=0.347	P1=0.960	No	No diff. found

4.8 Participant experience level

In order to determine whether participant C-arm experience level had any effect on their performance, we plotted the imaging task results for four different experience groups: No experience (1), low-experience (2), medium-experience (3), and high-experience (4). Performance was plotted for the four primary evaluation metrics: the number of X-rays, time, submitted lateral distance, and submitted angular difference. These results are presented in Figure 36 to Figure 37.

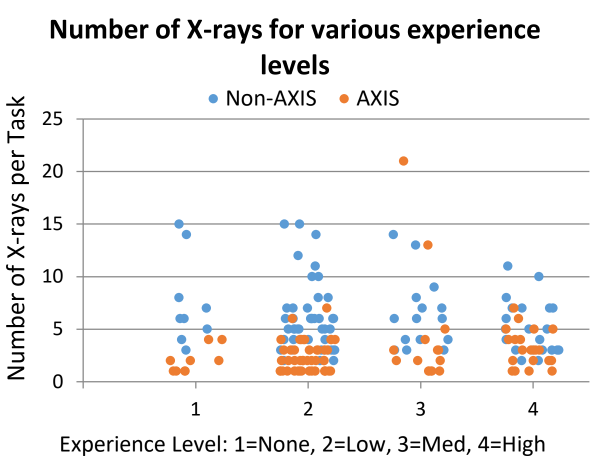

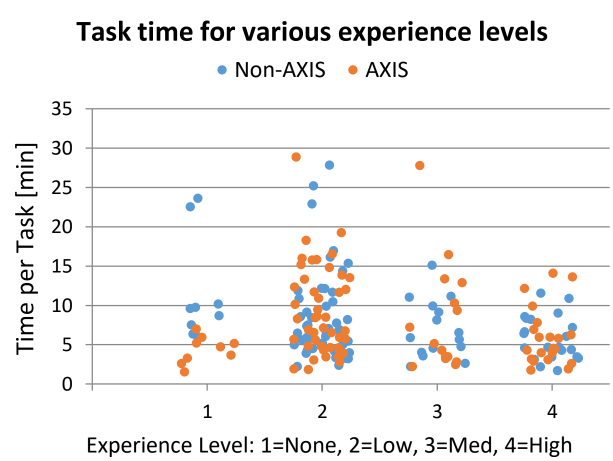

Figure 36: Number of X-rays (left) and task time (right) required per imaging task for various experience levels

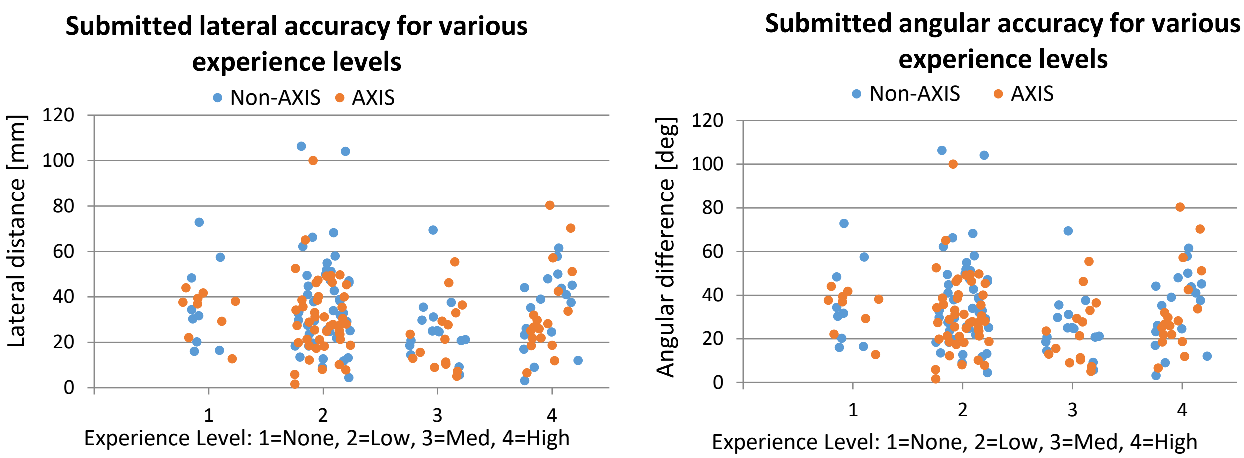

Figure 37: Lateral accuracy (left) and angular accuracy (right) achieved by various experience levels

To test for statistical significance, we performed one-way ANOVA tests on the four experience levels (none - 1, low - 2, med - 3, high - 4), followed by Tukey post hoc tests. These statistical tests were performed for the number of X-rays, time, submitted lateral distance, and submitted angular difference; the test results are summarized in Table 7. ANOVA testing suggested the possibility of detecting a significant difference for both AXIS and non-AXIS tasks in the time metric, as well as for the individual mean differences for the angular accuracy metric. However, the Tukey post hoc tests show that for the no-experience group (1), the discrepancy between the number of X-rays required in non-AXIS tasks compared to AXIS tasks was greater (an average of 5.4 more X-rays for non-AXIS tasks) than for the medium-experience group (3), and that the high-experience (4) group took an average of 6.3 more minutes to complete tasks compared to the no-experience group (1).

Table 7: One-way ANOVA testing with post-hoc Tukey tests for each level of experience

	One-Way ANOVA			Tukey Post Hoc Tests	
	F-ratio	P-Value	Test Result	Tukey Test	Test Result
NUMBER OF X-RAYS					
AXIS	1.325	0.288	No diff. found	-	No diff. found
Control	1.496	0.239	No diff. found	-	No diff. found
Mean Diff	2.254	0.106	No diff. found	**0 vs. 2, P=0.032**	**$\mu(0)-\mu(2)=5.4$ X-rays**
TIME [min]					
AXIS	3.181	0.041	**Reject H_0**	-	No diff. found

Control	3.676	0.025	**Reject H_0**	**0 vs. 3, P=0.028**	**μ(3)-μ(0)=6.3 min**
Mean Diff	2.646	0.070	No diff. found		No diff. found
LATERAL DISTANCE, SUBMITTED [mm]					
AXIS	0.507	0.681	No diff. found	-	No diff. found
Control	1.570	0.222	No diff. found	-	No diff. found
Mean Diff	**0.743**	0.537	No diff. found	-	No diff. found
ANGULAR DIFFERENCE, SUBMITTED [°]					
AXIS	0.922	0.444	No diff. found	-	No diff. found
Control	2.226	0.110	No diff. found	-	No diff. found
Mean Diff	3.285	0.037	**Reject H H_0**	-	No diff. found

4.9 Experts' Target Evaluations

In order to provide context regarding the acceptability of image accuracies resulting from the participants' evaluation exercises, the two orthopaedic surgeons performed the control evaluation task (without AXIS guidance) once for all six target images. The experts' results are present in Figure 38 through Figure 42.

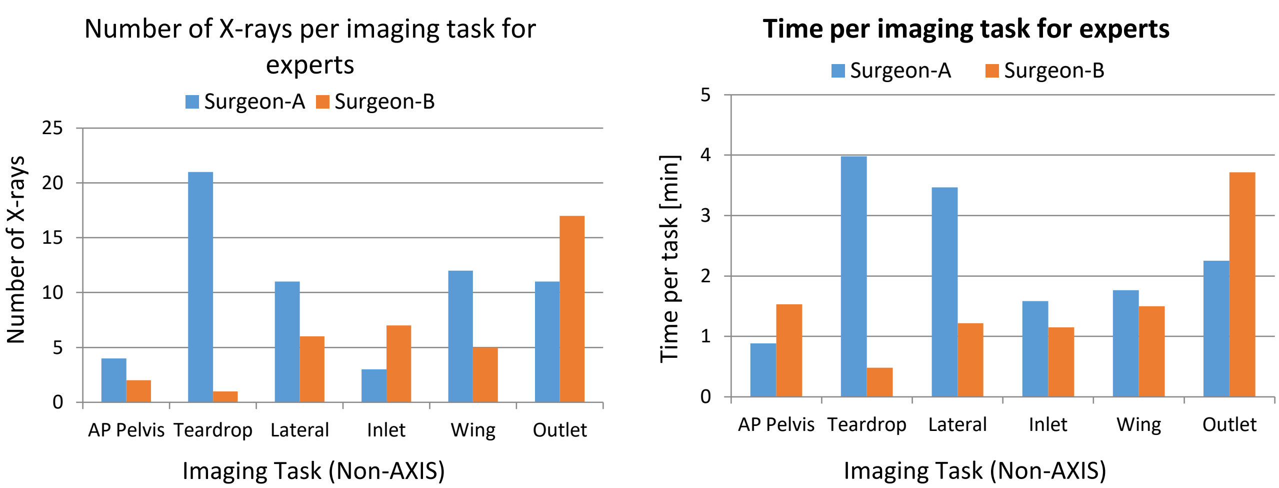

Figure 38: Number of X-rays (left) and time (right) required by experts for each imaging task

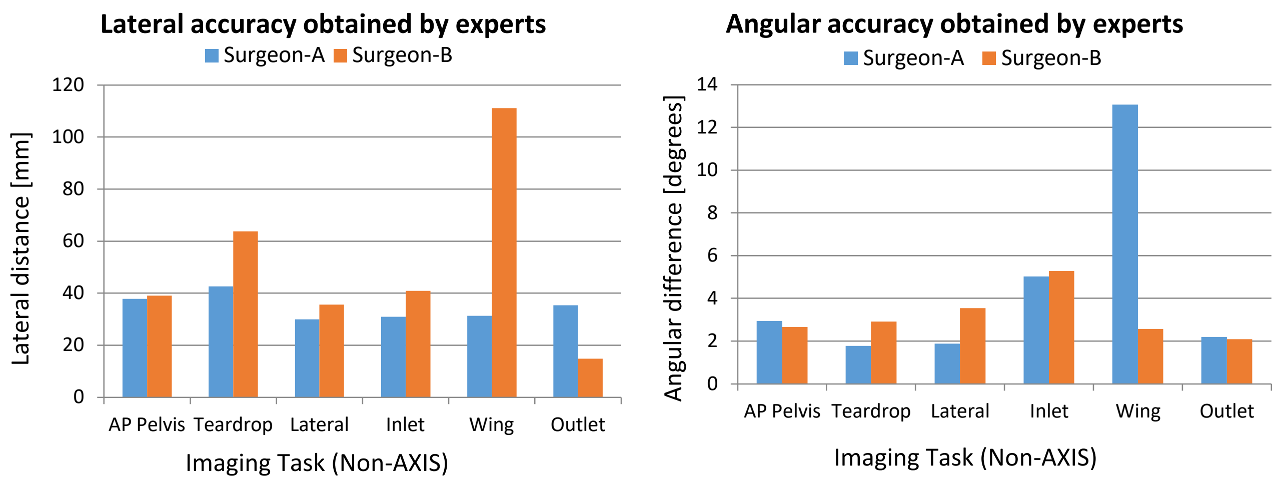

Figure 39: Lateral (left) and angular (right) accuracies achieved by experts at the end of each imaging task

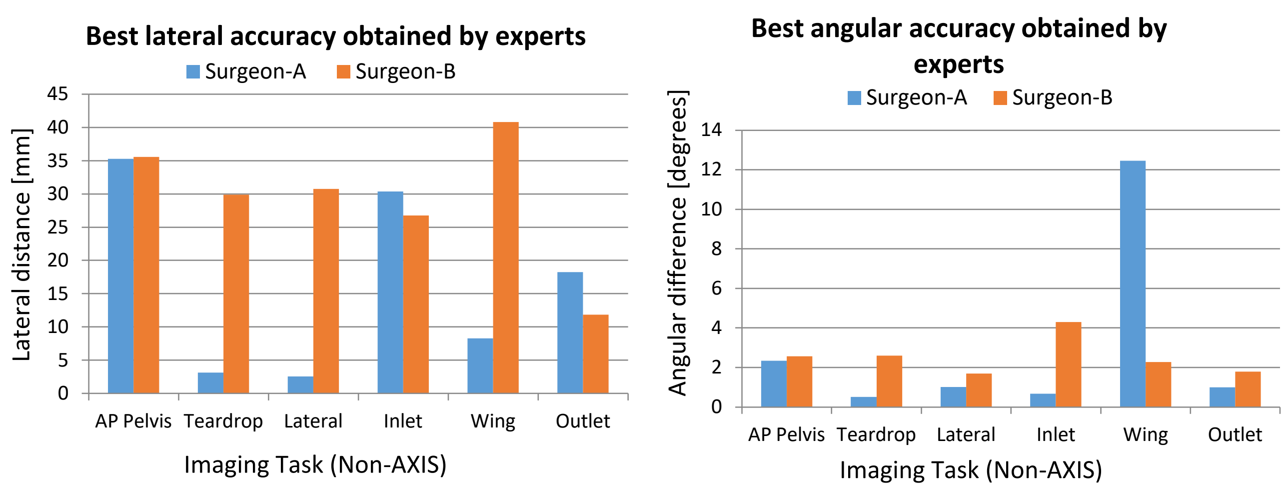

Figure 40: Best lateral (left) and best angular (right) accuracies achieved by experts for each imaging task

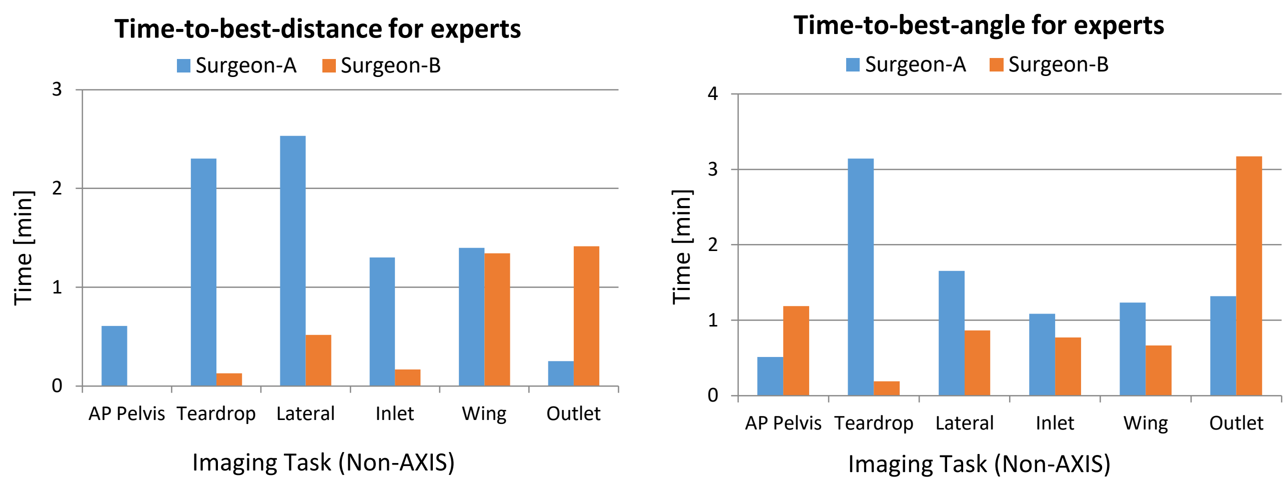

Figure 41: Time required by experts to achieve their best lateral (left) and angular (right) accuracies for each imaging task

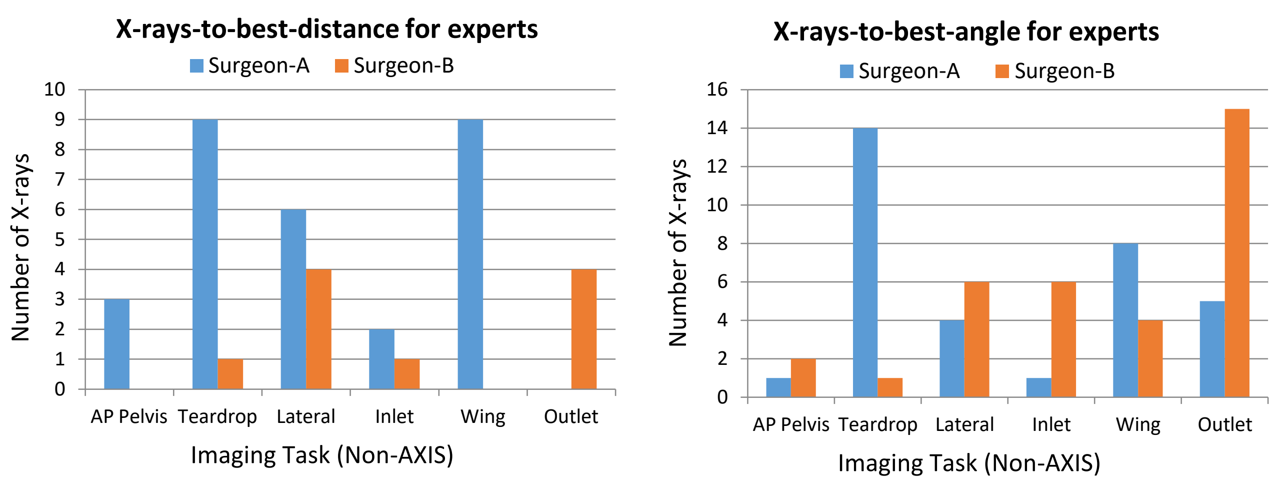

Figure 42: Number of X-rays required by experts to achieve their best lateral (left) and angular (right) accuracies for each imaging task

The results obtained by the experts were averaged for all six imaging tasks for each of the ten evaluation metrics. Their results were compared to those of the participants, as was presented in Figure 21 at the beginning of this Chapter. Of relevance, the point estimates show that the participants took fewer X-rays altogether, they took substantially more time for both task types, and they achieved somewhat better lateral distance accuracy than the experts (we did not perform statistical analyses on these differences).

4.10 Questionnaire Responses

After having completed the evaluation tasks, each participant was given a questionnaire to fill out. While certain questions are emphasized in this section, the full set of survey questions and a summary of the participant responses can be found in Appendix B, along with a summary of the additional comments made by each participant. All 30 of the study participants chose to complete the questionnaire. The average age of the participants was 27 years old, ranging from 19 to 51 years old. The frequency of different age groups is shown in Table 8.

Table 8: Number of participants in various age groups

Age group	Frequency
19-25	14
26-33	14
34+	2

Out of the 30 participants, half identified themselves as being female and the other half male. The participants' level of hands-on experience with a C-arm varied from having no experience at all to having professional work experience with the C-arm; two-thirds of the participants had no hands-on experience. Refer to Table 2 in Chapter 3 for a summary of the number of participants at each level of C-arm experience.

Figure 43 shows how the participants responded to questions regarding their confidence in completing the tasks: "*By circling the best answer, rate your level of confidence in your ability to capture the correct anatomical view during the standard X-ray C-arm evaluation exercises (without the AXIS)*" and "*By circling the best answer, rate your level of confidence in your ability to capture the correct anatomical view during the Artificial X-ray C-arm evaluation exercises (with the AXIS)*", respectively. The participants were asked to rate their confidence on a five-level Likert scale from "*No confidence at all*" for a value of '0', to "*Very confident*" for a value of '4'. On average, participants felt significantly more confident in their ability to capture the correct anatomical views when they were guided by AXIS ($p<0.0001$, with a difference in mean score of 1.5).

Figure 43: Participants' confidence in taking X-rays without AXIS guidance (a), and Participants' confidence in taking X-rays with AXIS guidance (b)

Figure 44 shows how the participants responded to the questions "*How would you rate usefulness of the Artificial X-ray Imaging System in guiding you to the desired view before taking real X-ray radiographs*" and "*How would you rate the accuracy and realism of the artificial X-ray images in comparison to the real ones*", respectively. Both questions used a five-level Likert scale from "*Poor*" for a value of '0', to "*Excellent*" for a value of '4'. On average, the participants found the usefulness of AXIS in guiding them to the desired view to be 'very good' with a mean score of 3.2 (standard deviation, 0.69), and they found the accuracy and realism of the artificial X-ray images to be 'good' with a mean score of 2.3 (standard deviation, 0.86), compared to real ones.

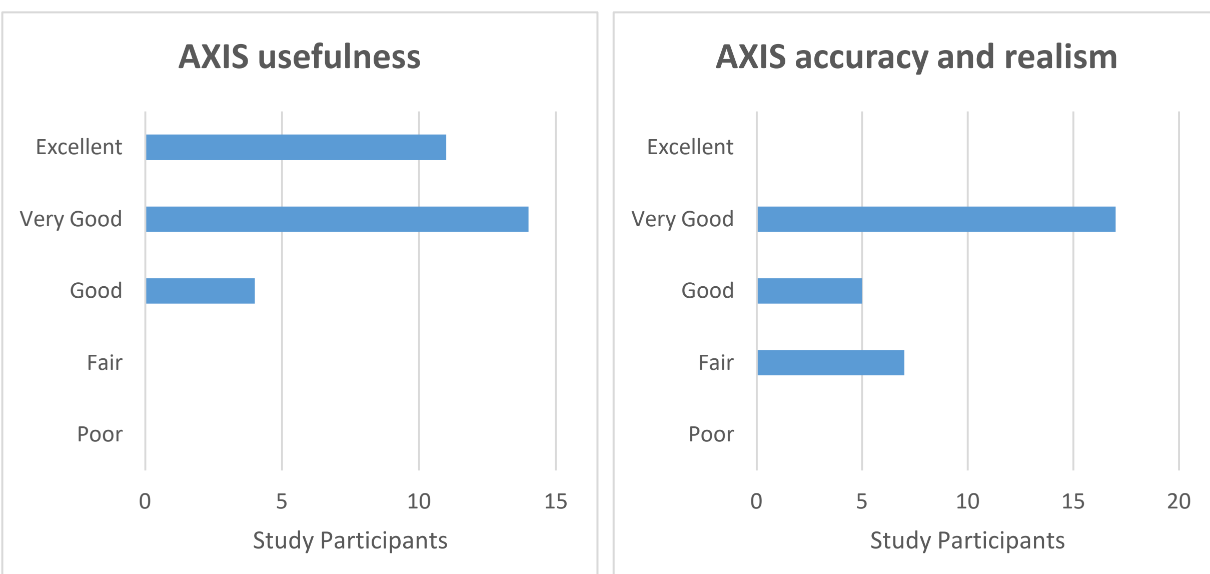

Figure 44: Participants' perception of AXIS usefulness (a), and participants' perception of the accuracy and realism of AXIS images (b)

Chapter 5

User Study Discussion

The purpose of this user study was to assess the utility of an Artificial X-ray Imaging System (AXIS) as an educational and intraoperative guidance tool. The system is aimed at improving C-arm performance during specific orthopaedic surgery imaging tasks in a simulated OR setting and focuses on users who are early in their training. In the study, we measured performance by the number of X-rays and amount of time required to achieve the target radiographic views for specific imaging tasks. To recapitulate from Section 1.8, we hypothesized that guidance with AXIS can significantly decrease the need for scouting X-rays, which MRTs normally take when trying to achieve the correct radiographic view, as well as decrease the amount of time required to do so. Additionally, we investigated how guidance with AXIS affects the accuracy of the images during tasks, by measuring the C-arm's pose throughout the tasks and comparing it to the target pose of the associated target image. In this chapter, the study results are interpreted in the context of image-guided orthopaedic surgery, some of the limitations of the study are brought to light, and recommendations are made for pursuing future work in this area.

5.1 Discussion of Results

We found that participants on average took significantly fewer X-rays overall, they took fewer X-rays to achieve their best lateral accuracies, and they achieved significantly better lateral accuracies for their submitted images when they were guided by AXIS. The paired t-tests additionally showed that the participants achieved greater lateral accuracies for their best-images and required fewer X-rays to achieve their best angle. The point estimates for the other evaluation metrics also showed superior performance on average when guided by AXIS, though these differences were not statistically significant. The questionnaire results revealed that, on average, participants felt significantly more confident in their ability to capture correct anatomical views when they were guided by AXIS. Moreover, the participants found the usefulness of AXIS in guiding them to the desired view to be 'very good' and they found the accuracy and realism of the artificial X-ray images to be 'good'.

5.1.1 Number of X-rays per task

It is to be expected that the number of X-rays required to achieve the imaging tasks is greater when the participants lack AXIS guidance because they must blindly move the C-arm towards the internal anatomical region of interest depicted in the target X-ray image shown to them at the beginning of the task. This would naturally require the use of scouting images to help guide them towards the proper position, a process that is understandably more difficult, especially for those who have limited background and knowledge in radiography and anatomy. With AXIS, the need for scouting X-rays is significantly reduced because AXIS provides immediate visual feedback regarding which anatomy is expected to be within the radiographical view, as well as how different C-arm movements affect the view, even if this information is only an estimate of the true anatomy. As mentioned in Section 4.6, AXIS guidance resulted in a 53% decrease in X-rays compared to without AXIS guidance; in a real OR setting, the patient and OR staff would benefit from an appreciable decrease in radiation exposure if the number of scout X-rays were reduced by half. Our finding that artificial X-ray guidance reduced the need for scout X-rays agrees with the findings reported by the other groups with similar systems that were described in Chapter 1. The CamC group reported an X-ray reduction of 28% during cadaveric intramedullary nail interlocking tasks when using their DRR-enhanced system (Wang 2010). The zero-dose navigation group reported a 90% decrease in radiation exposure during cadaveric guide-wire and cannulated screw insertion procedures when guided by their navigation system, which overlays 3D bone and implant models onto the DRRs (Müller 2011).

5.1.2 Task time

Between the AXIS and non-AXIS exercises, for both submitted and best image cases, there was no statistically significant difference in time required to achieve each task. We observed that during the AXIS tasks, when participants were attempting to move the C-arm towards the anatomical goal, they would often experiment with the rotations and translations of the C-arm to gain immediate feedback on how these affected the X-ray view and how it could be improved. They would also spend much of the time making minor adjustments once they were in the vicinity of the desired region, as was discussed in Section 4.4. Additionally, AXIS DRR generation takes approximately 0.5 seconds per image, meaning that when they make quick, fine-tune adjustments, they must wait for the image to update, adding more time to each task overall. On the other hand, in the non-AXIS case, the participants ended up requiring more X-rays on average to complete each task to make up for the lack of immediate feedback provided by AXIS guidance, meaning that for every X-ray they acquired, they needed to walk to the back of the lead shields to take an X-ray, then view the resulting image on the monitor and assess the result of the C-arm movements they just made.

The study was also designed with the assumption that the participants can autonomously interpret the X-ray images, which was not always the case, especially for the participants who had no previous experience with radiography and anatomy. The element of uncertainly and lack of confidence in interpreting the images contributed to additional task time. We therefore speculate that, in the AXIS case, whatever time is saved from having to take and assess more X-rays is made up for in spending time experimenting with the visual feedback afforded by AXIS and attempting to improve the image. Interestingly, as previously discussed in Section 4.4, participants tended to submit final images that had larger C-arm positioning errors than intermediate images they had acquired. However, in the real OR setting, we presume that the surgeon requesting the views would also be monitoring navigation progress through AXIS while the MRT manoeuvres the C-arm and could provide verbal feedback throughout this process, as well as make it known when the desired view is sufficiently accurate. This additional verbal feedback could significantly reduce the amount of time spent by MRTs in navigating the C-arm towards the correct view. Additional recommendations on improving time are discussed in Section 5.2.2.

Groups who evaluated similar systems on task time reported different results compared to our findings: the virtX group reported a 24% reduction in time when the participants got to practice beforehand with both the physical and virtual simulation training packages compared to the control group who did not practice (Bott 2008). In contrast, the zero-dose navigation group reported a 68% increase in screw insertion time when guided by their system (Müller 2011). In any case, a lack of time difference between the AXIS and non-AXIS tasks rather than the system causing additional time, such as in the zero-dose navigation case, is encouraging because added time could foster apprehension towards adopting artificial X-rays for guidance in the OR.

5.1.3 C-arm positioning accuracy

For the best image case from paired comparisons, and both the submitted and best image cases from group comparisons, the participants achieved greater lateral distance accuracy when guided by AXIS. However, statistically there was no difference between AXIS and non-AXIS tasks in achieving angle accuracy for either the submitted image case or the best image case. One possible reason for this result is that in the AXIS case, lateral distance accuracy can generally be achieved by choosing a prominent anatomical landmark in the target X-ray image, finding the corresponding landmark in the artificial X-rays, and ensuring it is in the same two-dimensional position on the artificial image as it is in the target X-ray. Of course, this method is also carried out in similar fashion in the non-AXIS tasks, with the exception of matching the landmark position onto real X-rays rather than the artificial ones. However, we speculate that this process is made much easier with the availability of immediate feedback in the artificial images.

On the other hand, achieving angular accuracy is more challenging because varying any combination of angles from all three axes results in subtle radiographical nuances that are caused by the overlap of specific anatomical features, which is better grasped when one has experience with radiography and anatomy, and has been trained to assess radiographic images. To provide a simple example, when trying to achieve lateral distance accuracy in an AP pelvis view, the foramina in the coccyx can be used to center the anatomy in the image in a similar fashion to the target X-ray, which is a rather straightforward process. However, to achieve angular accuracy, the C-arm must be orbited laterally around the pelvis in a way that aligns the pubic symphysis anteriorly with the coccyx posteriorly, so that they are symmetrical. The amount of rotation depends on the specific anatomy of the patient or pelvic model.

To illustrate this, Figure 45 below shows three consecutive X-ray images acquired by one participant during an AXIS-guided AP pelvis imaging task. Adequate lateral accuracy was achieved within one X-ray image and maintained throughout the task, as can be seen from how the foramina are relatively well-aligned with the vertical red dashed lines that are equidistant from the centre of the field-of-view. However, Figure 45a shows the angular discrepancy between the pubic symphysis anteriorly (depicted by the red arrow) and the coccyx posteriorly. The participant had to orbit the C-arm and acquired several X-rays in order to improve this angle.

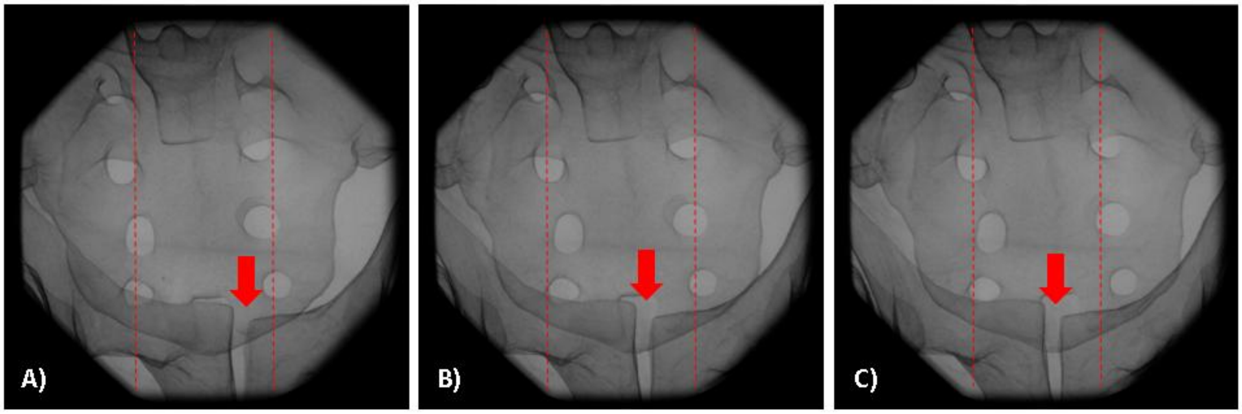

Figure 45: X-rays acquired by one participant in order to improve angular accuracy during the AXIS-guided AP pelvic imaging task

In the case of the AP pelvis imaging task, the requirement to rotate the C-arm in the orbital direction was relatively straightforward for most participants; however, in tasks that required a combination of rotations, such as the teardrop and down-the-wing imaging tasks, the participants had more difficulty. The teardrop view, for example, is achieved by combining orbital and tilt rotations, and the characteristic teardrop shape is made up of a confluence of cortices: inferiorly the sciatic notch, medially the inner cortex of the ilium, and laterally the outer cortex of the ilium. This C-arm and pelvis perspective effect can be difficult to grasp without any previous background in anatomy or radiography. Therefore, while AXIS guidance is helpful in improving lateral distance accuracy, it may not be sufficient on its own to overcome the difficulty of angular accuracy. However, as mentioned in the previous section in the context of avoiding lengthy minor adjustments by the MRT during imaging tasks when sufficient accuracy has already been achieved, in the real OR surgeons would provide verbal feedback in the same way they would with real scout images, lessening the need for AXIS to improve C-arm positioning accuracy. In any case, recommendations for improving C-arm positioning accuracy when guided by AXIS are discussed in Section 5.2.1 below. Other groups who have evaluated similar systems did not report any directly relevant comparable findings on C-arm positioning accuracy.

5.1.4 Additional factors: Treatment order and experience level

The statistical tests we performed based on treatment order did not provide any indication of performance improvement associated to either the AXIS-first or the control-first treatment order. However, two of the three time-related metric results are nearly significant, both of which were significant before applying the Holm-Bonferroni correction. These results indicate that whichever evaluation the participants performed first took longer to complete than the subsequent evaluation. This is not surprising as it agrees with the concept that performing a new, challenging task for the first time is bound to take longer than when we perform a similar task the second time around. Added task time with inexperienced MRTs would be expected in the OR regardless of the guidance tools they have access to. However, of much relevance, these near-significant results validate our initial study design decision of randomizing the task orders. Moreover, it is encouraging, that this sort of result was not the case with the number of X-rays: regardless of the task order, the participants required less X-rays when they were guidance by AXIS.

In terms of experience level, the ANOVA tests show that users with no previous experience tend to have a substantially higher discrepancy between the number of X-rays required without AXIS guidance and that required with AXIS guidance, compared to users with more experience. This result suggests that for users with low experience levels, AXIS could have a larger impact on reducing radiation exposure, compared to for users with more experience, which is promising given that the AXIS tool is aimed at improving the performance of MRTs with little to no hands-on C-arm experience. The ANOVA tests also showed that the users with higher experience levels took more time to complete the imaging tasks when they were not guided by AXIS, compared to the users without any experience. This result is somewhat surprising, given that, as discussed below, the experts took substantially less time when performing the six imaging tasks without AXIS compared to the participants' time for either of the evaluation types. We speculate that these users may be more aware of the subtleties of what constitutes an optimal image and invested additional effort to try to achieve this.

5.1.5 Experts' evaluations

When the two orthopaedic surgeons performed the six imaging tasks without AXIS guidance we found that, notably, they took more X-rays overall compared to the participants, they took substantially less time to perform the imaging tasks compared to the participants, and they achieved lower lateral accuracies than the participants. Though perhaps somewhat counterintuitive, these findings are perhaps more understandable on reflection: firstly, while orthopaedic surgeons are more experienced with radiography and anatomy, and therefore should be capable of completing the imaging tasks with fewer X-rays, they are likely more relaxed and comfortable with the idea of ionizing radiation exposure since they are confronted with this in their everyday practice, resulting in the tendency to take many more real X-rays throughout the tasks without as much concern as the less-experienced participants. Secondly, because they are much more experienced than the participants, it follows naturally that they are faster and more deliberate in the way they manoeuvre the C-arm and can assess the X-rays more efficiently, and as a result, can complete the imaging tasks more quickly. Finally, we speculate that the reason for the participants achieving better lateral accuracies than the experts is that, for the experts, as long as the anatomy in question is within the field of view, they likely consider the image to be adequate; in assessing the positioning of a screw, its location on the monitor is irrelevant, as long as the important components can be seen, whereas the study participants assume that they must replicate the target image as accurately as possible and therefore spend more time trying to refine the lateral accuracy. In terms of angular accuracy, on the other hand, the experts saw better results because, in assessing screw placement, for example, only correct angular visualization truly reveals if the screw is breaching undesired tissue, or in the case of anatomical measurement for screw length selection, only proper angulation can truly display the anatomy in a perpendicular fashion so it can be measured accurately.

5.1.6 Questionnaire responses

Overall, the responses obtained in the questionnaires were very promising: on average, the participants felt significantly more confident in their ability to position the C-arm correctly when they were guided by AXIS. Overall, the participants rated the system's usefulness to be 'very good', and the accuracy and realism of the artificial X-ray images to be 'good'. Additionally, both BCIT Medical Radiography instructors and both orthopaedic surgeons expressed satisfaction with the system's potential to improve C-arm performance in the OR, both by decreasing radiation exposure and by improving efficiency through the facilitation of clear communication between the MRT and the surgeon, as well as through improving the MRT's confidence with C-arms. Given the pilot nature of the system and user study, these results are encouraging, but also steer us towards the development of AXIS on several aspects. Additionally, in the survey comments sections, the participants provided a variety of constructive feedback, which helps navigate us towards the aspects that warrant the most attention in the future, as discussed in the following sections.

5.2 Limitations and Recommendations for Future Work

The user study has demonstrated the potential of AXIS as a guidance tool for new C-arm users to learn and practice the manoeuvering of C-arms, as well as for improving their performance with C-arms in the OR. The user study has revealed AXIS to be a guidance tool capable of reducing the number of scout X-rays required during imaging tasks, providing equivalent or better imaging accuracy, and improving the confidence of new C-arm users. Additionally, AXIS was found to require equivalent imaging task times compared to without it, which is promising in the context of easy integration into educational and OR settings. However, drawing on the suggestions provided by the study participants, a number of limitations should be addressed in order to directly improve AXIS, as well as develop its potential for acceptance into the OR.

5.2.1 Artificial and real X-ray image agreement accuracy

In terms of the AXIS design, the sources of image matching disagreement between the artificial X-rays and the real ones can be attributed at least in part to errors in the CT-to-manikin registration process, as was described in Section 2.4, as well as to the C-arm digitization process. Regarding the registration process, firstly, a rigid CT is registered to a non-rigid manikin that is positioned slightly differently each time it is placed on the surgical table. The main positioning inconsistencies result from the manikin's pelvis, which can be tilted anteriorly or posteriorly approximately over a 4°angle, as well as from its hips, which can be abducted and adducted over approximately 15° in total for each leg. This means that when the manikin is positioned on the surgical table, although we try to reposition it as consistently as possible, its posture differs compared to its posture when the CT scan was acquired, resulting in a mapping discrepancy between the manikin's anatomical landmarks within the CT and those in the physical manikin. Secondly, when the C-arm is positioned in its home position for the registration process, the C-arm's angle ruler is used, whose precision is +/- 5°. Finally, verification of the agreement between the DRRs and the X-rays was performed by visual inspection, leaving room for human error. Regarding the C-arm digitization process, digitization of points V1-V5 on the C-arm was performed visually by aligning the tip of the digitization probe with the point of interest during collection, making this step susceptible to human error as well. We estimate the precision of this step to be ~2 mm. Moreover, the C-arm was assumed to be a rigid body; however, slight misalignment (~2 mm) occurs between the source and detector when it is in certain positions that cause it to bow. While we did not explicitly perform tests to measure the angular and translational agreement accuracy between the DRRs and the X-rays, we estimate it to be within +/- 1 cm and +/- 3º, which we feel is sufficient to fulfill the goals of the user study.

Improvement on the slight mismatch between artificial and real X-ray images was a suggestion that was provided in the study questionnaire by 9 of the participants. In order to improve the design of AXIS for better OR and educational setting adoption, registration accuracy could be improved by using fiducial markers on the manikin and acquiring a CT scan that includes these so they can be accurately registered. However, since the manikin is non-rigid, the CT scan would have to be manipulated so that it is deformable to adapt to the slight pose variations of the manikin. This could be achieved by registering bone segments separately. Such improvements would not only benefit the registration accuracy but also the system's clinical applicability: given that we are developing AXIS for eventual integration into the OR, we will need to explore and implement methods that are better suited for intraoperative registration and tracking. We discuss these clinical considerations further in Section 5.2.5. C-arm tracking accuracy could be improved by instrumenting the source and detector with two separate sets of optical marker triads and tracking them separately. In light of these improvement suggestions, future work in this area should aim to establish a baseline for clinical acceptability of artificial and real X-ray image agreement accuracy.

5.2.2 AXIS image generation speed

An additional point of feedback provided by the participants in the study questionnaires was to increase the speed of DRR generation in order to avoid lag time between C-arm movements and AXIS visual feedback. Ten of the participants suggested improving AXIS speed. As explained in Section 2.7, the DRR generating algorithm used is based on Siddon's ray-casting method and, despite the availability of more efficient algorithms, Siddon's method was chosen because a C++ script based on this method is freely available and includes a MEX wrapper for interfacing with Matlab (Siddon 1985). The ideal approach to improving the speed of AXIS would be to rewrite the DRR code using one of the more efficient algorithms described previously in Section 2.7, such as those reported to be 3-7.5 times faster, proposed by Han or Jacobs (Han 2000; Jacobs 1996). Additionally, the code could be written so that the computations can be performed on the GPU. This approach would also require a MEX extension to be written so that the C++ DRR function could be implemented on the GPU. The group that proposed wobble-splatting to improve efficiency and image quality (Section 2.7) reported a 70-90% reduction in rendering time when the DRR computations were performed on a GPU compared to on a CPU. While any increase in AXIS speed would be beneficial as it would have a cumulative impact on user experience and OR procedure times, we cannot speculate on the specific extent to which the speed would be improved for either of these proposed approaches since it is highly dependent on several factors including the DRR image resolution desired, the number of voxels within the CT volume, the DRR algorithm used, and the GPU being used.

5.2.3 AXIS image quality

Finally, another frequent suggestion provided by the participants was to increase contrast and spatial resolution of the DRR images to better match that of the real X-rays. While none of the participants rated the AXIS realism and accuracy to be poor and only seven of them rated it to be fair, 9 participants still suggested improvements on image quality. To better prepare AXIS for OR and educational settings, image quality could be improved by acquiring a higher resolution CT scan; however this would decrease the speed of DRR generation as a trade-off. Another approach, similar to improving the speed of AXIS, would be to re-write the DRR code using one of the alternative DRR algorithms that yield more realistic X-ray image predictions, such as cylindrical harmonics or wobble splatting, as proposed in Section 2.7 (Wang 2002, Spoert 2007). Also, image-processing techniques could be explored further in order to fine-tune the output DRRs. Finally, using real CT volumes with AXIS instead of a manikin's CT would yield more realistic images by providing information from real bone structures, as well as surrounding soft tissues. Overall, AXIS image quality improvements could enhance the user's learning experience with the C-arm and eliminate uncertainties associated with lack of image resolution, in turn increasing its potential, as a system, to facilitate communication between MRTs and surgeons in the OR.

5.2.4 Providing additional cues for users

While some participants certainly benefited from AXIS guidance and expressed confidence either in person during the study or through the questionnaire, others still admitted to struggling, often attributing their struggle to lack of background in radiology and anatomy. An additional feature to AXIS that could serve as a supplementary capability during C-arm practice sessions would be offering cues in the GUI letting the user know in which rotational and translation directions, and by how much, the C-arm must be moved in order to reach the desired view. The users could also be made aware, through the GUI, when they have achieved the correct anatomical view, deemed acceptable by surgeons in a pre-established baseline assessment for accuracy. This feature could easily be integrated by using the C-arm's tracked pose, calculating its difference compared to the target pose in real time, and breaking it down into its x-, y-, and z-translation and rotational components. Also, during the user study, participants often expressed difficulties with anatomical orientation relative to the anteroposterior and cranial-caudal directions. A compass-like cue on the GUI indicating where the head is or where the toes are pointing could help the C-arm users in anatomical navigation.

Finally, as discussed in Chapter 1, there are several safety-related decision-making factors in the OR that have a direct impact on radiation exposure, including the distance between the X-ray source and the patient, and how the X-ray source is positioned relative to the surgical table. An AXIS feature that would help new C-arm users learn this concept is a scatter radiation visualization module that would show the AXIS user how different C-arm positions relative to the patient affect scatter radiation propagation and intensity. The virtX group has proposed a method to calculate the propagation and intensity of scattered radiation and has implemented its visualization as a training aid in their X-ray simulation software package (Wagner 2012). This feature was shown to improve learning and understanding of scatter radiation concepts during a user study performed by the virtX group (Bott 2008).

5.2.5 Clinical considerations for the operating room

In its current state, AXIS has shown itself to be a powerful tool for MRT education and hands-on practice in C-arm manoeuvring and operation. However, additional work is required with AXIS in order to address a number of clinical considerations before being acceptable for the OR. Firstly, the line-of-sight condition that comes with using an optical tracking system like Optotrak is a major limitation with regard to OR readiness. The number of staff involved in a surgical setting, as well as the abundance of tools and equipment in the surgical theatre would render the maintenance of line-of-sight between the position sensor and the markers very challenging. There are a number of alternative tracking options currently available that could address this issue, such as inertial measurement units (IMUs), laser distance sensors, electromagnetic tracking, or the use of computer-vision in conjunction with a camera. Our Surgical Technologies lab is currently developing a base-tracking system that consists of a downward-facing camera that tracks the C-arm's position by using OR floor features in a computer vision algorithm.

Another limitation of AXIS in its current form is that the manikin is not only considered to be a rigid body, but also to be rigidly fixed onto the surgical table. In the real surgical scenario, the patient's anatomy would be manipulated and moved around throughout the procedure by healthcare staff. In order to eliminate this limitation, the patient's bones of interest should be tracked throughout the procedure, and furthermore, if the procedure consists of a fracture treatment, methods should be explored in order to track the movement of individual bone fragments. This leads us into the final limitation of requiring a patient-specific equivalent of a CT scan to be registered to the patient in a real OR setting. Preoperative CT scans are not always requisitioned by the surgeon, and when they are, they would quickly diverge from the current intraoperative condition, whether due to postural changes or shifts in bone position during a fracture reduction procedure. A CT scan library could potentially be maintained for the purposes of generating patient-specific models intraoperatively, where, for example, similarly sized scans from the database could be utilized instead and scaled to the patient's size and shape, at the cost of some loss of fidelity between the CT representation and the actual patient anatomy. Finally, as previously suggested in Section 5.2.1, the bone fragments in question could potentially each be registered to bone segment CT volumes and tracked individually to address patient movement throughout procedures.

5.3 Thesis Contributions and Concluding Remarks

The utility of artificial X-rays on C-arm performance was shown to be highly promising for both educational and operating room settings. This utility was demonstrated through the design and deployment of AXIS during a user study conducted in a simulated OR setting. This artificial X-ray-generating tool is intended to guide inexperienced users during C-arm usage, and our studies showed that AXIS decreases the need for real scout X-rays by a factor of a half and also has the potential to improve X-ray imaging accuracy. In conjunction, the time required to complete orthopaedic imaging tasks in a simulated OR setting was not affected. Overall these results are encouraging, and will stimulate further development of the AXIS systems to include both training and intraoperative applications. In an OR setting, artificial X-ray images have the potential to offer a tremendous positive impact by significantly reducing radiation exposure to both patients and operating room staff.

Bibliography

Amiri, S., Wilson, D., Masri, B., Anglin, C. (2014). A low-cost tracked C-arm (TC-arm) upgrade system for versatile quantitative intraoperative imaging. *International Journal of Computer Assisted Radiology and Cardiology, 9: 695-711*

Bates, P., Starr, A., Reinert, C. (2011). The Percutaneous Treatment of Pelvic and Acetabular Fractures. *The Orthopaedic Clinics of North America*, 42(1): 55-67

Birkfellner, W., Seemann, R., Figl, M., Hummel, J., Ede, C., Homolka, P., Yang, X., Niederer, P., Bergmann, H. (2005). Wobbled splatting – a fast perspective volume rendering method for simulation of x-ray images from CT. *Physics in Medicine and Biology,* 50: 73-84

Blinch, J. (2010). Controlling Optotrak from Matlab. *Motor behaviour: Cognitive psychology and neuroscience perspectives*. https://motorbehaviour.wordpress.com/2011/09/02/controlling-optotrak-from-matlab/ (20/01/2016)

British Columbia Institute of Technology (BCIT). (2016). Courses; Program Matrix. *Medical Radiography, School of Health Sciences.* http://www.bcit.ca/study/programs/6510diplt#courses (20/09/2016)

Booij, L. (2006). Conflicts in the operating theatre. *Current Opinion in Anesthesiology,* 20: 152-156

Boone, J. (2000). X-ray Production, Interaction, and Detection in Diagnostic Imaging. Beutal, B., Kundel, H., Van Metter, R. *Handbook of Medical Imaging, Volume 1. Physics and Psychophysics, SPIE,* 3-74

Bott, O., Teistler, M., Duwenkamp, C., Wagner, M., Marschollek, M., Plischke, M., Raab, B., Stürmer, K., Pretschner, D., Dresing, K. (2008). virtX – Evaluation of a Computer-based Training System for Mobile C-arm Systems in Trauma and Orthopaedics. *Methods of Information in Medicine,* 47: 270-278

Bott, O., Wagner, M., Duwenkamp, C., Hellrung, N., Dresing, K. (2009). Improving education on C-arm operation and radiation protection with a computer-based training and simulation system. *International Journal of Computer Assisted Radiology and Surgery,* 4: 399-407

Bott, O., Dresing, K., Wagner, M., Raab, B., Teistler, M. (2011). Use of a C-arm Fluoroscopy Simulator to Support Training in Intraoperative Radiography. *Radiographics – Radiological Society of North America,* 31: 65-76

Chen, X., Wang, L., Fallavollita, P., Navab, N. (2013). Precise X-ray and video overlay for augmented reality fluoroscopy. *International Journal of Computer Assisted Radiology and Surgery,* 8: 29-38

Cleary, K., Ibanez, L., Ranjan, S., Blake, B. (2004). IGSTK: a software toolkit for image-guided surgery applications. *International Congress Series,* 1268: 473-479

De la Fuente, M., Belei, P., Ohnsorge, J., Skwara, A., Radermacher, K. (2007). Zero-dose C-arm navigation: an efficient approach based on virtual X-ray targeting. *International Journal of Computer-Assisted Radiology and Surgery.* 2(1): 256-272

Dresing, K. (2011). X-ray in trauma and orthopaedic surgery. Physicial and biological impact, reasonable use, and radiation protection in the operating room. *Operative Orthopadie und Traumatologie*, 23(1): 70-78

Dressel, P., Wang, L., Kutter, O., Traub, J., Heining, S., Navab, N. (2010). Intraoperative Positioning of Mobile C-arms using Artificial Fluoroscopy. *Proceedings of SPIE,* 7625.

Folkerts, M. (2012). DRR Code. https://sites.google.com/site/ucsdresearch/home/cart/code (14/07/2015)

Fornell, D. (2011). An Introduction to Mobile C-arm X-ray Systems. *Imaging Technology News.* http://www.itnonline.com/article/introduction-mobile-c-arm-x-ray-systems (02/12/2016)

Fujii, S., Oku, K., Tsukamoto, Y., Tanaka, M., Ninomiya, A., Fukami, R. (2003). Mobile Radiography Device. *United States Patent, US 6,609,826 B1*

Giordano, B., Grauer, J., Miller, C., Morgan, T., Rechtine, G. (2011). Radiation Exposure Issues in Orthopaedics. *The Journal of Bone & Joint Surgery,* 93(69): 1-10

Gong, R., Jenkins, B., Sze, R., Yaniv, Z. (2014). A Cost Effective and High Fidelity Fluoroscopy Simulator using the Image-Guided Surgery Toolkit (IGSTK). *Proceedings of SPIE,* 9036.

Grimson E., Kikinis, R., Jolesz, F., Black, P. (1999). Image-guided surgery. *Scientific American,* 280(6): 62-69

Han, G., Liang, Z., You, J. (2000). A Fast Ray-Tracing Technique for TCT and ECT Studies. *Nuclear Science Symposium, IEEE,* 1515-1518

Jacobs, F., Sundermann, E., Sutter, B., Christiaens, M., Lemahieu, I. (1998). A fast algorithm to calculate the exact radiological path through a pixel or voxel space. *Journal of Computing and Information Technology,* (6)1: 1-12

Klein, T., Benhimane, S., Traub, J., Heining, S., Euler, E., Navab, N. (2007). Interactive guidance system for C-arm repositioning without radiation visual servoing for camera augmented mobile C-arm (CAMC). *Bildverarbeitung für die Medizin,* 1: 21-25

Kroon, D. (2010). Read Medical Data 3D. *Mathworks, Matlab Central, File Exchange,* https://www.mathworks.com/matlabcentral/fileexchange/29344-read-medical-data-3d (10/07/2015)

Matthews, F., Hoigne, D., Weiser, M., Wanner, G., Regazzoni, P., Suhm, N., Messmer, P. (2007). Navigating the fluoroscope's C-arm back into position: An accurate and practicable solution to cut radiation and optimize intraoperative workflow. *Journal of Orthopaedic Trauma*, 21(10): 687-692

Mezger, U., Jendrewski, C., Bartels, M. (2013). Navigation in sugery. *Lagenbeck's Archives of Surgery*, 398: 501-514

Mount Sinai Medical Center (MSMC). (2016). Orthopaedic Care: Advantages of Minimally Invasive Surgery. http://www.msmc.com/orthorehab/advantages-of-minimally-invasive-surgery/ (17/11/2016)

Müller, M., Belei, P., de la Fuente, M., Strake, M., Weber, O., Burger, C., Radermacher, K., Wirtz, D. (2011). Evaluation of a fluoroscopy-based navigation system enabling a virtual radiation-free preview of X-ray images for placement of cannulated hip screws, A cadaver study. *Computer Aided Surgery,* 16(1): 22-13

Müller, M., Kabir, K., Gravius, S., de la Fuente, M., Belei, P., Strake, M., Wirtz, D. (2012) Fluoroscopy-based computer-assisted navigation for implant placement and hip resurfacing arthroplasty in the proximal femur: the zero-dose C-arm navigation approach. *Biomedical Engineering,* 57: 209-219

Northern Digital Inc. (2015). Optotrak Certus: Technical Specifications. https://www.ndigital.com/msci/products/optotrak-certus/#optotrak-certus-technical-specifications (14/01/2017)

Pally, E., Kreder, H. (2013). Survey of terminology used for the intraoperative direction of C-arm fluoroscopy. *Canadian Journal of Surgery,* 56(2): 109-112

Reaungamornrat, S., Otake, Y., Uneri, A., Schafer, S., Mirota, D., Nithiananthan, S., Stayman, J., Kleinszig, G., Khanna, A., Taylor, R., Siewerdsen, J. (2012). An on-board surgical tracking and video augmentation system for C-arm image guidance. *International Journal of Computer Assisted Radiology and Surgery,* 7: 647-665

Rosenstein A., O'Daniel M. (2006). Impact and implications of disruptive behavior in the perioperative arena. *Journal of the American College of Surgeons,* 203:96–105.

Siddon, R. (1985). Fast calculation of the exact radiological path for a three-dimensional CT array. *Medical Physics,* 12(2): 252-255

Siemens AG, Medical Solutions. (2006). System Description. *Operator Manuel, ARCADIS Orbic,* Section 2.

Spoerk, J., Bergmann, H., Wanschlitz, F., Dong, S., Birkfellner, W. (2007). Fast DRR splat rendering using common consumer graphics hardware. *Medical Physics,* 34(11): 4302-4308

Suhm, N., Müller, P., Bopp, U., Messmer, P., Regazzoni, P. (2004). The MEPUC concept adapts the C-arm fluoroscope to image-guided surgery. *International Journal of the Care of the Injured,* 35: S-A120-123

Suhm, N., Müller, P., Hehli, M., Koller, S., Bopp, U., Jacob, A., Regazzoni, P., Messmer, P. (2003). Adapting the fluoroscope to image-guided surgery*. Injury*, 34(4):307-311

Touchette, M., Blinch, J. (2016). Step-by-step instructions to control Optotrak from Matlab on a 64-bit Windows platform. *MathWorks File Exchange,* https://www.mathworks.com/matlabcentral/fileexchange/56281-step-by-step-instructions-to-control-optrotrak-from-matlab-on-a-64-bit-windows-platform (15/02/2017)

Wagner, M., Dresing, K., Ludwig W., Ahrens, C., Bott, O. (2012). SIScaR-GPU: fast simulation and visualization of intraoperative scattered radiation to support radiation protection training. *Studies in Health Technology and Informatics*, 180: 968-972

Wang, F., Davis, T., Vemuri, B. (2002). Real-Time DRR Generation Using Cylindrical Harmonics. *Medical Image Computing and Computer Assisted Intervention,* 2489: 671-678

Wang L., Weidert S. (2010) First animal cadaver study for interlocking of intramedullary nails under camera augmented mobile C-arm. A surgical workflow based preclinical evaluation. *Proceedings of IPCAI, lecture notes in computer science,* 6135: 56–66

Williams, T., Syrett, A., Brammar, T. (2009). W.S.B. – A fluoroscopy C-arm communication strategy. *Injury, 40: 840-843*

Zheng, G., Nolte, L. (2015). Computer-Assisted Orthopaedic Surgery: Current State and Future Perspective. *Frontiers in Surgery,* 2(66): 1-14

APPENDICES

Appendix A User Study Casebook

During the imaging tasks of the AXIS user study, the participants had access to a casebook binder, which included reference material for each of the six imaging tasks. The participants were allowed to refer to this reference book as much as they liked, to help guide them through the tasks. This appendix includes the pages included in the casebook binder. Note that the each of the two X-ray images were printed on one whole page, but they are minimized and presented together on one page here to save space.

AP Pelvis View – Main Goals

- X-ray source under table; C-arm position is usually straight up and down
- May need to adjust starting position (ex: if patient has pronounced lordosis)
- Lumbar spines should be lined up with tip of coccyx (posteriorly) and symphysis (anteriorly)
- Posterior features most important (ex: lumbar spines, coccyx)
- This view is used to assess symetry and overall shape of pelvic ring following surgery

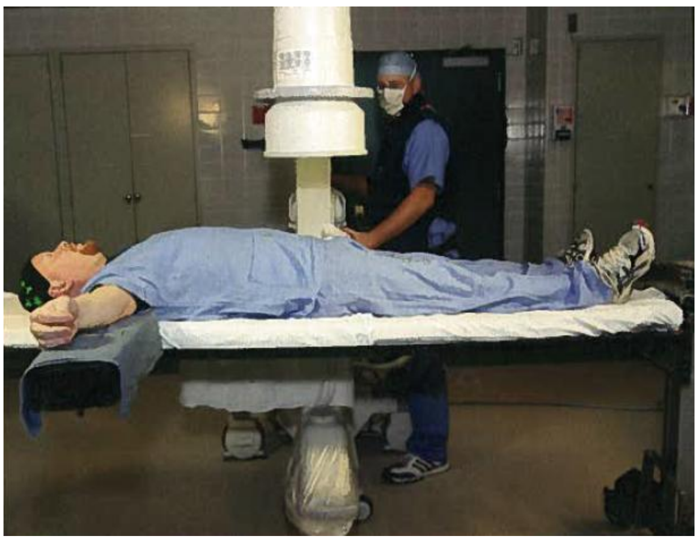

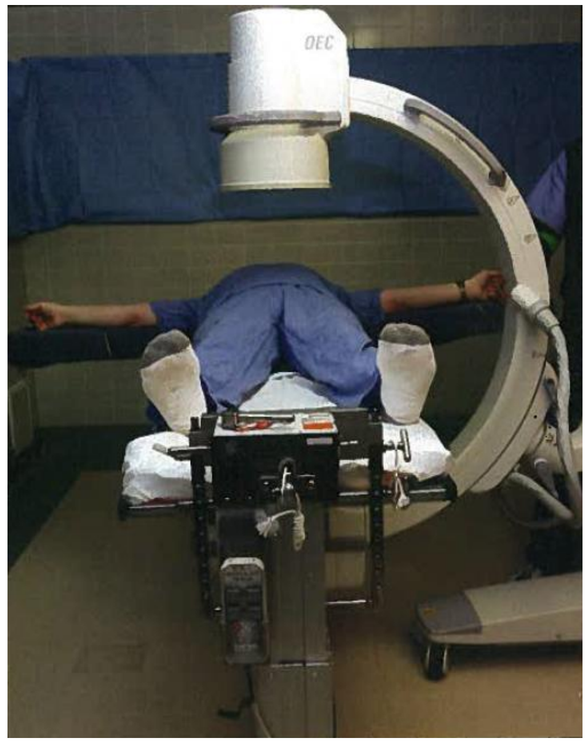

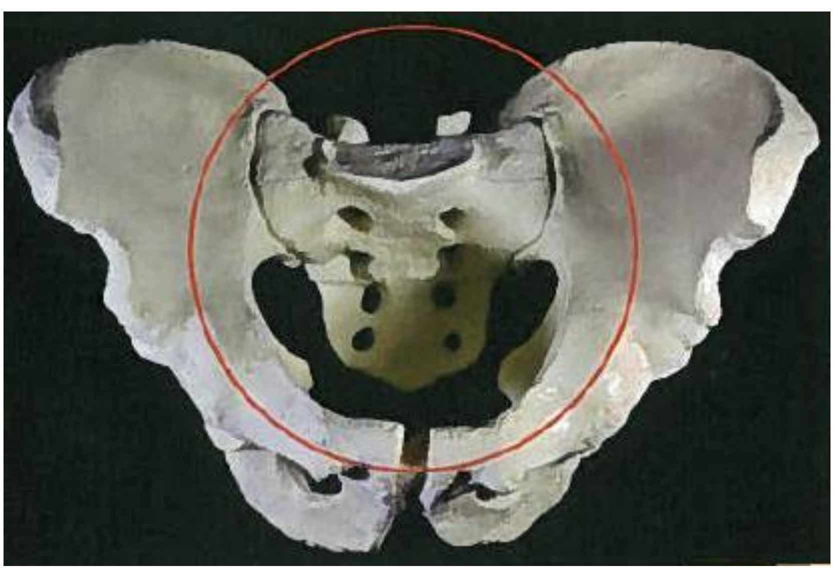

Surgeon A – AP Pelvis:

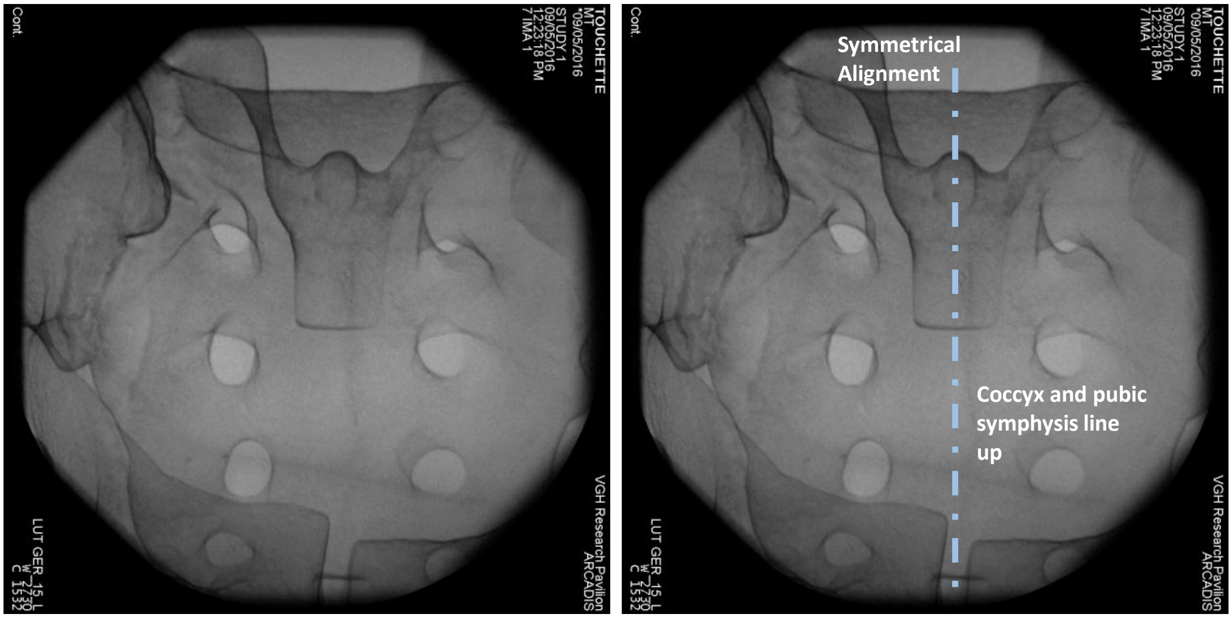

Teardrop / Teepee View – Main Goals

- Look for the characteristic "teardrop" or "teepee" structure in the X-ray
- This view is used to view the LC-2 channel, which is a long column of bone running from the AIIS (anterior inferior iliac spine) to the PSIS (posterior superior iliac spine). The direction of this column (if patient is supine) runs from anterolateral (AIIS) to posteromedial (PSIS).
- The teepee view looks directly down this thick column of bone

Surgeon A – Teardrop / Teepee (Left):

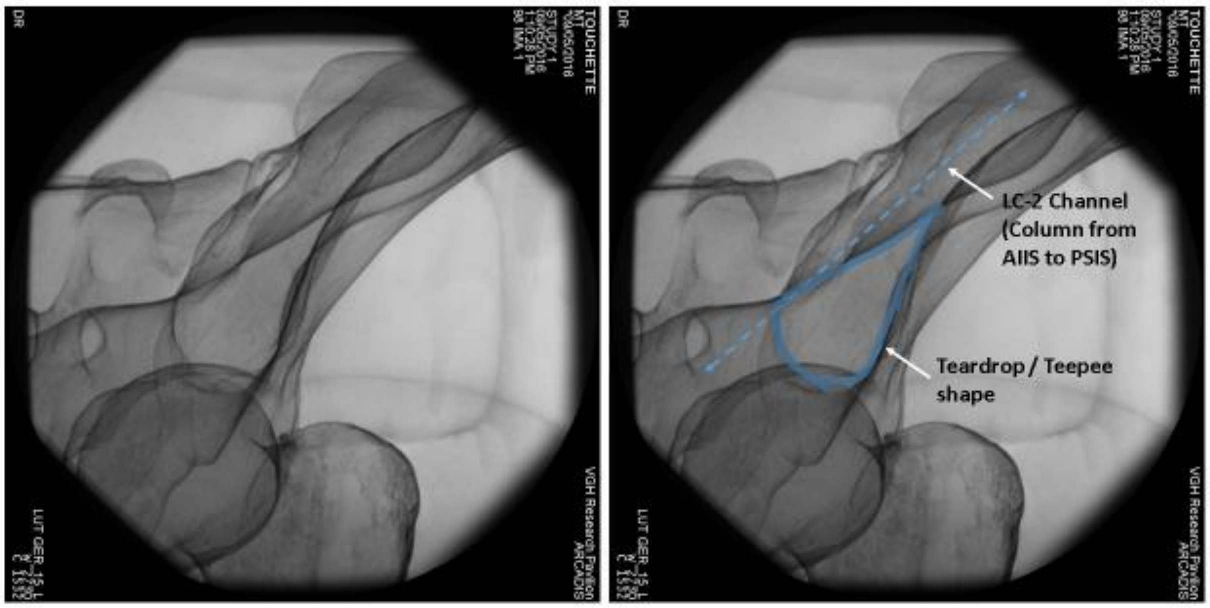

Pelvic Inlet View – Main Goals

- C-arm is tilted about 40 degrees (detector towards head, source below table; exact tilt depends on patient lordosis)
- Sacral promontory should overlap anterior cortex of first sacral vertebral body (S1)
- Lumbar vertebral spines should line up with the coccyx (posteriorly) and with symphysis (anteriorly)
- Posterior features are most important (ex: lumbar vertebral spines, coccyx)
- This view is used for assessing the posterior pelvic ring, sacrum, sacro-iliac joints, and symphysis

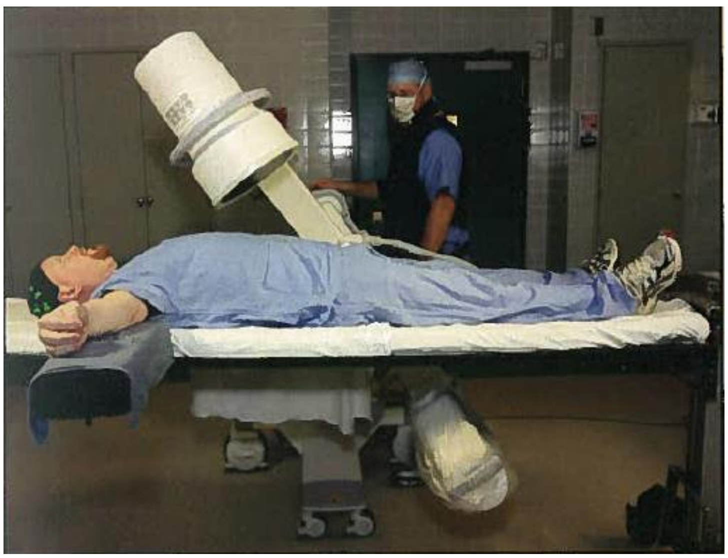

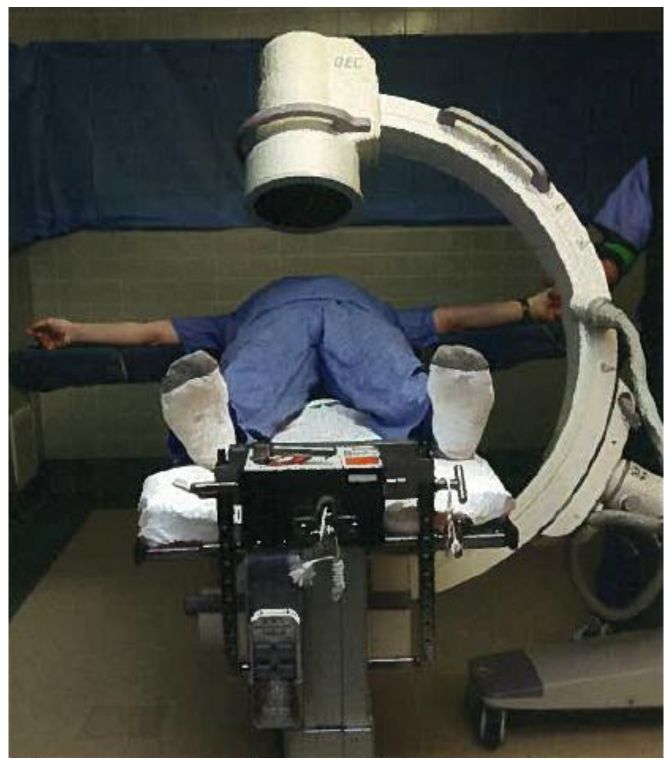

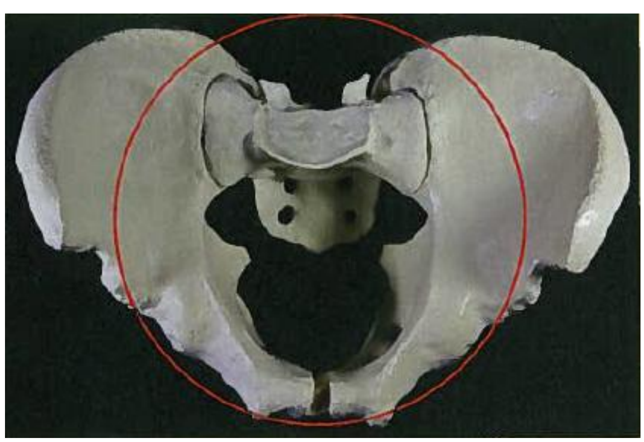

Surgeon A – Pelvic Inlet:

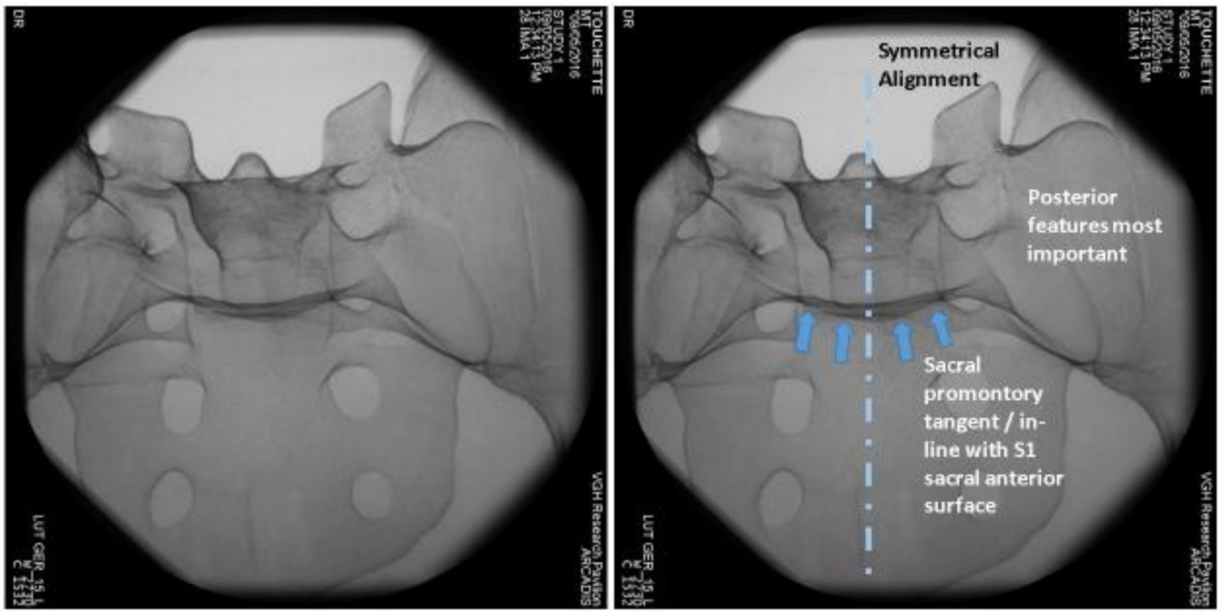

True Lateral Pelvis View – Main Goals

- The C-arm is lined up directly side-to-side (for this study, please have arm reach over patient instead of the customary underneath)
- Both sciatic notches should line-up with each other

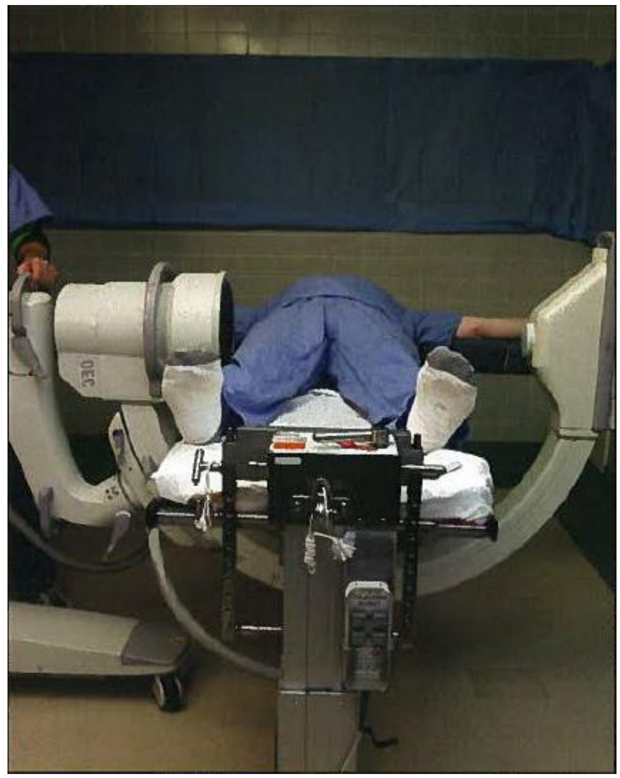

Surgeon A – True Pelvic Lateral:

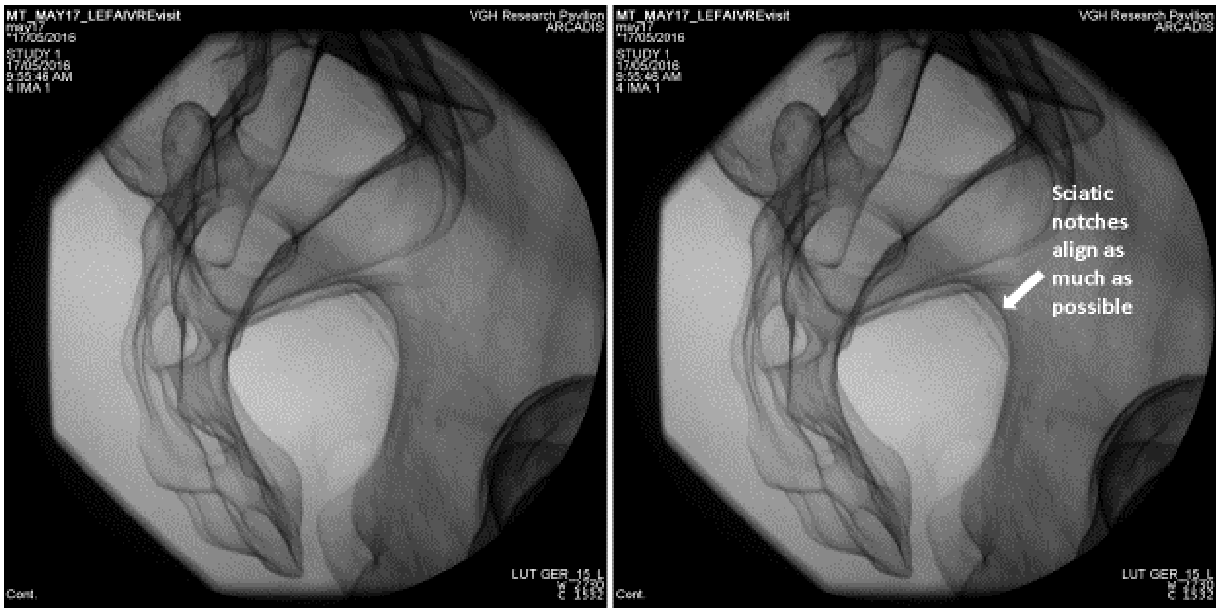

Down-the-Wing View – Main Goals

- The beam is aligned with the outer cortex of the posterior ilium (arrows in reference image) by tilting the C-arm towards the side of interest, and towards inlet view.
- All or part of the LC-2 channel can be viewed, which is a long column of bone running from the AIIS (anterior inferior iliac spine) to the PSIS (posterior superior iliac spine). The direction of this column (if patient is supine) runs from anterolateral (AIIS) to posteromedial (PSIS).
- The outline of the outer cortex of the posterior ilium can be seen
- The PSIS (posterior superior iliac spine) can be seen

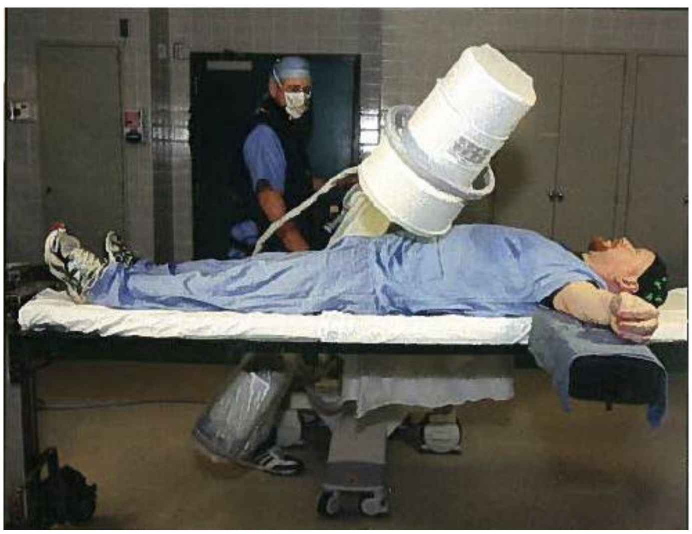

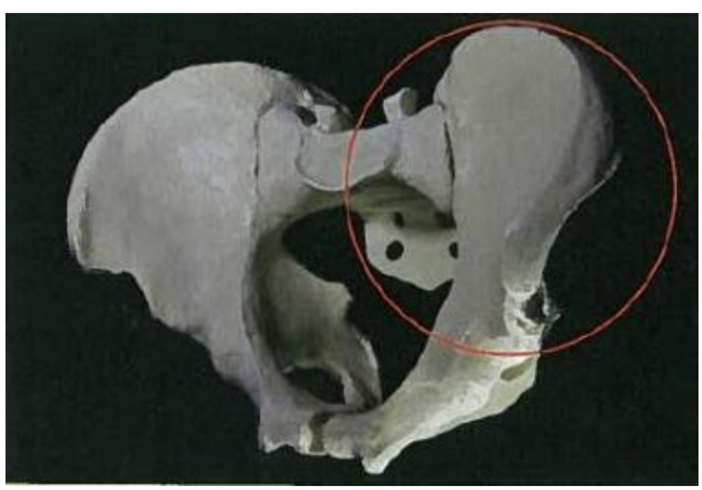

Surgeon A – Down-the-Wing (Left):

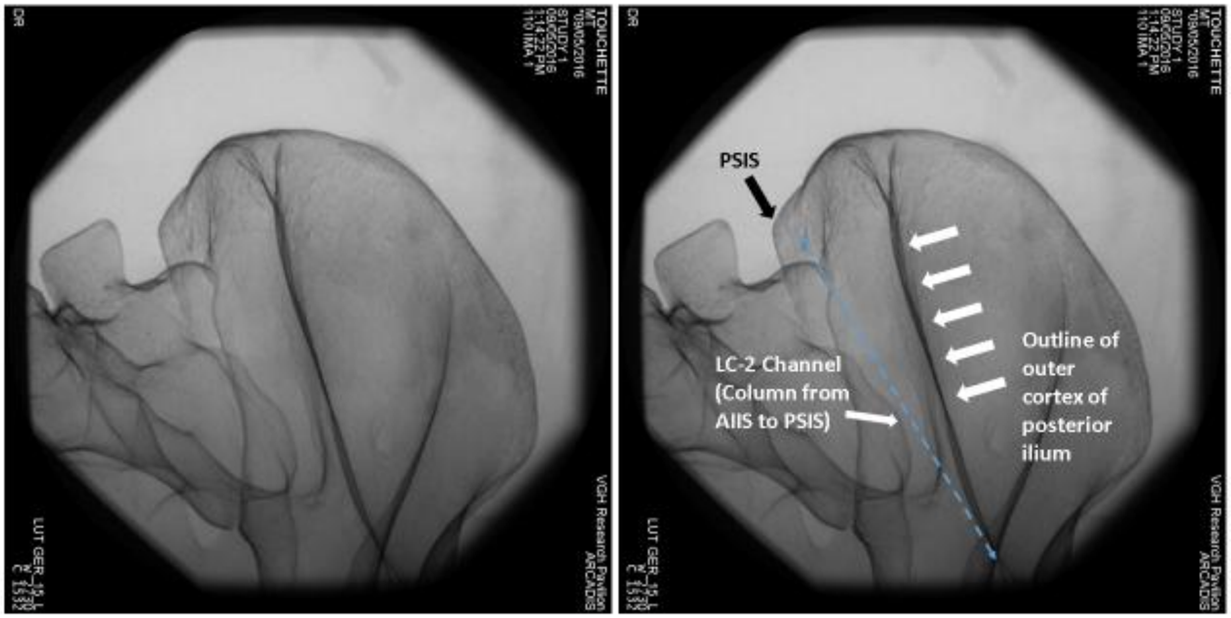

Pelvic Outlet – Main Goals

- C-arm tilted about 45 degrees (detector towards feet & source under table; exact tilt depends on patient lordosis)
- The top of the pubic symphysis should be level with the second sacral body (S2)
- The lumbar vertebral spines should line up with the sacrum (posteriorly) and symphysis (anteriorly)
- This view can be used to view fractures of the sacrum, pubic rami, or widening of the sacro-iliac joint

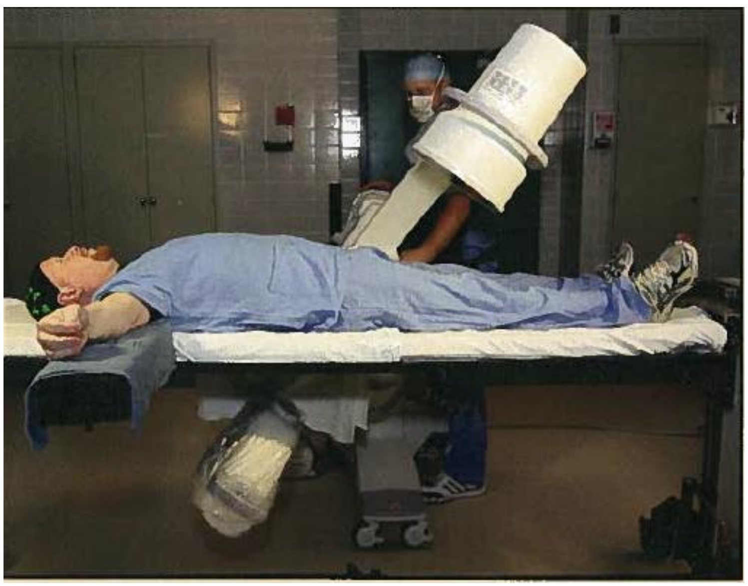

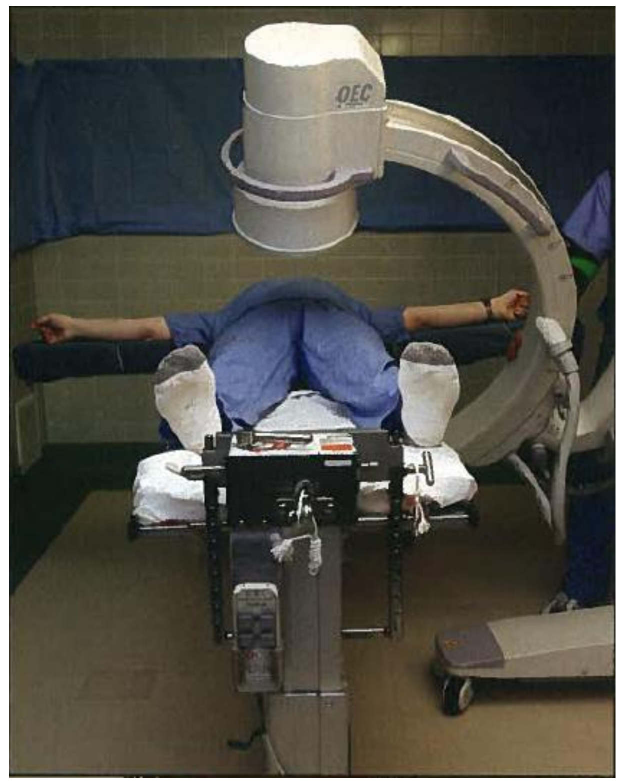

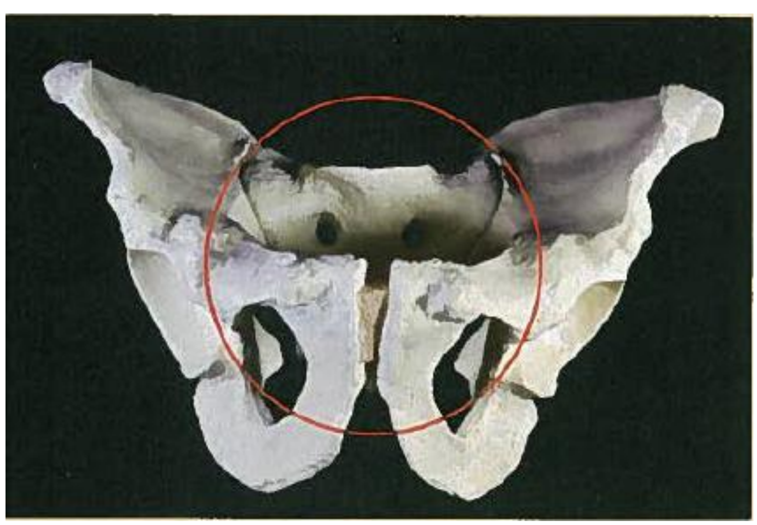

Surgeon A – Pelvic Outlet:

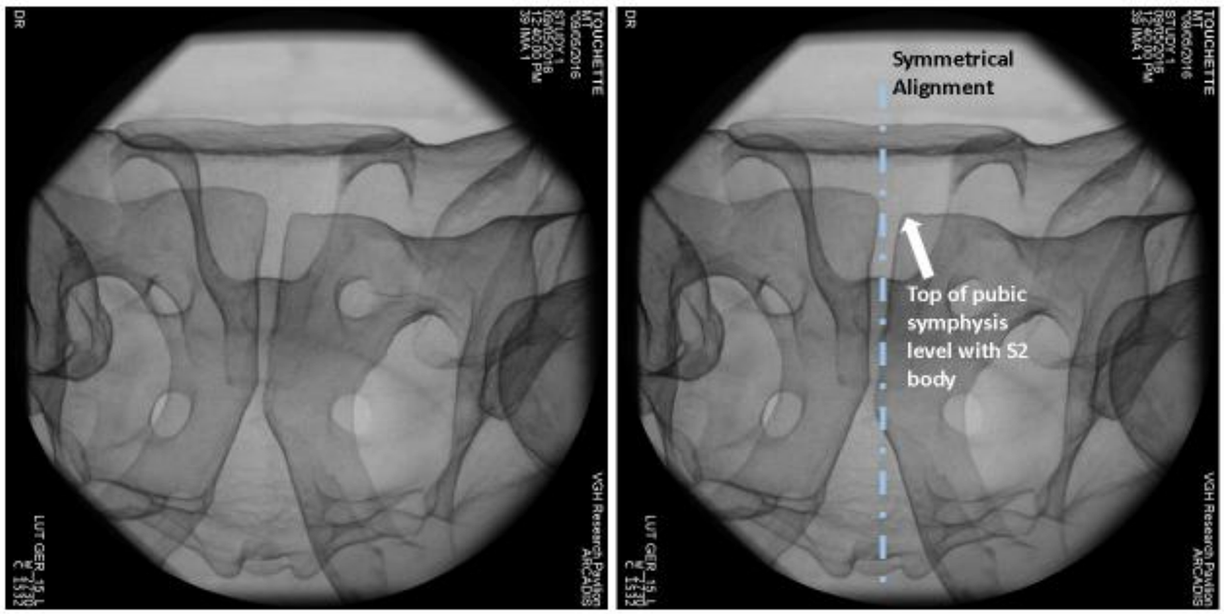

Appendix B AXIS User Study Questionnaire Responses

After each participant carried out the AXIS user study tasks, we provided them with a questionnaire, which all thirty participants agreed to complete. This appendix presents the questions included in the questionnaire, a summary of the numerical results, and a summary of the additional written information the participant may have provided in the "*Additional Comments*" sections.

1. What is your current age:

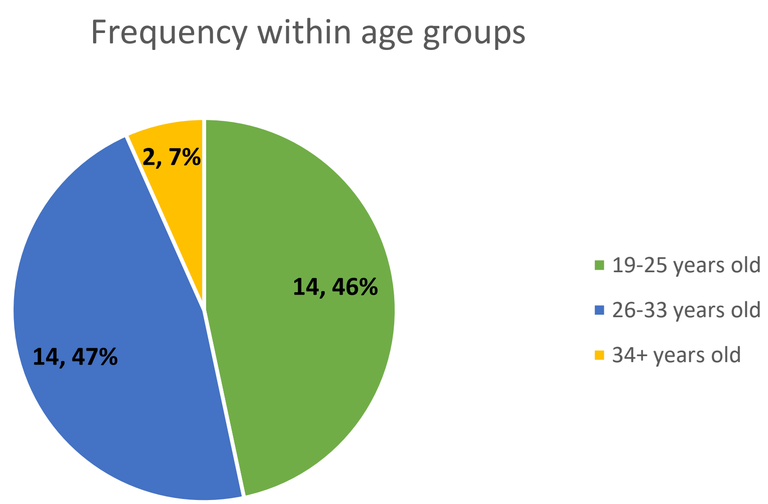

Average: 26.9 years
Standard Deviation: 5.97 years

2. What is your gender:

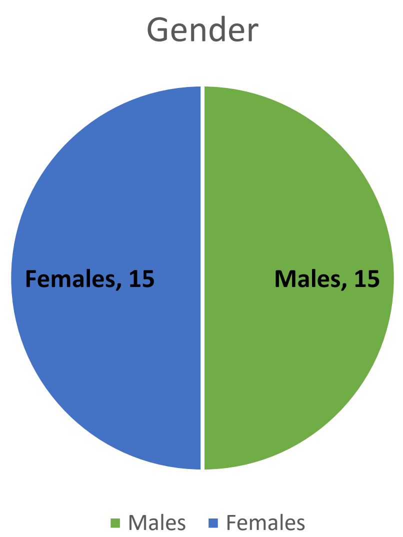

3. What was your experience with C-arm operation **<u>before</u>** the study?

Circle the best answer – my experience with C-arm operation was:

a. No hands-on experience; I've only learned about C-arm operation through readings and/or demonstrations
b. I've manoeuvered a C-arm in a course lab before but I've never taken real X-rays with it
c. I have operated a C-arm and taken X-rays under supervision during my rotations before
d. I have professional work experience with C-arm use

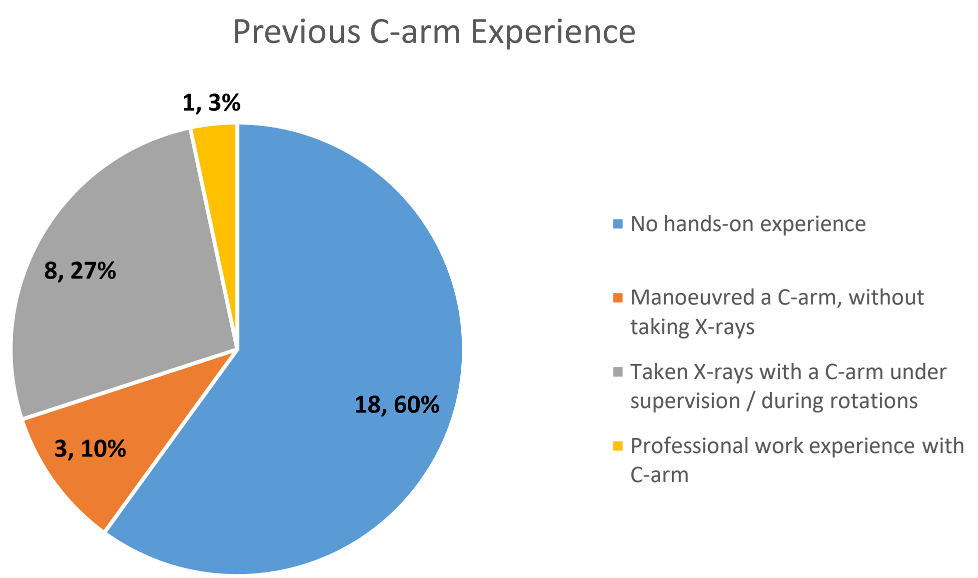

Average (0=No experience; 3=Professional work experience): 0.7
Standard deviation: 0.98

4. By circling the best answer, rate your level of confidence in your ability to capture the correct anatomical view in reasonable time during the standard X-ray C-arm evaluation exercises (**without the AXIS**). Additional comments are welcome (i.e. what did you have particular difficulties with; what did you feel confident about; what did you feel uncertain about?)

No confidence at all	Somewhat unconfident	Neutral	Somewhat confident	Very confident

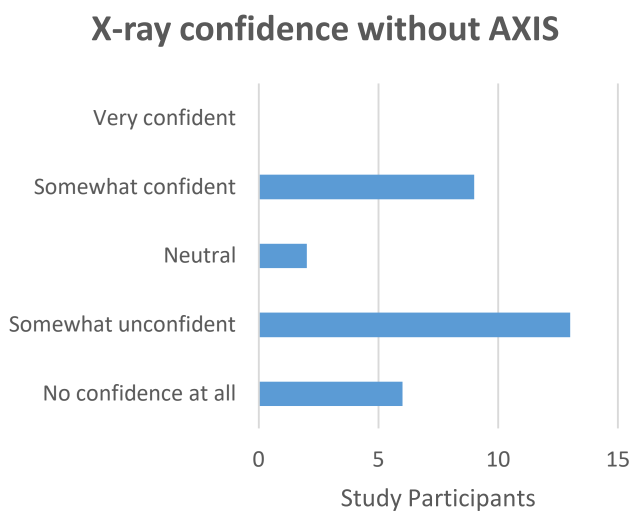

Average (0=No confidence; 4=Very confident): 1.5
Standard deviation= 1.14

Additional Comments:

New views, never attempted before today
Took a bit of time to use the C-arm but felt comfortable after first couple. Some of the images I had never seen before so it took some trial and error.
I'm confident with my knowledge of anatomy and angles required to obtain the image. I was unfamiliar with some of the views required which made it more difficult to mentally adjust angles to capture the correct view. The images obtained without AXIS were helped by completing them after first using AXIS. I already understood the unique anatomy of the phantom and was able to adjust prior to exposing.
I was uncertain about the views that I've never performed in OR (teardrop, inlet/outlet). Without looking at patient's landmark for positioning, it was hard to even locate where the required structures were.
New views I'd never heard of; I felt I was taking a long time but I was also really trying to match the picture in the book.
Felt uncertain about the rotation and resulting views at first; but after the first view / joint, I was better able to predict how to manoeuvre the C-arm to get the desired images.

Without previous experience using a C-arm, I felt as if I was definitely guessing the positioning of the images. What I found most difficult was understanding whether or not I was turning the system in the correct direction to adjust my view the way I intended.
I had more difficulty with imaging when the C-arm needed to be adjusted at 2 or more angles.
No imaging experience, so unsure about how to adjust from the initial image even if I had an idea about how to get the end image (how much movement was needed to move a certain amount); Took a long time trying to figure out which direction to move based on what I wanted to do.
Was very hard for me to tell if I was anywhere close to the region I was to be taking an X-ray of beforehand. Took a few initial X-rays for me to even get the correct placement, then subsequent images to do minor adjustments in positioning / angle / etc.; Took a lot of tries for me to get an image I was not even fully confident about, and a lot more time.
Unfamiliar with using X-ray on
I could capture a reasonable X-ray after about 6 snap shots and about 15 minutes. The shots with multiple axis tilts were particularly difficult.
It took some thinking to determine what correct C-arm orientation would result in proper images (especially for the teardrop view)
Tried to replicate pictures of C-arm orientation in binder -> felt like I was guessing; Took a while to wrap my head around how C-arm adjustments changed image orientation.
By trial and error I guess, that's how I did it. The first image would always be somewhat or very "off", but I just tell myself "let's just take this image to see how it looks.
Confidence grew across the 3 attempts as familiarity with C-arm grew; What is considered "reasonable time"?
Especially ok when capturing simple views such as just the AP view.
I am not super familiar with the pelvis, so it was very difficult at first to predict how the motion would affect the image.
I got to use the C-arm with AXIS first so using it without after made me feel a lot more uncertain, however with a little bit of practice prior, I don't feel I'm in the "no confidence at all" category.
First image I took was always a guess based on the pictures provided.
It was definitely a learning curve, even for the first 3 tests, as to how the C-arm works. The C-arm also did not move precisely from the base (base movement) which made fine adjustment difficult.
No. Literally no reference to start. Binder of info is not good enough.
Can get images eventually, but involves trial and error. First X-ray images were way off and required large adjustments.
Finding the correct views - or close to- was not very challenging, however matching the image to the one provided in terms of smaller details was difficult.
Having the sample views from an experienced surgeon helped to capture the desired characteristics. I tried to compare my X-rays to the ones in the manual to see if they are valid.
Difficulties with finding the right angles of the C-arm. Also finding the correct part of the anatomy of the patient.
The X-rays seemed to change considerably in between different configurations that I tried. This severely hindered any intuitive understanding of what I was looking at.

5. By circling the best answer, rate your level of confidence in your ability to capture the correct anatomical view in reasonable time during the Artificial X-ray C-arm evaluation exercises (**with the AXIS**). Additional comments are welcome (i.e. what did you have particular difficulties with; what did you feel confident about; what did you feel uncertain about?)

No confidence at all	Somewhat unconfident	Neutral	Somewhat confident	Very confident

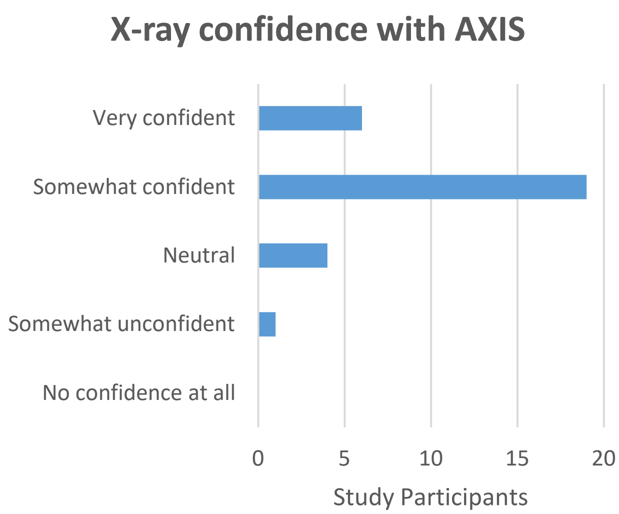

Average (0=No confidence; 4=Very confident): 3.0
Standard deviation: 0.69

Additional Comments:

Guess work is eliminated --> Need for repeats were due to slight imprecision between AXIS & captured image, although slight.
It can get you in the ballpark and then you fine adjust the C-arm. Very interesting program. After the first image I could sense how far off AXIS was from the actual fluoro image making the next two images easy to acquire.
I thought the AXIS was a great tool. It helped me get to an approximate position before taking the first X-ray image. The only thing that I had difficulty with is the AXIS didn't seem to pick up slight movements well.
I found AXIS very useful when ballparking the correct view, as well as for the fine tune adjustments when adjusting the angle of the 'C' and cranial-caudal angles. When the cranial-caudal angle was significant however, the red circle of AXIS was not very accurate.

I was way more confident operating the C-arm with AXIS. To be able to see which adjustment I am making and to see if I'm doing a right correction, I think it will be helpful for stressful OR cases or rare views which I've never done before; I found the screen is very small so it was hard to see the exact location of the C-arm.
For the most part it was great (except last image); It gave me a great starting point, especially for new views; I definitely needed to expose less often.
Using AXIS definitely made capturing desired views easier; It was nice to get feedback after making adjustments to the C-arm without having to take an X-ray to see what the image would look like.
The AXIS helped me with my problem of not being sure about which way to turn the C-arm as I was adjusting it. Being able to watch the image adjust as I adjusted the C-arm was quite helpful.
AXIS made it much easier to locate the region of interest with the C-arm
AXIS gave a general idea as to how the image changed when I moved in a certain direction, so it was easier to see when I was moving the wrong way; Had difficulties seeing if little movements were having an effect on the image, it's easier to see what happens with the larger movements.
Definitely way easier than without AXIS. Much quicker to get my bearings and identify the region to be X-rayed; Not as useful for the minor adjustments in angle / position as for initial positioning; Was still not 100% confident in my submitted X-rays (mainly as a result of my unfamiliarity with X-rays) but was definitely easier to get to an image I was willing to submit than without AXIS.
I felt faster and had better adjustment capabilities with the AXIS system. I would likely feel very confident with slightly reduced lag and if the C-arm was easier to adjust by small amounts.
Real time feedback from the AXIS made the thinking effort reduced significantly. Some minor adjustments still had to be made due to the AXIS being slightly out of sync with the C-arm. It should also be noted that difficulty in acquiring the wing view was due to my lack of hip anatomical knowledge.
Felt way better! Set up approximately like the binder picture then searched the AXIS for features I could recognize and adjusted from there.
It requires initial orientation, correct view that takes some getting used to but as soon as I see the correct view I'm quite confident that the X-ray image is the right one. So getting things right at the first "shot".
The first effort showed some lack of correlation in the AXIS view vs. the actual X-ray. It was much more useful for identifying features that were difficult to obtain.
One view was particularly difficult (lateral) very helpful to see how a given motion would affect views.
You are able to see how small motions of the C-arm will change the image with fewer X-rays.
Having the AXIS present is very helpful, especially for capturing more hidden parts.
Let me compare the landmark features on the image to the AXIS and then line them up where it looked the same.
Real time feedback helped a lot. Pelvis tilt in the outlet view was different between AXIS & the dummy which added an additional X-ray. Overall, AXIS was much more confidence inspiring.
Let's me try before I irradiate a pour soul w/ X-rays.
Still need a significant amount of time and images, but first image is closer to the goal.
I found the AXIS system very helpful in getting immediate feedback on adjustments, but didn't feel it helped me when trying to match the precise orientation of the X-rays to the reference image provided.
AXIS definitely was helpful by showing real-time views. Lower lag time (faster response time) would help even more.

The first case I did with AXIS (it was also the first of the study) took me a long time because I misunderstood the anatomical view required. It wasn't an issue with AXIS or with the C-arm. I was looking for a view that was not correct. Also, it was the first X-ray I ever took. I think the more X-rays I took the faster and easier to get to find the angles of the C-arm for the views.
I was not completely sure that I captured the optimal view. Other than that, I was quite relaxed with changing viewpoints. The real-time feedback was really helpful.

6. How would you rate usefulness of the *Artificial X-ray Imaging System* in guiding you to the desired view before taking real X-ray radiographs (circle the best answer)?

Poor **Fair** **Good** **Very Good** **Excellent**

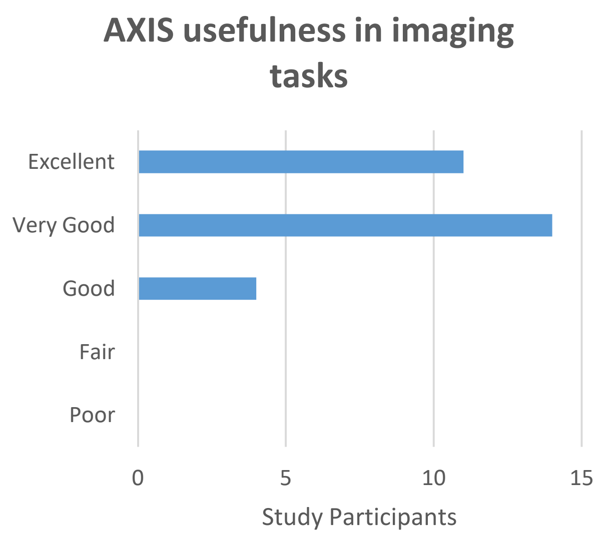

Average (0=Fair; 4=Excellent): 3.2
Standard deviation: 0.69

Additional Comments – What was useful? What was not as useful?:

(See previous comment); Useful for reducing unnecessary exposure; Slight imprecision still produced acceptable images, but required some modifications to achieve optimum.
For the challenging views it gets you in the ballpark. I could see this reducing a lot of dose to the patient.
It definitely eliminates the preliminary images taken with X-ray; ultimately saving dose.

Useful --> to fine tune angle; Not as useful --> I became too obsessed with finding the "text book" image. This took extra time.
To be able to see if you are in the right location & making a right correction, this would be very useful in the clinical situation.
It was useful; it made capturing desired images a lot easier.
The only problem I encountered was with the calibration of the system.
Useful: Can visualize the anatomy easily; Could be better: The colours from AXIS should match the X-ray output (i.e. white for bone)
Getting a general idea about what was happening as I moved the C-arm was very useful; Since the AXIS image didn't quite match the X-ray image, it wasn't as useful in being accurate or with details
Easy to use and made me more confident
Excellent to get initial placement & first image, good but not as useful to make minor corrections to get the "perfect" image.
Slow to load
Very useful for spatially orienting yourself + reducing the number of X-rays
Higher resolution and better AXIS / C-arm synchronization would have increased my rating to "excellent". Also, refresh rate was slightly slow.
Zoom was a little different than X-ray but once I figured that out it was so easy to use.
Visual aid is very important for getting the right X-ray image.
Took time to get used to.
Difficult to see alignment of the sciatic notches on AXIS
But you need a CT for registration.
It was very useful to see where the laser was pointing before taking the image. When I did not have the AXIS, I was mostly guessing where my laser was generally pointing.
Having no knowledge of C-arm operation it was super helpful.
Very helpful for gross placement.
Low fps; No frame of reference; Low resolution; 3D C-arm or guidance cues would be good.
Most images were very helpful and allowed me to get semi-accurate results right away. The tilt of the pelvis being off in one case caused some trouble.
(See prev) I found it especially useful in understanding the effects of certain orientation changes.
Refer to my previous answer.
In my personal case, as I started the study with the AXIS and it was the first time I took X-rays, I started to move the C-arm around to look for the right position instead of thinking what the best position was first. Without the AXIS you need to make sure you get the right angles and views before shooting. With AXIS I tend to just move the C-arm around to try new views.
Useful- Real-time feedback in particular.

7. How would you rate the *accuracy and realism of the artificial X-ray images* in comparison to the real ones (circle the best answer)?

Poor **Fair** **Good** **Very Good** **Excellent**

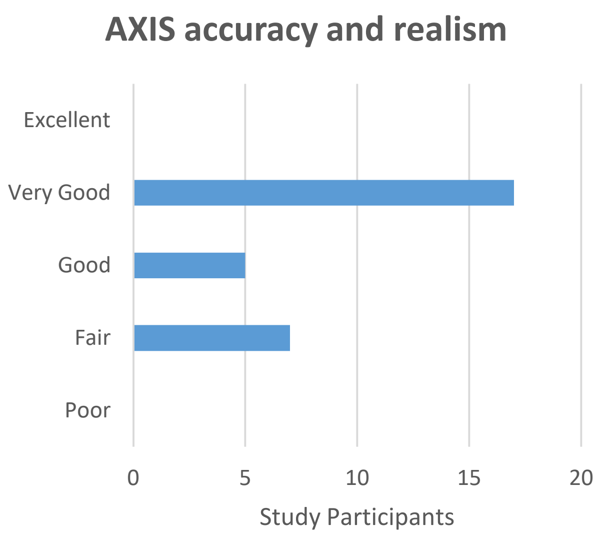

Average (0=Poor; 4=Excellent): 2.3
Standard deviation: 0.86

Additional Comments:

Almost equivalent to low dose but nowhere near fluoroscopy diagnostic images.
It is pretty close, after the first image I adjusted for how much it was off.
AXIS pretty much replicated the X-ray image. Very realistic and quite accurate.
The angles seemed to be quite accurate. The images were very realistic. The location was not always accurate.
Cephalad-caudad & orbit angles were slightly off from the actual ones.
The quality of the images on the AXIS system were good.
Not all X-ray details were visible, but most were.
Generally the images matched
Quite similar: enough to be a useful guide to taking an X-ray image.
Major landmarks were displayed very clearly; Minor landmarks could be seen with some effort (not that much effort though); Refresh rate was slow - faster DRR would've made adjustments quicker; Orientation between AXIS and C-arm slightly out of sync. Resulted in extra fluoro shot in last view (pelvic outlet).

Could recognize all the features I was looking for. Responded very quickly to my C-arm adjustments.
Maybe the correlation was a little off? But definitely more useful than doing by without the AXIS program.
There were some slight differences but overall felt similar to the actual X-ray views.
The artificial X-rays were very grainy and the colors were inverted, but good for overall guidance.
The image on AXIS was blurrier than the actual x-ray, however it was clear enough that I could see what my x-ray was supposed to show.
Some things were slightly off such as rotation on head-to-toe axis but it was constant so I just adjusted for it.
A bit different resolution (i.e. better res for the X-ray) but it was still extremely useful for gross alignment: pelvic tilt was a bit off for the last view (outlet).
Definitely not great. Some work to do on quality of image.
Most images were very accurate, one view was off.
There's something different about the grey-scheme. Also the resolution is not amazing, which makes seeing some of the smaller features hard.
Things to be improved (in my idea): faster response time, higher resolution, better contrast.
I could see some discrepancy in pixel values - but overall the image patterns and major anatomical details seemed to agree very well.

8. What did you like about using the C-arm guided by the Artificial X-ray Imaging System? Do you have any suggestions for improving the C-arm with the Artificial X-ray Imaging System?

Love seeing an image composite before exposure --> adjustments could be made on the fly allowing for more rapid assessment; Tweak the calibration slightly to match with acquired image --> though it is still acceptable.
I like knowing that you can get in the rough area and not be exposing the patient; Nothing to suggest.
I liked seeing where I actually am on the mannequin before taking an X-ray. Something that could make AXIS better is being able to detect tiny movements made by the C-arm.
The lag time between adjustments could be shorter. I found myself over adjusting while I was waiting for the imaging to catch up. I think physicians would become impatient.
I like the AXIS because it doesn't use radiation; The AXIS monitor screen can be bigger; If image quality can be improved, it will be easier to position the C-arm even more.
Very helpful; Things that would be nice would be clearer images and ability to track what is happening with the patient live; It was great being able to get the idea of where I was at before exposing though.
With no background in Radiology, I can't give feedback on areas of improvement. However, I felt more confident with AXIS than without it. Additionally, I felt as though I took less X-rays with AXIS to achieve the desired views.
I found it extremely useful to be able to see which anatomical features were caught in the field of view. Possible improvements may include reduction in delay of the image and image clarity.
See question 6; Another improvement can be increasing the frame rate so the display updates more quickly.
Liked seeing the live view of the movements; Larger image on screen to see from farther away; Less grainy / clearer images.
I liked everything about it!

Very good setup & easy to use; Once or twice I wanted to adjust the C-arm by standing on the side of it that interfered with the sensors on the AXIS, causing the picture to disappear but that was easy enough for me to avoid afterwards.
Perhaps providing real-time guidance to the user. For example, a sample of the desired image can be given to the artificial X-ray imaging system, and then based on that and the current image of the user, some of feedback be provided to the user (tilt the C-arm; move it forward; etc)
Seemed close in terms of predicting where images would be
Easy to spatially orient yourself when positioning C-arm
It was interesting moving the C-arm around and acquiring live feedback from AXIS as it provided me with an intuitive understanding of C-arm views with the hip; Assurance in image prior to X-ray exposure made me more confident in taking the shot without overthinking what the output would look like.
Felt less like I was blindly searching for an image. Sorry, can't think of any suggestions.
Visual aid is very useful. It tells me what I sort of image I would get, instead of leaving it to chance or trial and error.
It was useful to have a guide to show where roughly the C-arm arm should go - although I did not rely on it as much as I thought. It would be useful to have a more definitive correlation between the contrast (colours) on the AXIS and on the actual X-rays.
It is nice to see the effect of a given adjustment.
I like the real-time feedback.
As someone with no experience, an xy-axis type of orientation would be helpful but I feel those with anatomy would be fine using the system.
Real time (lag didn't really bother me); Similar rendering (i.e. black & white; close to what an X-ray looks like)
GOOD: "Preview" of image; Reasonably realistic; Changed as I moved the arm. BAD/IMPROVEMENTS: No reference frame; 3D scene?; Add the blue/ yellow/ green [C-arm's tilt, orbit, and wig-wag lock/unlock buttons] cues to the image
It was very useful to conceptualize in 3D space what the different motions of the C-arm did in real time without using an X-ray. Improvements would be better images and faster refresh rate.
I liked having near-instantaneous feedback on adjustments made. A faster update / frame rate would be nice, and matching the image style to the C-arm would make it more intuitive.
It gave me the confidence to know that the X-rays I took were the ones I was looking for; I guess the single-shot images appearing when moving the C-arm could update faster. Sometimes the image gets stuck and you have to wait.
What I liked: The red circle identifying the field of view; Real-time feedback (the slight lag was not a problem for me).

9. What do you consider to be the most challenging aspect of operating a normal C-arm? Which tasks/procedures would you most like to have guidance for?

None; New procedures that I am inexperienced with required the most guidance --> pelvic views are challenging.

The challenging part of operating a normal C-arm in the OR is the difficult views like the teardrop and other view where you are putting the C-arm in multiple angles. Without guidance I feel as a student you would end up giving the patient more dose to try and get the image and could make the doctor upset as you take more time positioning.
For IM nails, getting the holes aligned is quite difficult and we end up using a lot of fluoro time. AXIS would help with that.
Understanding what the surgeon wants to see on the image. AXIS is extremely helpful for guiding centering and including required structures.
When a patient is draped during an operation, it is challenging to locate the patient's anatomy; I find a tibia/fibula OR case to be challenging with a normal C-arm - AXIS would be very useful.
Finding the anatomy is definitely the most challenging, especially when you're trying to find the surgeon's pin and then get it at the specific angle he wants; Trauma, any orthopaedics for big parts really.
Finding the correct position of the C-arm to get the views you want would be the most challenging; I found the reference images provided to be very helpful
I think the most challenging part was being able to visualize and understand which direction was the correct one when it came to adjusting the arm in an effort to improve the view of a particular feature.
Some of the views required during surgery are very precise, so it is difficult to know whether you have aligned the arm correctly without taking an X-ray.
Knowing how much movement translated to what movement in the image; Reminders on how to move the C-arm to get a certain perspective / move the image in a certain direction.
Most difficult part is having a concept of spatial reasoning. I liked having the screen because I could see what I was taking an X-ray of.
Was not confident in knowing what adjustments to make in the C-arm position (angle, position, etc) for an adjustment I identified and wanted to make on the X-ray image.
It does not have real-time guidance system.
Orienting the C-arm with respect to the patient to capture an image with sufficient information.
How multiple degree of freedom adjustments would affect my shot as I would in cases attempt a multi-dimensional adjustment manoeuvre.
Challenging to visualize how angles of C-arm change orientation of pelvis in image. AXIS helped so much with this.
Having the correct spatial orientation in your head.
Challenging to get a good grip on how much each movement of the C-arm translated to an image shot.
Difficult to get the precise adjustments. Sometimes it felt like the base would not stay in the exact location desired.
Normal C-arm is hard due to lack of external anatomical landmarks, and the number of degrees of freedom that should be coordinated.
I think the reaction time for the image to appear on the AXIS could be faster. When I moved the C-arm, I had to wait couple of seconds for the correct image of the x-ray to appear.
Know where I was before the first X-ray.
Fine movement at the base was challenging; Did not have to change the distance of the source but this seemed intimidating.
Physically moving it. Often moved too little or far; No idea what I'm looking at.
Most challenging is understanding how different motions will affect the image produced. Any tasks involving tilt and rotation are especially difficult.

The orientations which are not in -or orthogonal to - anatomical planes, i.e. those that require adjustments in several d.o.f. and for which adjustments of one d.o.f. requires compensation in another.
Weight / non-trivial manoeuver for inexperienced rad-techs.
First, I think you need to have some experience operating C-arms. Also you need to know very well the anatomy of the patient. Third, you need to have as well 3D visualization to understand from where to take the shots and how. I guess this last point is the one coming with experience and it would be great to have guidance.
Electronic controls, perhaps, to move the C-arm around. Perhaps a joystick to control its movements?

10. Imagine an *Artificial X-ray Imaging System* that guided you to the desired anatomical view with an artificial fluoroscopy mode (continuous artificial X-ray mode, or "video" mode) as compared to the single-shot images used in this study. What is your perceived usefulness of a live artificial fluoroscopy mode?

Not useful at all	Not very useful	Neutral	Somewhat useful	Very Useful

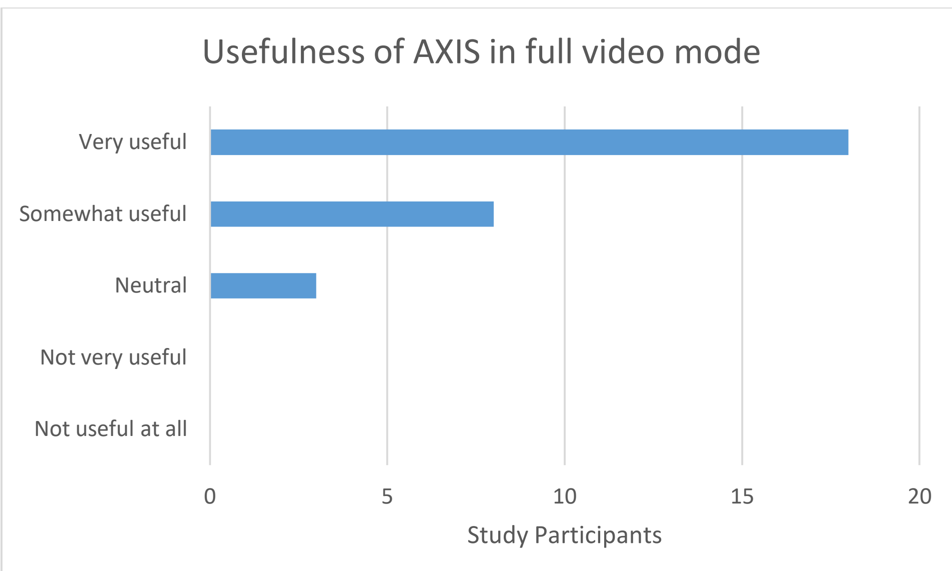

Average (0=Not useful at all; 4=Very useful): 3.5
Standard deviation: 0.69

Additional Comments:

AXIS produced something similar to fluoro…
Especially if you can decrease lag time.
A smooth, continuous video would help with smaller adjustments.
It would reduce the amount of patience required by user.

Definitely not necessary but may appear a bit "smoother" as you move C-arm around.
I don't understand, as I felt the AXIS was almost a 'video' since it updates all the time.
Photos worked just fine. Video would be more to look at but not needed.
Once trained, I imaging the placement would be a lot easier without AXIS but having it available would be great (even if it reduces radiation exposure by 1 X-ray, it is worthwhile).
I think the faster the updating, the better, but I don't see it being much more useful than the current system.
The slight lag did not bother me at all. I was too busy in controlling the C-arm - so I was not looking at the screen continuously.

11. Please include any additional comments or suggestions you wish to make:

Great study with applications for healthcare & education.
Very interesting study! I hope to one day see this in the OR or in training facilities to help students get comfortable using a C-arm.
AXIS will make an amazing education tool to understand how angles affect the view of anatomy; AXIS could prove very useful in the OR to help bridge the communication gap between surgeon and technologist. I think if I had done the non-AXIS imaging first, it would have taken longer and I would have needed more exposures. I learned a lot about patient specific anatomy by doing AXIS supported imaging first.
I think the AXIS is an extremely useful tool for the C-arm. I am sure that the AXIS will help many medical radiation technologists.
This sounds very interesting; I hope to see it in the OR one day :)
Thanks for letting me participate in the study!
Great job!
Very cool system!
No additional comments / suggestions
Good job!
Investigator was very useful in observing and not interfering with study.
Really cool system! Great job :)
I guess I would be interested in how you expect to use the system, since it does seem to require data beforehand. It would be great for training to get a better idea of how C-arm motions change the X-ray image.
Cool!; Market for this?; Automate this?; Why not add more cues on the preview as to what moving the C-arm does?; More precise angles [ruler] on C-arm good
Definitely think the AXIS helped me to learn the C-arm system much faster than I would have without.
Great study!